Gastrointestinal Laboratory
Department of Small Animal Clinical Sciences
College of Veterinary Medicine and Biomedical Sciences
Texas A&M University
&
Klinik für kleine Haustiere
des Fachbereichs Veterinärmedizin
der Freien Universität Berlin

RNA SEQUENCING, GENE EXPRESSION ANALYSIS, AND IMMUNOHISTOCHEMICAL STUDIES IN DOGS WITH CHRONIC HEPATITIS AND HEPATIC FIBROSIS

Inaugural-Dissertation
zur Erlangung des Grades eines
Doktors der Veterinärmedizin
an der
Freien Universität Berlin

vorgelegt von
Vera Eulenberg
Tierärztin aus Neuwied

Berlin 2018
Journal-Nr.: 4044

mbvberlin | mensch und buch verlag

Gastrointestinal Laboratory
Department of Small Animal Clinical Sciences
College of Veterinary Medicine and Biomedical Sciences
Texas A&M University
&
Klinik für kleine Haustiere
des Fachbereichs Veterinärmedizin
der Freien Universität Berlin

RNA SEQUENCING, GENE EXPRESSION ANALYSIS, AND IMMUNOHISTOCHEMICAL STUDIES IN DOGS WITH CHRONIC HEPATITIS AND HEPATIC FIBROSIS

Inaugural-Dissertation
zur Erlangung des Grades eines
Doktors der Veterinärmedizin
an der Freien Universität Berlin

vorgelegt von
Vera Eulenberg
Tierärztin aus Neuwied

Berlin 2018
Journal-Nr.: 4044

Gedruckt mit Genehmigung des Fachbereichs Veterinärmedizin

der Freien Universität Berlin

Dekan:	Univ.-Prof. Dr. Jürgen Zentek
Erster Gutachter:	Univ.-Prof. Dr. Barbara Kohn
Zweiter Gutachter:	Prof. Dr. Jonathan Lidbury
Dritter Gutachter:	Univ.-Prof. Dr. Salah Amasheh

Deskriptoren (nach CAB-Thesaurus):
dogs; hepatitis; chronic hepatitis; gene expression; biopsy; chemokines; polymerase chain reaction; immunohistochemistry

Tag der Promotion: 08.03.2018

Bibliografische Information der *Deutschen Nationalbibliothek*
Die Deutsche Nationalbibliothek verzeichnet diese Publikation in der Deutschen Nationalbibliografie; detaillierte bibliografische Daten sind im Internet über <http://dnb.ddb.de> abrufbar.

ISBN: 978-3-86387-886-3
Zugl.: Berlin, Freie Univ., Diss., 2018
Dissertation, Freie Universität Berlin
D188

ABBREVIATIONS

ACE	Angiotensin converting enzyme
ALT	Alanine transaminase
αSMA	Alpha-smooth muscle actin
CAV-1	Canine adenovirus type 1
CCL	Chemokine (C-C motif) ligand
CCR	C-C chemokine receptor
CH	Chronic hepatitis
CTGF	Connective tissue growth factor
COMMD1	Copper metabolism domain containing 1
CXCL	Chemokine (C-X-C motif) ligand
CYGB	Cytoglobin
diH2O	Deionized water
EBDO	Extrahepatic bile duct obstruction
ECM	Extracellular matrix
FDR	False discovery rate
GSH	Glutathione
HE	Hepatic encephalopathy
HSC(s)	Hepatic stellate cell(s)
Mas	Ang (1-7) receptor
MMPs	Matrix metalloproteinases
MPS	Mononuclear phagocytic system
NF-kB	Nuclear factor kappa B
NK cell	Natural killer cell
NOX	NADPH oxidase
PDGF	Platelet derived growth factor
qPCR	Quantitative polymerase chain reaction
RAS	Renin angiotensin system

ROS	Reactive oxygen species
SAMe	S-adenosylmethionine
TGFβ-1	Transforming growth factor beta-1
TIMP-1	Tissue inhibitor of metalloproteinases 1
vWF	Von Willebrand factor

1. Introduction 8

2. Literature Review 10

2.1 The Liver 10

2.1.1 History 10

2.1.2 Embryology 12

2.1.3 Anatomy 12

2.1.4 Histology 13

2.1.5 Physiology 17

2.2 Chronic Hepatitis 20

2.2.1 Causes of Chronic Hepatitis 20

2.2.2 Clinical Symptoms and Clinical Pathology 22

2.2.3 Diagnosis and Treatment 22

2.3 Hepatic Fibrosis 23

2.3.1 Causes of Hepatic Fibrosis in Dogs 23

2.3.2 Consequences of Hepatic Fibrosis 27

2.3.3 Pathophysiology of Hepatic Fibrosis 28

2.3.4 Diagnosis 35

2.3.5 Treatment 40

3. Objectives 43

3.1 RNA Sequencing and Gene Expression Analysis 43

3.2 Immunohistochemistry 43

4. Material and Methods 44

4.1 RNA Sequencing and Gene Expression Analysis 44

4.1.1 Animals 44

4.1.2 RNA Extraction 44

4.1.3 High-throughput RNA Sequencing and Data Analysis 45

4.1.4 Reverse Transcription and Quantitative Polymerase Chain Reaction 45
4.1.5 Statistical Analysis 47
4.2 Immunohistochemistry 48
4.2.1 Dog Liver Tissue for Immunohistochemistry 48
4.2.2 Immunostaining of Dog Liver Tissue Sections 48
4.2.3 Analysis of Stained Sections 49
4.2.4 Statistical Analysis 49

5. Results 50
5.1 RNA Sequencing and Gene Expression Analysis 50
5.1.1 Dog Characteristics 50
5.1.2 RNA Sequencing Data Analysis 52
5.1.3 Quantitative Polymerase Chain Reactions 66
5.2 Immunohistochemistry 68
5.2.1 Specificity of the Primary Antibody 68
5.2.2 Immunostaining of Dog Liver Sections 69
5.2.2.1 αSMA 69
5.2.2.2 Ki67 71
5.2.2.3 TIMP-1 72
5.2.2.4 αSMA and Picrosirius Red 73

6. Discussion 75
6.1 RNA Sequencing and Gene Expression Analysis 75
6.2 Immunohistochemistry 79

7. Conclusions 82

8. Summary 83

9. Zusammenfassung 84

10. References 85

11. Appendix 98

11.1 Legend of Figures 98

11.2 Legend of Tables 98

11.3 Supplementary Materials 99

Table S1 99

Table S2 100

Table S3 115

12. Publications 142

13. Danksagung 143

14. Selbständigkeitserklärung 144

1. Introduction

Chronic hepatitis (CH) is the most common cause for hepatic fibrosis in dogs. In the majority of CH cases, the etiology remains unknown after diagnostic testing and the disease is referred to as 'idiopathic CH' (Bexfield 2017; Poldervaart et al. 2009; Watson 2004). One proven cause of CH, however, is copper accumulation in hepatocytes, which can be primary or secondary. Primary copper accumulation due to diminished biliary copper excretion can occur because of mutations in copper metabolism genes (e.g., *COMMD1*, copper toxicosis of the Bedlington terrier). Copper levels in the liver are relatively high (5,000-12,000 ppm) (Rolfe and Twedt 1995; Strombeck and Guilford 1990) and copper concentrates in the centrilobular zones. If the copper accumulation occurs secondary to cholestasis, it concentrates in the periportal zones and it seldom reaches such high concentrations (Rolfe and Twedt 1995; Spee et al. 2006). Unlike in humans, viral causes of CH seem to play a minor role in dogs, although canine adenovirus type I (CAV-1) has been reported as a possible causing agent. Other infectious agents (e.g., *Leptospira* spp.) (Bexfield 2017) have been postulated but not proven to cause canine CH. Additionally, an autoimmune etiology has been suspected in some breeds, but has not been proven yet (Bexfield 2017).

Chronic hepatitis is defined as a condition that lasts more than 4-6 months and is characterized by hepatocellular apoptosis and necrosis, an inflammatory reaction with a mononuclear infiltrate, and elevation of serum alanine transaminase (ALT) activity (Ettinger, Feldman and Cote 2017; Van den Ingh 2016). Regeneration and fibrosis are usually present (Van den Ingh 2016). Hepatic fibrosis is recognized as the formation of excess 'scar tissue', a wound healing response to chronic injury and inflammation (Ma et al. 2015; Ramachandran and Iredale 2012; Friedman 2007). During fibrogenesis, a progressive accumulation of fibrillary extracellular matrix (ECM) components takes place (Pinzani and Rombouts 2004). The amount of interstitial matrix increases, with increased amounts of the fibrillary collagen types I, III and V, the non-fibrillary collagen types IV and VI, and other ECM components such as proteoglycans and glycosaminoglycans (Gressner et al. 2008; Friedman 2007). The total collagen content in a fibrotic liver is 3-10 fold higher than that of a healthy liver (Friedman 2007). Hepatic fibrosis is a dynamic process and continuous remodeling of the deposited ECM takes place (Younis et al. 2016). Collagen deposition and resolution happens simultaneously. In advanced fibrosis and

cirrhosis cross-linking of matrix proteins has occurred, which renders the ECM more resistant to degradation (Grenard et al. 2001). Cirrhosis is considered the ‘end-stage’ of liver disease. The deposited and remodeled ECM connects (‘bridging’) and disrupts the functional architecture of the liver (Xu et al. 2016).

Diagnosis of CH and hepatic fibrosis requires histopathologic examination of a liver biopsy specimen and at the time of diagnosis, hepatic fibrosis is frequently advanced. As it is often not possible to determine the underlying cause of canine CH, treatment remains symptomatic and supportive. Effective antifibrotic drugs are currently not available.

The pathogenesis of canine hepatic fibrosis is complex and not completely understood. In human hepatic fibrosis, the activation of myofibroblast precursor cells has been recognized as the key event in fibrogenesis. This leads to the increased deposition of ECM components. Several cells have been reported to be a source of myofibroblasts, but hepatic stellate cells (HSCs) are generally believed to be the main source for myofibroblasts in CH. The transdifferentiation of quiescent HSCs to myofibroblasts is a multi-step process that involves cytokines/chemokines, growth factors, reactive oxygen species (ROS), and apoptotic bodies derived from hepatocytes (Crosas-Molist and Fabregat 2015; Czaja 2014; Mallat and Lotersztajn 2013; Friedman 2007). Upon activation the HSC changes from its quiescent, vitamin A-rich state to a highly fibrogenic (myofibroblastic) phenotype. They lose the ability to store vitamin A and acquire the ability for proliferation, chemotaxis, and ECM production.

Hepatic fibrosis can proceed to cirrhosis and lead to severe consequences. The formation of fibrotic scar tissue can impede portal blood flow and reduce functional hepatic mass. The results are portal hypertension with the associated clinical symptoms, such as ascites and hepatic encephalopathy (HE), or liver failure. However, hepatic fibrosis has been shown to be reversible, when the underlying cause for the disease is removed and a specific treatment is applied (Ramachandran et al. 2015).

This study aimed to determine differential gene expression in dogs with CH compared to healthy control dogs to elucidate the pathophysiology of chronic hepatic disease in dogs. RNA sequencing and data analysis were performed and upregulation of selected genes was confirmed by quantitative polymerase chain reaction (qPCR). Immunohistochemistry was performed to investigate selected markers at the protein level.

2. Literature Review

2.1 The Liver

2.1.1 History

The liver, as largest organ of the abdominal cavity, must have been known to hunters since primeval times (Mani 1959). The first systematic examination of the liver, however, was carried out during ‘haruspicy’, the inspection of the entrails of sacrificed animals to predict the future or to discover the will of the gods. The Assyro-Babylonian culture was famous for reading omens out of sheep livers and the ‘art of hepatoscopy’ was taught systematically to priest (‘baru’) scholars with the use of liver models. One of these models, a Babylonian clay model of a sheep’s liver dated to 2,000 BC, is conserved at the British Museum. The Babylonian ‘hepatoscopy’ was a systematic and detailed examination and description of all outer liver parts and is presumed to be the precursor of anatomy. Also, the Etruscans and Romans practiced haruspicy (called ‘hostiae consultatoriae’). From this time another model of a sheep’s liver exists – the ‘bronze Liver of Piacenza’, dated to 100 BC. The Etruscan/Roman tradition of ‘hepatoscopy’ survived until the end of the Roman Empire (476 AD) and was usually carried out when advice was needed in important state affairs. A big liver meant luck and a small or incomplete liver was considered a bad omen. And also, Emperor Caligula could not find the papillary process of his sheep’s liver in the year of his assassination (41 AD). However, the first ‘medical’ document that contains a description of liver anatomy and physiology comes from the ancient Egyptians. The Egyptian medical papyrus is dated to 1,550 BC, but is probably much older. Today it is called ‘Papyrus Ebers’ and it is currently kept in the library of the University of Leipzig, Germany. It describes the liver linked to its vessels, the hematopoietic function of the liver, and the congestion of the liver as a pathological process. In addition, it contains the first description of a patient suffering from a liver disease with symptoms of anorexia, abdominal pain, and nausea. He was reportedly cured with ‘herbal medication’ that ‘opened the liver’. During the time of the Greek natural philosophers (600/500 BC), the liver was recognized as essential organ (‘a stab in the liver was deadly’) and as key organ for alimentary processes. The bile was described as cause for many acute illnesses and phlebotomy was established as a

treatment for abdominal and liver diseases. The ‘Corpus Hippocraticum’ (about 400 BC) was a collection of medical works of different authors related to the Greek physician Hippocrates. It was recognized that the cause for ascites and icterus is liver disease and that liver diseases can be diagnosed by abdominal palpation. Additionally, liver lobe torsion was described (‘the man, whose liver lobe was twisted; I shook him and the pain stopped’). Aristoteles mentioned the detoxification and storage function of the liver and was the first, who described the liver capsule and the bile ducts. At approximately 250 BC, Erasistratos defined the term ‘parenchyma’. For him it was a simple ‘blood clot’, the matrix of all viscera. ‘Liver cirrhosis’ was recognized as cause of ascites for the first time. For Galen (about 200 AD) then, the liver parenchyma turned into an ‘organ’, responsible for liver functions like hematopoiesis.

The next known descriptions of liver cirrhosis came from the physicians J. Browne in 1685 and R. Laennec in 1819 (Lee 2000). The first liver biopsy was performed in 1833 by an English surgeon, E. Stanley, and in 1845 G. Budd described two causes of human hepatic fibrosis – the parasite *Fasciolopsis bushi* and hepatic vein occlusion (later named: Budd-Chiari syndrome, 1898). In 1860 F. von Frerichs first described a familial disorder in copper metabolism (later known as Wilson’s disease, 1912) that is accompanied by liver fibrosis. The French physician V. C. Hanot described biliary fibrosis in 1875 (‘Hanot disease’). The first diagnostic liver biopsy was performed in 1895 by an Italian surgeon L. Lucatello. In 1935, H. Kalk used a laparoscope for the first time to take liver biopsies. During the following years major progress was made in the treatment of liver diseases: in 1959 the physician J. Walshe treated successfully Wilson’s disease with penicillamine; in 1972 A. Hofman, dissolved gallstones with oral administration of chenodeoxycholic acid, and in 1987 alpha interferon was used as a treatment for viral hepatitis C (Lee 2000).

The connection of chronic liver inflammation and an increase in connective tissue was made by J. Mueller in 1843 (Gressner et al. 2008). R. Virchow added 1858 that the increase in connective tissue comes from a cellular source. The search began for cell types engaged in ECM production. In 1869 F. Boll was the first, who discovered a star-shaped cell with cytoplasmatic granules. They were described more detailed in 1876 by C.W. von Kupffer and in 1952 by T. Ito. In 1996, the cell – considered to be a main producer of ECM during fibrogenesis – was named ‘hepatic stellate cell’.

2.1.2 Embryology

The liver consists of the connective tissue capsule, the parenchyma and the hepatic sinusoids. The parenchymal cells are of endodermal origin. They arise from an endodermal layer in the floor of the foregut. The resulting 'hepatic diverticulum' grows through the ventral mesogastrium into the septum transversum. Interaction with the surrounding mesenchyme is important to form the connective tissue capsule, the liver ligaments, endothelial cells, liver resident macrophages (Kupffer cells), and HSCs (Hyttel 2010). The hepatoblasts multiply and the liver grows out of the septum transversum and into the abdominal cavity. The hepatoblasts differentiate into hepatocytes, the predominant parenchymal cells of the liver (Hyttel 2010). The hepatic diverticulum also forms the bile duct system and the gallbladder by branching progressively during development (Latshaw and Latshaw 1987). The liver grows around the vitelline veins and breaks them up into channels, the hepatic sinusoids. The cranial part of the right vitelline vein builds the hepatic veins and the portal vein arises from the right and left vitelline vein and their middle anastomosis. The hepatic artery is a branch of the coeliac artery, which derives from the vitelline arteries (part of the ventral branches of the aorta) (Latshaw and Latshaw 1987).

2.1.3 Anatomy

The liver is the largest gland in the body. In dogs, it is situated almost entirely in the intrathoracic part of the abdominal cavity, right behind the diaphragm. The diaphragmatic (or parietal) surface is highly convex. The surface of the liver that is facing the abdominal organs (visceral surface) is concave and in contact with the stomach, the pancreas, the duodenum and the cranial pole of the right kidney (Kumar 2013). In dogs and cats, the liver can be divided into four lobes: the right, left, quadrate and caudate lobe. Right and left lobe can be subdivided into a right lateral, a right medial, and a left lateral and left medial lobe. The quadrate lobe can be found between the right medial and the left medial lobe. In a fossa between the right medial and the quadrate lobe lies the gallbladder. The caudate lobe is part of the visceral liver surface and can be further divided into a papillary process and a caudate process. The papillary process forms part of the gastric impression of the left lateral lobe. The caudate process is the most caudal part

of the liver and the part, which can be palpated when the liver becomes enlarged (Strombeck and Guilford 1990). The caudate process also forms the renal fossa. The duodenal impression is the most lateral part of the caudate process and the right lateral lobe. The liver is covered by visceral peritoneum, which fuses with a thin underlying fibrous capsule. Both, serosa and fibrous coat, form the liver ligaments (Evans and Miller 2013). Five ligaments and the lesser omentum provide attachment of the liver to the diaphragm, the body wall and the visceral organs. Parietal connection to the diaphragm is maintained by the coronary, the right triangular (between the right lateral liver lobe and the right crus of the diaphragm), and the left triangular (between the left lateral liver lobe and the left diaphragmatic crus) ligament. The falciform ligament arises from between the right medial and the left medial liver lobe and connects the liver to the diaphragm and the ventral body wall caudally to the umbilicus (Evans and Miller 2013; Kumar 2013). The hepatorenal ligament connects the renal fossa of the caudate process and the ventral surface of the right kidney. The lesser omentum (hepatogastric/hepatoduodenal ligament) is a peritoneal fold that attaches the liver to the lesser curvature of the stomach and the cranial duodenum. The porta hepatis can be found on the visceral surface of the liver. Here, the portal vein, the hepatic arteries, and nerves enter and the biliary duct leaves the organ. Also, the caudal vena cava enters the liver through the caudate process on the visceral surface. Hepatic venules, which contain blood from hepatic arterioles and portal venules, become hepatic veins that join the vena cava on its way through the liver. The portal vein brings blood from the gastrointestinal tract to the liver sinusoids to deliver nutrients but also for detoxification of possible harmful agents. Approximately, 25-33 % of the cardiac output reaches the liver and this highly oxygenated blood maintains perfusion of the liver (Strombeck and Guilford 1990).

2.1.4 Histology

The histological organization of the liver consists of connective tissue and parenchyma. The capsular connective tissue extends into the interstitium, is most prominent in the portal areas and divides the liver as interlobular connective tissue into hepatic lobules, which is most evident in the porcine liver (Banks 1993). The intralobular connective tissue is a fine network of reticulin fibers that surround cells and sinusoids (Dellmann and Brown 1987). The hepatic lobule is the smallest morphological unit in the liver. It is a hexagonal structure around a central vein and consists of rows of hepatocytes and hepatic sinusoids. Blood flows from the periphery of each

lobule through the sinusoids toward the central vein. An alternative morphological unit is the portal lobule, a triangular structure, which includes one portal triad and three central veins. The functional unit of the liver is the hepatic acinus, which is a quadrilaterally shaped, combining two central veins and two portal triads. It consists of three zones according to the oxygen content of the blood. Zone 1 is the innermost zone (around the portal triad) where the oxygen content is highest and where cells are metabolically most active. But, cells of this zone may also be the first that are exposed to toxic agents entering the liver (Dellmann and Brown 1987). Zone 3 is the area nearest to the central vein with the lowest oxygen and nutrient supply and zone 2 is the zone in between with intermediate metabolic cell activity (Samuelson 2007). **Figure 1** shows the normal histological organization of the canine liver (hematoxylin & eosin stain; **A**) and explains the morphological and functional units of the liver (**B**).

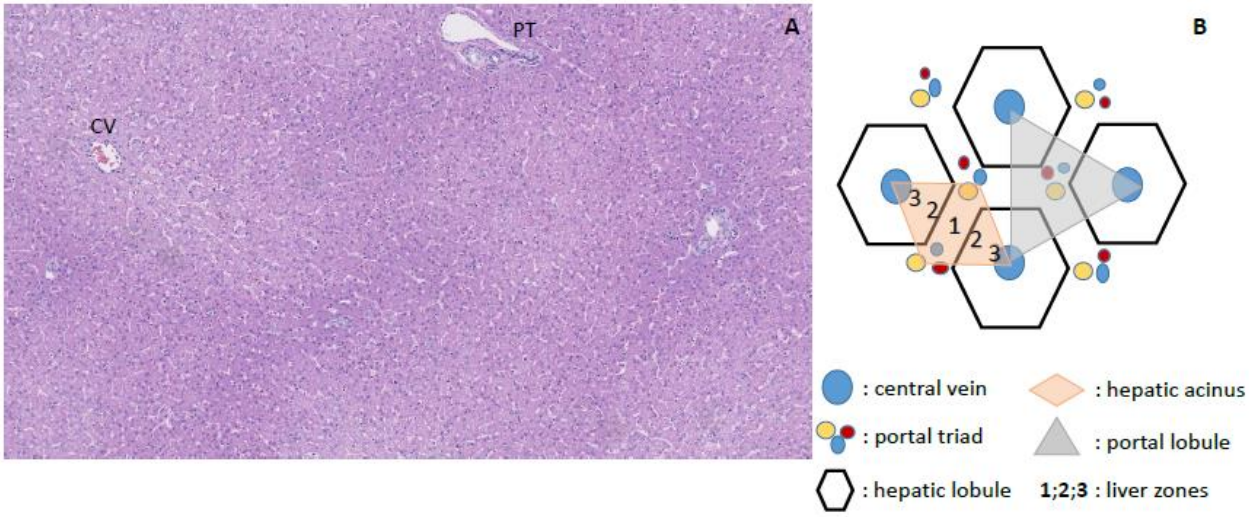

Figure 1: Histological Organization of the Canine Liver. A: Liver of a healthy dog. Hematoxylin & eosin stain. CV: central vein; PT: portal triad. **B:** Schematic presentation of the morphological and functional liver units: hepatic lobule, portal lobule, and hepatic acinus with the metabolic liver zones.

Hepatocytes. Hepatocytes account for 60-80 % of liver cell mass (Washabau and Day 2013). They have an eosinophilic cytoplasm and large amounts of mitochondria and rough endoplasmatic reticulum. Nuclei are centrally positioned and the nucleoli are prominent.

Binucleated cells and anisokaryosis can be found. Hepatocytes are organized in cords, from the central vein to the limiting plate. The rows are separated by the sinusoids and the perisinusoidal space. Hepatocytes have many metabolic functions. For example, they extract nutrients from the portal blood and oxygen from the arterial perfusion, detoxify endogenous and exogenous toxins, and they synthetize and secrete bile components (Washabau and Day 2013).

Cholangiocytes. Cholangiocytes or biliary epithelial cells contribute with 3-10 % to the total liver cell mass. They are cuboidal cells lining the intra- and extrahepatic ducts of the biliary tree. They modify the hepatocyte-derived bile and provide 30 % of the total bile volume by secreting water, bicarbonate, and cations into the bile (Washabau and Day 2013).

Kupffer cells. Kupffer cells are liver resident macrophages and part of the mononuclear phagocyte system (MPS). About 2-5 % of liver cells are liver resident macrophages and they are situated upon the endothelial lining of the sinusoids, but they may also extend across the sinusoidal lumen (Banks 1993; Washabau and Day 2013). They capture and phagocytize aged red blood cells and are involved in the metabolism of hemoglobin and in iron storage. Another function is immune surveillance. They are a first defense against invading pathogens and producers of inflammatory mediators during pathologic conditions. Besides liver resident macrophages, monocyte derived macrophages play a role in liver immunology, as well as in fibrosis progression and resolution. Other liver resident immune cells are *natural killer cells* (NK cells) in the hepatic sinusoids and *endothelial cells*, which line sinusoids, blood vessels and lymphatic vessels (Washabau and Day 2013).

Hepatic stellate cells. Hepatic stellate cells, also called vitamin A-storing cells, lipocytes or Ito cells, are located in the perisinusoidal space. In the healthy liver, they maintain a dendritic cell shape with close contact to hepatocytes and sinusoidal endothelial cells. A main function is the storage of vitamin A-droplets and the regulation of vitamin A homeostasis. During pathologic conditions, they change to a myofibroblastic phenotype with the ability to migrate and produce ECM components (a main mechanism in the development of fibrosis).

Smooth muscle cells. Smooth muscle cells are located around the hepatic artery or the hepatic veins and their derivatives. They contribute to 2-5 % to the total liver cell mass and their function is the regulation of the hepatic microcirculation (Washabau and Day 2013).

Portal fibroblasts. Portal fibroblasts are located in the mesenchyme of the portal tracts. They surround the hepatic bile ducts and are important for the integrity of the portal triads (Washabau and Day 2013). Their role as a source of myofibroblasts during fibrogenesis is still controversial (Wells 2014).

Progenitor cells. Stem cells are undifferentiated cells with a capacity to self-renew. Stem/progenitor cell populations contribute to the normal organ and to regeneration. Liver stem cells are Wnt-responsive (Wnt is a signaling molecule released by endothelial cells). Without this signal, they differentiate into mature liver cells (Wang et al. 2015; Washabau and Day 2013). An overview of the different types of liver cells, their function, and recognized cell markers is given in **Table 1**.

Table 1: Liver Cell Types

Cell Type	Function	Other Names	Cell Marker(s)
Hepatocyte	Metabolism; detoxification; formation & Secretion of bile; storage; regeneration	Liver cell	HepPar1; Albumin; Annexins; Ki67
Cholangiocyte	Formation of bile components	Biliary epithelial cell	CK7; CK19
Kupffer cell	Immune surveillance; part of MPS; Iron storage	Liver resident macrophage; Browicz-cell	CD68; CD14; CD11d; CD163; F4/80; Ly6C
Hepatic stellate cell	Vitamin A storage; ECM production; supportive function in hematopoiesis	Ito cell; Lipocyte; Vitamin A-storing cell; Perisinusoidal cell	αSMA; Desmin; GFAP; FAP; CYGB
Portal fibroblast	Integrity of portal tracts; fibrogenic function; vascular remodeling	Fibroblast	THY-1; Mesothelin; Fibulin 2; Elastin; Col15A1; NTPD2
Endothelial cell	Immune surveillance; part of MPS; lining of blood vessels	-	CD31; CD34; vWF
Natural killer cell	Immune surveillance; part of MPS	NK-cell; Pit cell	NCR1
Dendritic cell	Immune surveillance; part of MPS	-	CD1; CD11c; MHCII+
Smooth muscle cell	Regulation of microcirculation	Myocyte	αSMA
Progenitor cell	Regeneration	Stem cell; Oval cell	α-Fetoprotein; CD29; CD44

Information provided in this table is from human/rodent studies/literature – cell marker expression is variable depending on species and/or *in vivo* or *in vitro* conditions. Abbreviations: ECM: extracellular matrix; αSMA: alpha smooth muscle actin; GFAP: glial fibrillary acidic protein; FAP: fibroblast activation protein alpha; CYGB: cytoglobin; THY-1: thymocyte antigen 1 (CD90); Col15A1: collagen type 15 alpha subunit 1; NTPD2: ectonucleoside triphosphate diphosphohydrolase 2; CD: cluster of differentiation; CK: cytokeratin; MPS: mononuclear phagocyte system; HepPar1: hepatocyte paraffin 1; Ki67: antigen identified by monoclonal antibody Ki67; NCR1: natural cytotoxicity triggering receptor 1; MHCII: major histocompatibility complex II; NK-cell: natural killer cell.

2.1.5 Physiology

The multiple functions of the liver can be summarized into six main categories: (1) metabolic; (2) secretion (of bile); (3) detoxification; (4) storage; (5) phagocytic, and (6) hematopoietic (in the embryogenic and fetal liver).

Metabolic Function. The metabolic function of the liver can be subdivided into *anabolic* and *catabolic*. *Anabolic* functions include e.g., gluconeogenesis, triglyceride and cholesterol synthesis, synthesis of proteins, and formation of bile components and bile. *Catabolic* functions are glycogenolysis, oxidation of fatty acids, and deamination of amino acids. An important anabolic function is to maintain normoglycemia. If blood glucose concentration decreases and the body's stores of carbohydrates are exhausted, glucose can be formed from amino acids and lactate (gluconeogenesis). During fasting 25 % of the liver's glucose production comes from gluconeogenesis. Decreased blood sugar and diminished carbohydrates are a stimulus for the release of cortisol. This mobilizes proteins from cells. The amino acids derived from these proteins are then converted into glucose in the liver (Hall and Guyton 2011). Carbohydrates can be used as an energy supply or stored in the form of glycogen. The liver converts excess carbohydrates into acetyl-CoA, fatty acids and finally into triglycerides. Triglycerides are transported in very low density lipoproteins from the liver to the adipose tissue for storage (Hall and Guyton 2011). Several kilograms of fat can be stored in the body, whereas the storage of glycogen is limited and the glycogen supplies are usually exhausted after 24 hours of fasting. Amino acids of dietary proteins can be converted into triglycerides as well. Moreover, the liver synthetizes cholesterol, phospholipids, and most lipoproteins (Hall and Guyton 2011). Additionally, the intermediate acetyl-CoA can be used for the formation of ketone bodies (acetocetic acid, β-hydroxybutyric acid, and acetone), which can serve as a form of energy if other energy forms are not available. The liver also synthetizes the major plasma proteins: albumin, fibrinogen, all α-globulins and some β-globulins. Plasma protein formation by the liver can be as high as 30 g/day. Other proteins synthetized by the liver are ceruloplasmin, ferritin, serum enzymes, and most coagulation factors, except von Willebrand factor (vWF), which is produced by endothelium, megakaryocytes, and connective tissue. About 80 % of the cholesterol that is formed by the liver is converted into bile salts. Glycogenolysis as catabolic function is the

breakdown of the stored glycogen to regenerate glucose. Epinephrine and glucagon can both activate phosphorylase and induce rapid glycogenolysis (Hall and Guyton 2011). Another catabolic function of the liver, the oxidation of fatty acids to acetyl-CoA, takes place in the mitochondria. The transport of fatty acids into the mitochondria is a carrier-mediated process and dependent on carnitine. The β-oxidation of fatty acids liberates large amounts of adenosine triphosphate, which provides energy for cellular processes. Amino acids are used for energy, or they are degraded and stored. The main step in their degradation is removal of the amino group (deamination). Deamination is initiated by the activation of the enzyme aminotransferase, as a result of an excess of amino acids in the cells (Hall and Guyton 2011).

Bile Secretion. Bile is the source for fat digestion and absorption and an excretory route for metabolites or xenobiotics (Washabau and Day 2013). Hepatocytes are responsible for the initial secretion of bile components. This secretion contains bile acids, cholesterol and other organic components. Cholangiocytes add a second portion of bile components, a watery solution of sodium and bicarbonate ions (Hall and Guyton 2011). Secretion by the hepatocytes takes place continuously, whereas secretion by the cholangiocytes is regulated by hormones, especially by secretin. The bile flows from the bile canaliculi towards the terminal bile ducts, the hepatic duct and the common bile duct. It is secreted directly into the duodenum or flows through the cystic duct into the gallbladder, where it is stored and concentrated. The stimulus for gallbladder contraction is mainly cholecystokinin, which is released by the duodenal mucosa when fatty food reaches the small intestine (Hall and Guyton 2011).

Detoxification. Portal blood brings nutrients, bacteria, bacterial antigens and xenobiotics to the liver. The liver has the ability to detoxify xenobiotics (drugs, chemicals, carcinogens), and endobiotics (steroids, fatty acids, prostaglandins, vitamins) by oxidation (phase I) (Washabau and Day 2013a). Enzymes of the cytochrome p450 family are the most important detoxifying enzymes of phase I. In phase II, the xenobiotic metabolites are conjugated, for example with glutathione (GSH), by glutathione S-transferases. Ammonia is a by-product of amino acid metabolism and can also be produced by urease bacteria in the gastrointestinal tract. Excessive ammonia in the blood is highly toxic and can cause HE, hepatic coma, and death. After entering the portal circulation and reaching the liver it undergoes conversion into urea in the urea cycle (Hall and Guyton 2011). Glutathione, a major antioxidant of the liver, is also responsible for

scavenging of ROS. In addition, cytoglobin (CYGB) has been found to be an important ROS scavenger in HSCs (Yoshizato et al. 2016).

Storage. The liver plays a role in the storage of vitamins and iron. In the liver, 95 % of the total body vitamin A can be found. Hepatic stellate cells are the main vitamin A-storing cells, but hepatocytes are also capable of storing vitamin A. In addition, all water soluble vitamins are stored in the liver, except for vitamin C (Washabau and Day 2013). Iron is stored in the liver intracellularly in the form of ferritin, and copper can be incorporated into copper proteins, e.g. ceruloplasmin (Washabau and Day 2013). As mentioned above, the liver stores carbohydrates, especially glucose, in the form of glycogen.

Phagocytosis. The phagocytic function of the liver is maintained by the MPS. It is a defense against microorganisms and responsible for the removal of harmful substances from the portal circulation (Strombeck and Guilford 1990). Liver resident macrophages, a main component of the liver MPS, are involved in the capture and destruction of old red blood cells and the storage of iron during hemoglobin breakdown. Sinusoidal endothelial cells are important for the recruitment and migration of leukocytes into the liver tissue. They also function as antigen presenting cells; they internalize antigens by receptor-mediated endocytosis and present the peptides to T-cells to maintain tolerance or to initiate an immune response.

Hematopoiesis. Hematopoiesis is the formation of blood cells from hematopoietic stem cells. In the embryo, blood formation occurs in the yolk sac. In further development, it occurs in the spleen, liver, lymph nodes and later in the bone marrow. Additionally, hematopoiesis can also occur in the liver (extramedullary hematopoiesis) when the bone marrow fails to provide an adequate environment for hematopoietic stem cells (Kordes et al. 2013). It has been demonstrated that rat HSCs possess molecular markers of bone marrow mesenchymal stem cells and that they associate with hematopoietic sites in the fetal rat liver. They did not differentiate into blood cells themselves, but supported the maintenance and development of hematopoietic stem cells (Kordes et al. 2013).

2.2 Chronic Hepatitis

The most common cause of hepatic fibrosis in dogs is CH. Chronic hepatitis is defined as a condition that lasts more than 4-6 months and is characterized by hepatocellular apoptosis and necrosis, an inflammatory reaction with a mononuclear infiltrate, and elevation of serum ALT activity (Ettinger, Feldman and Cote 2017; Van den Ingh 2016). Regeneration and fibrosis are usually present (Van den Ingh 2016). Several studies tried to evaluate the prevalence and the age and breed distribution of chronic hepatic disease in dogs (Andersson and Sevelius 1991; Bexfield 2017; Bexfield et al. 2012; Poldervaart et al. 2009; Watson et al. 2010). A postmortem examination of 200 dogs in the United Kingdom revealed a prevalence for CH of 12 %. Breeds reported to have an increased risk for developing CH are American and English cocker spaniels, Dobermann pinschers, English springer spaniels, Dalmatians, Great Danes, Cairn terriers, Labrador retrievers and Samoyeds (Bexfield 2017). Reported median ages at diagnosis ranged from 5-8 years (Andersson and Sevelius 1991; Bexfield 2017; Bexfield et al. 2012; Poldervaart et al. 2009).

2.2.1 Causes of Chronic Hepatitis

Causes of CH can be classified into primary and secondary causes. Primary causes can be infectious agents (e.g., viruses or bacteria), genetic or autoimmune diseases, drugs or toxins. Secondary hepatitis can occur with systemic infections, neoplastic disease, or disease in other organ systems like pancreatitis or inflammatory bowel disease (Sterczer et al. 2001). A possible viral cause of CH in dogs is CAV-1. Unvaccinated dogs develop fulminant (acute) hepatitis when they are infected. It has been proposed that this virus plays a role in CH as well (Cerquetella et al. 2012). In a study with 11 partially immunocompetent dogs that were experimentally infected with CAV-1, seven of them developed CH and fibrosis. But the virus was only detectable at an early stage postinfection (Gocke et al. 1967). In other studies where PCR screening and immunohistochemical staining were performed CAV-1 could not be detected in dogs with chronic liver disease (Boomkens et al. 2004; Boomkens et al. 2005; Chouinard et al. 1998). In an immunohistochemical study on paraffin-embedded liver sections of 53 dogs with hepatic inflammation, CAV-1 was detected in five livers (Rakich et al. 1986). Other infectious agents that may lead to CH in the dog are *Leptospira* spp. and *Leishmania* spp. Reports exist,

where dogs with persistent infection with *Leptospira interrogans* serogroups Australis or Grippotyphosa developed CH (Adamus et al. 1997; Bishop et al. 1979). In the study about leishmaniasis most of the dogs (20/26) developed a subclinical chronic granulomatous hepatitis with fibrosis in the portal areas (Rallis et al. 2005). Additionally, *Heterobilharzia americana* infection (which plays a role as differential diagnosis in the US) can involve multiple organs and has been shown to cause chronic granulomatous hepatitis in dogs (Corapi et al. 2011; Kvitko-White et al. 2011; Rodriguez et al. 2014). Copper toxicosis, an accumulation of copper in hepatocytes, is a well-recognized cause of CH in the Bedlington terrier. A homozygote deletion of exon 2 in the *COMMD1* gene leads to a defect in a copper transporting protein and to an inhibition of biliary copper excretion (Cerquetella et al. 2012). This results in massive centrilobular copper accumulation and the development of cirrhosis (Dirksen and Fieten 2017). Wilson's disease, a similar disorder in humans, is caused by mutations in the *ATP7B* gene (Coronado et al. 2008). A recent study in Labrador retrievers showed a significant association of high hepatic copper concentrations with a mutation in the *ATP7B* gene for this breed (Dirksen and Fieten 2017; Fieten et al. 2016). Chronic hepatitis associated with high hepatic copper concentration has been reported for other breeds, such as the West Highland white terrier, the Dalmatian, or the Doberman pinscher as well (Watson 2017). Inherited primary disease is suspected, but the mechanisms require further investigation. Autoimmune hepatitis in humans is characterized by hypergammaglobulinemia, detection of autoantibodies, hepatic necrosis and an infiltration of lymphocytes and plasma cells in the periportal areas. An autoimmune etiology is suspected in some dog breeds (i.e., Dobermans, English springer spaniels), but has not been proven yet (Bexfield 2017; Watson 2017). Aflatoxicosis and anticonvulsive drug therapy have been reported to cause CH in dogs (Bunch et al. 1982; Chaffee et al. 1969; Dayrell-Hart et al. 1991; Newberne 1973; Poffenbarger and Hardy 1985). The anticonvulsive drug primidone led to hepatic cirrhosis in a German shepherd dog (Poffenbarger and Hardy 1985). In another study with 18 dogs phenobarbital therapy was linked with chronic hepatic disease; necropsy results, that were provided for ten dogs, revealed chronic hepatic fibrosis or cirrhosis in eight of them (Dayrell-Hart et al. 1991). Similiarly, Bunch et al. reported advanced hepatic disease in five dogs that received either phenobarbital, primidone or phenytoin (Bunch et al. 1982). However, for the majority (>60 %) of dogs with CH, the etiology cannot be determined.

2.2.2 Clinical Symptoms and Clinical Pathology

Clinical symptoms are either not present in the early stages of CH, or they are non-specific (Bexfield 2017; Favier 2009; Strombeck and Guilford 1990). Most frequently reported are lethargy (40->50 %), reduced appetite (40-50 %), vomiting (40-50 %), weakness or weight loss (30-40 %), polyuria/polydipsia (30-40 %) and diarrhea (20-30 %). However, 5-10 % of dogs in more advanced stages of the disease show no clinical signs at all (Strombeck and Guilford 1990). Laboratory findings are non-specific, but may include elevated liver enzyme activities, e.g., for ALT and alkaline phosphatase (AP), or coagulation abnormalities in more advanced disease (Bexfield 2017). In 80-90 % of affected dogs, a 5-18 fold increase of ALT activity is present. Elevated ALP activity (2-3 fold) has been reported for >80 % of dogs (Strombeck and Guilford 1990).

2.2.3 Diagnosis and Treatment

Diagnosis of CH requires the histopathological examination of a liver biopsy specimen. A grading of inflammation and necrosis (activity of the disease) and staging of the fibrosis should take place. A routine stain for copper is recommended, as well as the determination of the copper concentration in the liver tissue.

Current therapeutic options for the treatment of idiopathic CH in dogs can be found in **Table 2**. The principles of treatment are: a) reducing inflammation b) preventing further oxidative damage c) inhibiting or reducing fibrosis and d) supportive therapy. For copper associated CH, specific treatment is possible and includes chelation therapy for reducing hepatic copper accumulation, supplementation with zinc salts and a low-copper diet (**Table 2**). This has been shown to decrease hepatic copper accumulation effectively. Supportive therapy for CH in general, includes an appropriate diet, with highly digestible proteins and carbohydrates, normal amounts of fat, and vitamin supplements (Bexfield 2017).

2.3 Hepatic Fibrosis

2.3.1 Causes of Hepatic Fibrosis in Dogs

The most common cause of hepatic fibrosis in dogs is CH and at the time of diagnosis of CH, fibrosis is usually present. The fibrosis often co-localizes with necrosis and, especially for idiopathic CH, is initially present in the periportal zones of the liver (Cullen 2009). With more advanced fibrosis, portal-portal or portal-central bridging fibrosis may develop with eventual formation of discrete nodules (Van den Ingh 2016). In a retrospective study, copper accumulation was the underlying cause in 36 % of dogs with CH (Poldervaart et al. 2009). In >60 % of dogs with CH, no underlying cause can be found and these patients are referred to as having idiopathic CH. Granulomatous hepatitis is an uncommon form of CH in dogs (Poldervaart et al. 2009) and may be the result of infectious diseases such as schistosomiasis (Rodriguez et al. 2014), histoplasmosis (Chapman et al. 1993), *Angiostrongylus vasorum* infection (Cook et al. 2015), leishmaniosis (Rallis et al. 2005), or with lymphoma and histiocytosis (Chapman et al. 1993). Regardless of the underlying cause of CH, chronic inflammation leads to fibrosis.

Lobular dissecting hepatitis is a distinct type of CH that typically occurs in young dogs at an average age of two years. It has been reported in a number of breeds, including the Standard poodle, Rottweiler, German shepherd, Golden retriever, and American cocker spaniel. This disease has a rapid clinical course and a poor prognosis with a short survival time (Mizooku et al. 2013). Lobular dissecting hepatitis is histologically characterized by a diffuse infiltrate of inflammatory cells and dissection of the lobular parenchyma with reticulin fibers (type III collagen) surrounding single or small groups of hepatocytes (van den Ingh and Rothuizen 1994). The cause of lobular dissecting hepatitis is not known.

Extrahepatic bile duct obstruction (EBDO) can result in fibrosis around biliary ducts presumably due to proliferation of portal myofibroblasts. Causes for extrahepatic bile duct obstruction in dogs include pancreatic or biliary tumors, inflammation, or cholelithiasis (Rothuizen 2008).

Cholangitis is less well described in dogs than in cats (Tamborini et al. 2016) and with chronicity can lead to biliary fibrosis. Biliary fibrosis can progress to portal-portal bridging fibrosis and biliary cirrhosis (Cullen 2015). Destructive cholangitis, characterized by loss of bile

ducts with accompanying inflammation can also lead to biliary fibrosis (Cullen 2015; Osumi et al. 2011). Idiosyncratic drug reactions have been implicated in causing this uncommon disease (Gabriel et al. 2006).

Right-sided heart failure or obstruction of the cranial vena cava lead to increased central venous pressure and passive venous hepatic congestion. Liver perfusion is impaired and ischemia and necrosis occur (Li et al. 2012). Chronically, this can lead to centrilobular fibrosis. A similar pattern can develop following toxin ingestion (Cullen 2015).

In addition, ductal plate abnormalities are a group of developmental disorders of the biliary system that can be associated with increased hepatic ECM, portal hypertension, abdominal effusion, and HE. The most severe form is called congenital hepatic fibrosis and is characterized by portal-portal bridging fibrosis, multiple small bile ducts, and discontinuous biliary profiles. Ductal plate abnormalities, including congenital hepatic fibrosis, were reported in a series of 30 boxer dogs (Pillai et al. 2016) and in other breeds (Brown et al. 2010; Kaneko et al. 2016). Pathologists may misdiagnose these conditions as fibrosis secondary to CH.

Table 2 summarizes relevant causes of hepatic fibrosis in dogs and lists the current treatment options.

Table 2: Causes of hepatic fibrosis in dogs

	Definition	Etiology	Signalement	Fibrosis pattern	Current Treatment	Principle of Treatment
Chronic idiopathic hepatitis	Lymphoplasmacytic inflammation of the liver	Unknown (immune-mediated?)	American/English cocker spaniels, Labrador retrievers, Doberman pinscher overrepresented; Average age 4-7 years	Periportal	Glucocorticoids: -Prednisolone 1 mg/kg/day, PO -Prednisolone and Azathioprine 0.5 mg/kg/day each, PO (6-12 weeks)	Antiinflammatory Immunomodulatory
					Ursodeoxycholic acid (UDCA): 15 mg/kg/day, PO	Antioxidant (anti-fibrotic)
					Vitamin E 10-15 IU/kg/day, PO	Antioxidant
					-S-adenosylmethionine (SAMe) 20 mg/kg/day, PO -Silymarin 3-6 mg/kg/day, PO	
Copper toxicosis	Copper accumulation in hepatocytes	Primary: genetic disorder	Bedlington Terrier and others (s. text)	Perivenular	-Penicillamine 10-15mg/kg, PO, twice daily -Trientine 10-15mg/kg, PO, twice daily (month-years)	Treatment of underlying cause (Chelation)
		Secondary: to cholestasis/hepatitis	All breeds; all ages	Periportal		
					Zinc 5-10 mg/kg, PO, twice daily, 1hr before meal (>3 months)	Supportive (Inhibition of absorption)
					-copper-restricted diet	Supportive
Other toxic hepatopathies	Oxidative damaged to hepatocytes	Drugs; chemicals; metals; toxins	All breeds; all ages	Perivenular	Removal of toxic agent	Treatment of underlying cause
					-Vitamin E -SAMe -Silymarin	Antioxidant

Table 2: Causes of hepatic fibrosis in dogs (continued)

Lobular dissecting hepatitis	Rapid development of fibrosis (with inflammation)	unknown	All breeds; Neonatal – young, adult dogs	Pericellular	No treatment available	Antifibrotic Colchicine treatment may be appropriate (0.03mg/kg/day, PO)
EBDO	Biliary duct obstruction with bile duct epithelial proliferation	Cholelithiasis, Inflammation, Neoplasia of biliary tract/pancreas	All breeds; all ages	Periportal	Surgical decompression	Treatment of underlying cause
Right-sided heart failure	Impaired liver perfusion; ischemia and necrosis	Heartworm disease, DCM, congenital, neoplasia, etc.	All breeds; all ages	Perivenular	RHF treatment	Treatment of underlying cause

PO: per os; UDCA: ursodeoxycholic acid; SAMe: S-adenosylmethionine; ppm: parts per million; EBDO: extrahepatic bile duct obstruction; DCM: dilated cardiomyopathy; RHF: right-sided heart failure.

2.2.2 Consequences of Hepatic Fibrosis

Hepatic fibrosis can proceed to cirrhosis, the end-stage of liver disease. Hepatocyte swelling, increased HSC contractility, fibrosis, and the formation of regenerative nodules impede portal blood flow, leading to hepatic (sinusoidal) portal hypertension (Washabau and Day 2013). Portal hypertension in dogs and cats is defined as a portal vein pressure above 10 mmHg (from experimental studies of anaesthetized animals estimated normal values are 6-9 mmHg) (Buob et al. 2011; Schmidt et al. 1980). Direct measurement of the portal vein pressure is an invasive technique, which requires direct puncture of the portal vein, and therefore is rarely performed in dogs and cats. An indirect method that has been performed in veterinary patients is the catheterization of the splenic pulp. But, values obtained from this measurement seem to be 0.5-1.5 mmHg higher than for the direct measurement (Buob et al. 2011; Schmidt et al. 1980). In most cases, it is assumed that portal hypertension is present when associated clinical symptoms can be observed. Hepatic portal hypertension can, for example, contribute to the development of ascites and lead to the opening of vestigial blood vessels that bypass the portal circulation (acquired portosystemic collaterals) (Buob et al. 2011). Portosystemic shunting can result in HE, where ammonia dysmetabolism and a variety of other factors, such as neurosteroids and inflammatory mediators, cause astrocyte swelling and neurological dysfunction (Lidbury et al. 2016). Development of ascites is the consequence of a combination of splanchnic arterial vasodilation, decreased cardiac output and the activation of the renin angiotensin system, which leads to sodium and water retention (Sanyal et al. 2008). In addition, high sinusoidal pressure drives fluid into the interstitial space (Buob et al. 2011). Treatment of portal hypertension concentrates on managing its complications (i.e., fluid and diuretic therapy (ascites), treatment of HE with lactulose, and angiotensin converting enzyme (ACE) inhibitors to reduce sodium and water retention). However, the optimal treatment would be to remove the underlying cause (i.e., the reduction or resolution of fibrosis).

The progressive replacement of hepatocytes with fibrous tissue is another consequence of chronic hepatic disease, which can result in hepatic synthetic failure. If this develops, coagulopathies may occur (Cerquetella et al. 2012). Dogs with liver disease traditionally were thought to be hypocoagulable as they can have prolonged clotting times (prothrombin and activated partial thromboplastin), hypofibrinogenemia, and mild to moderate thrombocytopenia (Poldervaart et al. 2009; Prins et al. 2010; Shih et al. 2007). Despite this, spontaneous bleeding is rare (Fry et al. 2017). In a recent study, dogs with CH

were found to have variable TEG results (Fry et al. 2017). In this study of 21 dogs, five were hypocoagulable, nine were normocoagulable, and seven were hypercoagulable. In a retrospective study of canine portal vein thrombosis hepatic disease was a common concurrent condition, suggesting that hypercoagulability may have clinical consequences in these patients (Respess et al. 2012).

A severe complication in human patients with liver cirrhosis and ascites is the hepatorenal syndrome, which has a very poor prognosis. The definitive treatment in humans is liver transplantation (Dundar and Yilmazlar 2015). And also in cirrhotic dogs with ascites, impairment of renal function due to low renal perfusion has been reported (Strombeck and Guilford 1990).

2.2.3 Pathophysiology of Hepatic Fibrosis

Hepatic fibrosis and myofibroblasts

Hepatic fibrosis is a wound healing response to chronic injury and inflammation with an imbalance between ECM deposition and removal, leading to excess ECM accumulation (Ramachandran and Iredale 2012). In the normal liver, fibril-forming collagens (type I, III, V, and XI collagens) can be found in the capsule, in large vessels, and the portal regions (Friedman 2007). Only small amounts of type I and III collagen are present in the subendothelial space. Additional components of the normal ECM include glycosaminoglycans and proteoglycans (e.g., hyaluronan, fibronectin, tenascin or laminin) and other collagens (type VI, XIV, and XVIII) (Friedman 2007). In human patients and rodent models of liver disease, early deposition of ECM components takes place along the subendothelial space (Bircher 1999; Friedman 2007). In humans, von vWF expression is used as a marker of this process and expression of vWF, varying in distribution from diffuse to periportal, was also found in 69 % of dogs with chronic liver disease (Vince et al. 2016).

The main mechanism of fibrogenesis is the activation of myofibroblast precursor cells, which results in the progressive deposition of ECM. Several cells have been reported to be sources of ECM production during hepatic fibrosis: HSCs, liver resident fibroblasts (portal or centrilobular), epithelial cells that undergo epithelial-to-mesenchymal transition, bone marrow-derived fibrocytes, and smooth-muscle cells that surround blood vessels (Gressner et al. 2008; Pinzani and Rombouts 2004). In human patients, hepatic stellate cells are generally believed to be the main source for myofibroblasts in CH, while portal fibroblast are considered to play an important fibrogenic role in cholestatic liver disease (Crosas-Molist and

Fabregat 2015; Iwaisako et al. 2014). Evidence suggests that also in dogs perisinusoidal HSCs are involved in the pathogenesis of hepatic fibrosis (Boisclair et al. 2001).

The transdifferentiation of quiescent HSCs to myofibroblasts is a multi-step process that involves cytokines/chemokines, growth factors, ROS, and apoptotic bodies derived from hepatocytes (**Figure 2**) (Czaja 2014; Friedman 2008; Mallat and Lotersztajn 2013; Friedman 2007). In the early phase of activation, the HSC acquires responsiveness to cytokine stimuli by exposure to fibronectin or apoptotic bodies derived from damaged hepatocytes (Friedman 2008). In the next phase, cytokines and growth factors, produced by neighboring cells such as liver resident macrophages, hepatocytes, endothelial cells, lymphocytes, and platelets, bind to specific receptors on the HSC membrane. Stimulation of intracellular signaling pathways results in altered gene expression and a phenotypic change of the HSC (Friedman 2007). The last phase is the maintenance of activation, which involves paracrine and autocrine mechanisms (Friedman 2008).

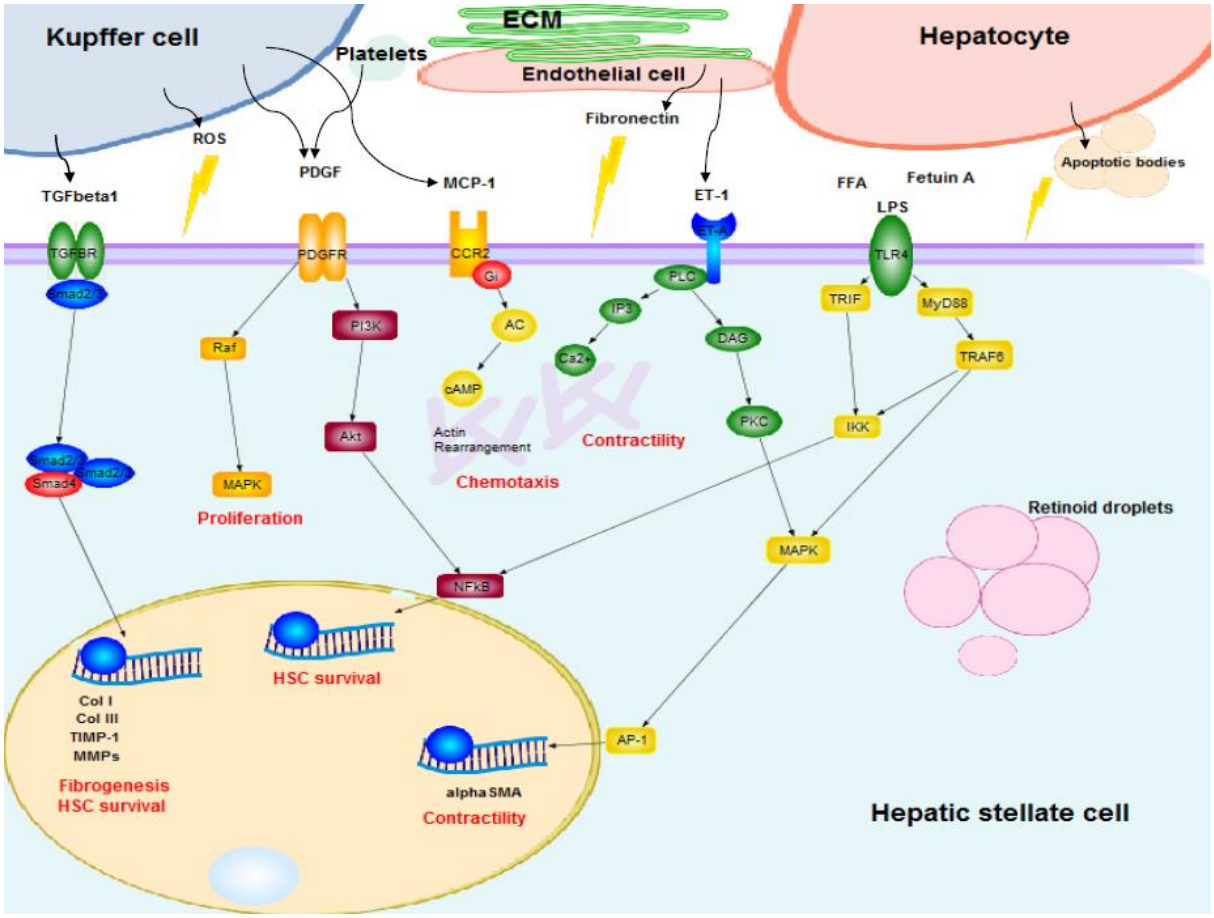

Figure 2: Mechanisms of Hepatic Stellate Cell Activation. Major mediators of HSC activation, involved signaling pathways, and the effect on HSCs.
Abbreviations: HSC: hepatic stellate cell; TGFβ-1: transforming growth factor beta 1; ROS: reactive oxygen species; PDGF: platelet derived growth factor; MCP-1: monocyte chemoattractant protein-1 (CCL2); ECM: extracellular matrix; ET-1: endothelin-1; FFA: free fatty acids; LPS: lipopolysaccharide; TGFBR: transforming growth factor beta receptor; PDGFR: platelet derived growth factor receptor; CCR2: C-C motif chemokine receptor type 2; ET-A: endothelin-1 receptor type A; TLR4: toll-like receptor 4; Smad: smad protein; Raf: raf-1 protein; PI3K: phosphatidylinositol-3-kinase; Gi: inhibitory G protein; AC: adenylate cyclase; PLC: phospholipase C; IP3: inositol 1,4,5-trisphosphate; DAG: diacylglycerol; TRIF: TIR-domain-containing adapter-inducing interferon-β; MyD88: myeloid differentiation primary response gene 88; MAPK: mitogen-activated protein kinase; Akt: protein kinase B; cAMP: cyclic adenosine monophosphate; Ca2+: calcium ion; PKC: protein kinase C; IKK: IκB kinase enzyme complex; TRAF6: TNF receptor associated factor 6; NFκB: nuclear factor kappa B; AP-1: activator protein-1 transcription factor; Col I: collagen type I; Col III; collagen type III; TIMP-1: tissue inhibitor of metalloproteinases 1; MMPs: matrix metalloproteinases. Figure generated with http://www.cellillustrator.com).

Myofibroblast precursor cells

Hepatic stellate cells have a dendritic morphology and are located in the perisinusoidal space in close contact with hepatocytes and sinusoidal endothelial cells. Upon activation HSCs change from their quiescent vitamin A-rich state to a highly fibrogenic (myofibroblastic) phenotype. This is characterized by diminution of vitamin A droplets, enlargement of the rough endoplasmatic reticulum, a ruffled nuclear membrane, and the appearance of contractile filaments (Friedman 1993; Friedman 2008; Gressner et al. 2008;

Friedman 2007). They acquire an increased ability for proliferation, chemotaxis, contractility, and ECM production. Activated HSCs can further promote their myofibroblastic phenotype and survival by paracrine and autocrine cytokine cross-talk with surrounding cells (e.g., the secretion of chemokine (C-C motif) ligand (CCL) 2 or 5 or the release of tissue inhibitor of metalloproteinase-1 (TIMP-1)) (Friedman 2008). The increased contractility of activated HSCs is due to the expression of the cytoskeletal protein alpha-smooth muscle actin (αSMA) (Friedman 2007). Regulators of HSC contractility include endothelin-1, nitric oxide, and angiotensin II (Oakley et al. 2009; Friedman 2007). A specific tissue marker for activated canine hepatic stellate cells has not been discovered yet.

Portal fibroblasts are located in the mesenchyma of the portal tracts. They surround the hepatic bile ducts and are important for the integrity of the portal triads (Washabau and Day 2013). In human biliary fibrosis, portal fibroblasts seem to be the source of myofibroblasts in the portal area (Lua et al. 2016). In rodent studies with bile duct ligated-induced fibrosis, it has been shown that they contribute to >70 % of matrix deposition during early injury (Iwaisako et al. 2014). However, their contribution during more advanced disease is still controversial and newer studies suggest that HSCs are the major collagen producing cells in both biliary and non-biliary fibrosis (Wells 2014). Nevertheless, portal fibroblasts seem to have a role in vascular remodeling during advanced fibrosis and cirrhosis (Lemoinne et al. 2015; Lemoinne et al. 2016). Activated portal fibroblasts express thymocyte differentiation antigen 1, mesothelin, fibulin-2, elastin, the alpha 1 chain of collagen type XV, as well as ectonucleoside triphosphate diphosphohydrolase 2 (Karin et al. 2016; Lua et al. 2016).

Epithelial-to-mesenchymal transition is a process where epithelial cells acquire mesenchymal features (Kalluri and Weinberg 2009). It has been recognized that epithelial-to-mesenchymal transition can occur through hedgehog or transforming growth factor beta-1 (TGFβ-1) signaling pathways and that both cholangiocytes and hepatocytes can undergo this process (Choi et al. 2011; Omenetti et al. 2011; Omenetti and Diehl 2011; Sancho et al. 2012). However, newer studies show that there is no evidence of cholangiocyte or hepatocyte epithelial-to-mesenchymal transition in mouse models of hepatic fibrosis (Chu et al. 2011; Taura et al. 2010). Therefore, epithelial-to-mesenchymal transition is not thought to play a major role in the pathogenesis of hepatic fibrosis.

Mediators of myofibroblast precursor cell activation

Platelet-derived growth factor. Early ECM changes (e.g., the production of fibronectin by endothelial cells) and apoptotic bodies from damaged hepatocytes are initiators of HSC activation (**Figure 2**) (Friedman 2008; Friedman 2007). Hepatic stellate cells acquire responsiveness to further paracrine activation by neighboring cell types via expression of certain cell surface receptors (Friedman 2008; Friedman 2007). Platelet-derived growth factor (PDGF) is the most potent factor that induces proliferation of HSCs (Borkham-Kamphorst et al. 2007; Borkham-Kamphorst and Weiskirchen 2016; Friedman 2007). It is released by platelets, but also by sinusoidal endothelial cells, activated liver resident macrophages, and myofibroblasts during ongoing disease (Gressner et al. 2008; Pinzani and Marra 2001; Friedman 2007). Downstream signaling involves the Ras/ERK (extracellular signal-regulated kinase) and phosphoinositol 3-kinase-pathways, which enhance proliferation and migration, and promote survival of the HSC (Lechuga et al. 2006; Pinzani and Marra 2001). Additionally, PDGF, as chemoattractant, guides HSCs to the site of injury (Friedman 2007; Seppa et al. 1982). Increased expression of PDGF mRNA has been demonstrated in liver from dogs with CH (Kanemoto et al. 2011).

Transforming growth factor beta-1. Fibrogenesis in HSCs is mediated by TGFβ-1 (Friedman 2008; Friedman 2007). Transforming growth factor beta-1 is considered to be the major factor accelerating hepatic fibrosis (Inagaki and Okazaki 2007). Hepatocytes, liver resident macrophages, sinusoidal endothelial cells, platelets, and activated HSCs all produce TGFβ-1 (Gressner et al. 2008). Downstream signaling involves phosphorylation and thus activation of the Smad2 and Smad3 proteins (Inagaki and Okazaki 2007). After forming complexes with Smad4 proteins, they are translocated to the nucleus where they interact directly on Smad-binding elements and alter gene expression for example, causing upregulation of collagen type I and III, and TIMP-1, and downregulation of matrix metalloproteinases (MMPs) (Inagaki and Okazaki 2007; Pinzani and Marra 2001; Pinzani and Rombouts 2004). The result is an increased capability of HSCs to produce ECM components and the inhibition of ECM removal. Transforming growth factor beta-1 also seems to be an important mediator of lysyl oxidase expression. Lysyl oxidases are copper dependent amine oxidases that are important for cross-linking of ECM proteins and further activation of myofibroblast precursor cells (Perepelyuk et al. 2013). Transforming growth factor beta-1 and phosphorylated Smad2/3 expression were shown to be upregulated in the liver of dogs with CH, lobular dissecting hepatitis, and cirrhosis (Spee et al. 2006). Serum concentrations were increased in dogs with moderate to severe hepatic fibrosis (Neumann et

al. 2008). Increased TIMP-1 mRNA expression has also been demonstrated in liver from dogs with CH (Dirksen et al. 2017; Kanemoto et al. 2011).

Connective tissue growth factor. Connective tissue growth factor (CTGF) is another fibrogenic signal for HSCs. It is involved in promoting the adhesion of HSCs to the ECM (Gao and Brigstock 2004; Friedman 2007). It has been shown that CTGF is increased in the fibrotic human liver and in animal models of hepatic fibrosis (Kovalenko et al. 2009). Connective tissue growth factor production is considered to be TGFβ-1/Smad2/3-dependent, but other induction ways have been reported (e.g., by endothelin-1 or angiotensin II) (Kemp et al. 2004; Kiryu et al. 2012; Sferra et al. 2017). As CTGF is recognized as profibrogenic mediator, its inhibition could be an interesting option for new antifibrotic therapies (Blom et al. 2002; Sferra et al. 2017). Also, CTGF has been evaluated as noninvasive biomarker in human patients with chronic hepatitis (Dendooven et al. 2011; Kovalenko et al. 2009). Patients with advanced disease showed higher serum levels of CTGF and this was linked to the stage of fibrosis (Dendooven et al. 2011; Kovalenko et al. 2009).

Endothelin-1. Endothelin-1 is a vasoactive peptide produced by endothelial cells and by activated HSCs in human cirrhotic livers (Friedman 2008; Pinzani et al. 1996). Endothelin-1 acts through the two receptors: endothelin-1 receptor type A and endothelin-1 receptor type B, which can be found on quiescent and activated HSCs (Pinzani et al. 1996). This promotes proliferation, contraction, and the maintenance of the activated state (Friedman 2008; Rockey et al. 1998).

Reactive oxygen species, such as superoxide anion, hydrogen peroxide, or hydroxyl radicals are generated by the “respiratory burst” of phagocytic cells of the innate immune system as a first defense mechanism against invading pathogens (Alfadda and Sallam 2012; De Minicis and Brenner 2007). But, excessive production of ROS leads to necrosis of surrounding cells and inflammation. The healthy liver contains several enzymatic and non-enzymatic antioxidant systems to detoxify excessive ROS. During liver disease, these antioxidant systems can become depleted, which intensifies inflammation. Reactive oxygen species formation by phagocytic cells (e.g., liver resident macrophages) is mainly the result of the enzyme nicotinamide adenine dinucleotide phosphate oxidase (NOX) 2. Besides NOX2, six other members of the NOX family have been identified so far: NOX1, NOX3, NOX4, NOX5, dual oxidase 1, and dual oxidase 2. Some of these have been shown to play a role in liver fibrosis: HSCs and hepatocytes express NOX2, NOX1, NOX4, dual oxidase 1, and dual oxidase 2, which may play a role in the maintenance of the activated HSC state (Crosas-Molist and Fabregat 2015; De Minicis and Brenner 2007; Liang et al. 2016; Sancho

et al. 2012). In human patients with cirrhosis, it has been shown that NOX1 and NOX4 proteins are increased (Lan et al. 2015). Moreover, NOX4 expression showed a correlation with the stage of fibrosis (Bettaieb et al. 2015; Sancho et al. 2012). Knocking down NOX4 in mouse models has been shown to attenuate HSC activation and reverse the myofibrotic phenotype (Lan et al. 2015; Sancho et al. 2012). Although oxidative stress plays an important role in a variety of canine and feline hepatobiliary diseases (Center et al. 2002), its role in fibrogenesis has not yet been studied.

Renin angiotensin system. The local renin angiotensin system (RAS) may play a role in the pathogenesis of hepatic fibrosis (Lubel et al. 2008). A simplified view of the RAS is to describe it in two axis: the ACE/angiotensin II/angiotensin II receptor type I-axis (pathway A), and the ACE/angiotensin (1-7)/angiotensin (1-7) receptor-axis (pathway B) (Santos et al. 2013). The first step in both axes is the cleavage of angiotensin I to angiotensin II by ACE. In pathway A, angiotensin II binds to angiotensin II receptor type I, activating profibrotic mechanisms (e.g., the induction of TGFβ-1) (Liu et al. 2008). In pathway B, a second enzyme (ACE2) cleaves angiotensin II, which results in the formation of angiotensin (1-7). The G-protein coupled Mas receptor has been recognized as the main receptor for angiotensin (1-7), and binding of angiotensin (1-7) to Mas seems to activate a counter-regulatory pathway with antifibrotic, antiinflammatory, and vasodilatory effects (Santos et al. 2013). Cultured activated human HSCs have been shown to express RAS components and synthesize angiotensin II (Bataller et al. 2003), which has been proposed to be a trigger for the profibrogenic mediator CTGF (Kiryu et al. 2012). In rodent models angiotensin (1-7) treatment, and thus enhancement of the antifibrotic RAS pathway, has been shown to reduce hepatic fibrosis (Lubel et al. 2009; Pereira et al. 2007). Furthermore, the administration of ACE inhibitors or angiotensin receptor blockers, which leads to the inhibition of the profibrotic RAS pathway, have been shown to attenuate hepatic fibrosis (Jonsson et al. 2001; Kurikawa et al. 2003; Lubel et al. 2008).

Reversibility of hepatic fibrosis

In the past, hepatic fibrosis was thought to be an irreversible process. However, more recent studies in humans and rodent models have shown that resolution of fibrosis, even in more advanced disease, is possible (Issa et al. 2004; Ramachandran and Iredale 2012; Friedman 2007). In contrast, dense cirrhosis with intense ECM cross-linking, nodule formation, and low cell density in the “fibrotic scars” is still considered irreversible (Issa et al. 2004; Friedman 2007). Several studies have shown that fibrosis regression takes place

after specific treatment and removal of the causing agent in human patients (Ramachandran et al. 2015). As fibrosis is now recognized as continuous remodeling process, where either net collagen deposition or resolution takes place (Younis et al. 2016), inhibiting mediators of collagen deposition or enhancing mediators of ECM degradation may result in the regression of fibrosis. The balance between MMPs and TIMPs seems to play an important role in this regulation process (Ramachandran and Iredale 2012). Tissue inhibitor of matrix metalloproteinase-1 overexpression has been shown to accelerate fibrosis due to inhibition of metalloproteinases, but also due to inhibition of HSC apoptosis. Tissue inhibitor of matrix metalloproteinase-1 activity decreases quickly during fibrosis resolution (Benyon et al. 1996; Iredale 2007; Iredale et al. 1996; Iredale et al. 1992; Pellicoro et al. 2012). Monocyte-derived macrophages with a pro-resolution phenotype seem to be important in the reversal of fibrosis, as they produce MMPs, which degrade the ECM or mediate apoptosis of myofibroblasts (Iredale 2008; Ramachandran and Iredale 2012; Wynn and Vannella 2016). Additionally, natural killer cells (NK cells) can induce apoptosis of HSCs and thus contribute to the inhibition of fibrosis. The main mechanism for the resolution of fibrosis seems to be the apoptosis or senescence of activated myofibroblasts (HSCs), which removes the source of TIMP-1, resulting in increased matrix metalloproteinase activity and the degradation of ECM.

2.2.4 Diagnosis

Histopathology. For definitive diagnosis of CH and hepatic fibrosis, histopathological examination of a liver biopsy specimen is required. However, liver biopsy is expensive and associated with a risk of hemorrhage and other complications (e.g., post biopsy pain, peritonitis, shock, or complications related to general anesthesia) (Bigge et al. 2001; Lidbury 2017). In small animal medicine the following liver biopsy techniques are used: ultrasound-guided percutaneous needle biopsy, laparoscopic biopsy, and surgical biopsy during laparotomy. No matter which technique is used, only a small portion of the organ is sampled. Since many lesions (including fibrosis) are heterogeneously distributed throughout the hepatic parenchyma, liver biopsy is susceptible to sampling error (especially when determining the fibrotic stage) (Bedossa et al. 2003; Kemp et al. 2015). There can be substantial variation in the distribution of lesions between liver lobes and therefore it is important to collect samples from several lobes (Kemp et al. 2015). In addition, it is recommended that pathologists should be presented with specimens containing at least 11

portal triads (Cholongitas et al. 2006; Rothuizen and Twedt 2009). Evaluation of samples with fewer portal triads than this resulted in underestimation of the fibrosis stage in human patients (Bedossa et al. 2003; Colloredo et al. 2003).

In human patients, histological scoring schemes are widely used to provide a more objective assessment in patients with CH. They assess hepatic necrosis and inflammation (grade), which gives an indication of disease activity and fibrosis (stage) and provides information about the chronicity of the disease (Goodman 2007). These schemes include the Ishak scheme (Ishak et al. 1995) and the simpler METAVIR scheme (Bedossa and Poynard 1996). In general, schemes with fewer levels are more clinically applicable as there is usually better interobserver agreement (Goodman 2007). Several studies have used a scoring scheme adapted from the Ishak scheme (Van den Ing 2016) to stage hepatic fibrosis in dogs with chronic hepatitis (Fieten et al. 2014; Fieten et al. 2013). When six board-certified veterinary pathologists used this scheme to stage hepatic fibrosis from picrosirius red stained sections in 50 dogs, they were in complete agreement in 53.0 % of the time, differed by 1 score level in 42.3 % of the time, and differed by more than 1 score level in 4.7 % of the time. In conclusion, agreement was interpreted as being fair (Lidbury et al. 2017). However, the hope is that the scheme can be refined to improve interobserver agreement. Before applicable in clinical patients, it is also important to demonstrate its prognostic significance.

While fibrosis may be apparent on hematoxylin and eosin stained sections (**Figure 3**), there are other histological stains that differentially stain collagen fibers and allow a better assessment of fibrosis. These include Masson's trichrome which stains type I collagen fibers, picrosirius red (**Figure 3**) that stains type I and III collagen fibers, and reticulin which stains reticulin fibers (type III collagen) (Lidbury 2017).

Computerized image analysis has been used to provide quantification of hepatic fibrosis in humans (Chevallier et al. 1994; Pilette et al. 1998). This technique entails differentially staining of collagen fibers with a histochemical stain such as picrosirius red. The histological section is then digitized, and image analysis software is used to calculate the fibrotic proportion of the section. This technique does not detect key features in the progression of fibrosis, such as the development of bridging fibrosis, therefore it should not be considered to be a direct replacement for the histological assessment of fibrosis (Chevallier et al. 1994).

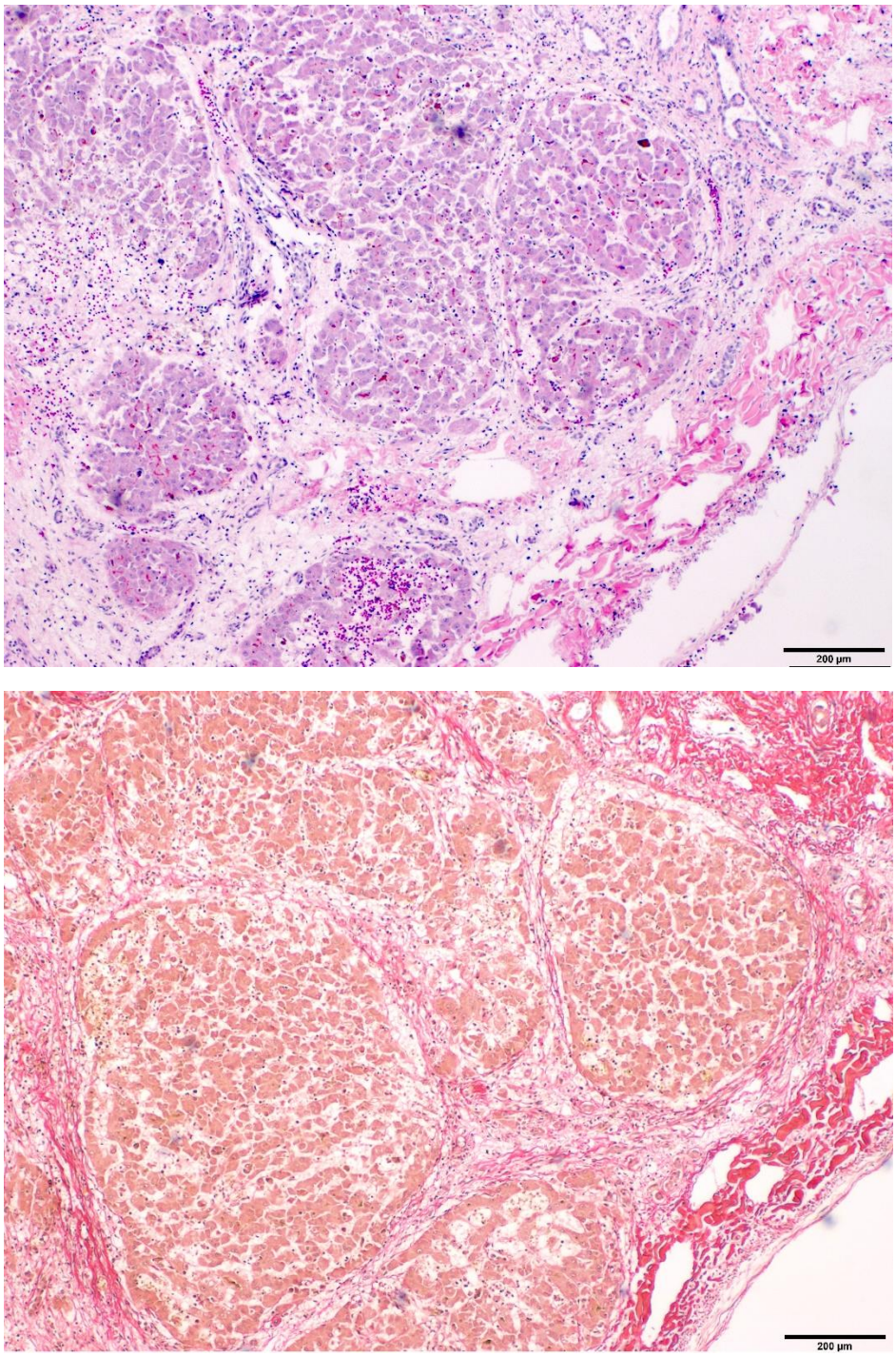

Figure 3: Hepatic Fibrosis in a Dog with CH. Hepatic fibrosis has progressed to fibrosis stage four ('very marked') with nodule formation. **a** Hematoxylin & eosin. **b** Picrosirius red.

Serum biomarkers. Because of the disadvantages of liver biopsy described above, serum markers of hepatic fibrosis have been developed for use in humans. In general, biomarkers of hepatic fibrosis can be divided into direct and indirect markers (Plebani and Basso 2007). Direct markers are proteins and other molecules involved in the pathogenesis pathways of fibrosis (e.g., TGFβ-1, tumor necrosis factor-α, angiotensin II) or those involved in the degradation or remodeling of the ECM (e.g., hyaluronic acid, procollagen peptides, MMPs, TIMPs, chitinase-3-like protein 1). With some of these markers, accurate diagnosis of advanced fibrosis stages is possible (Pereira et al. 2004; Plebani and Basso 2007). Hyaluronic acid appears to be the most promising (Plebani and Basso 2007), for example in a meta-analysis of hepatitis C patients the sensitivity and specificity for diagnosing cirrhosis were 82 % and 89 %, respectively (El Serafy et al. 2017). In human patients, these direct markers of fibrosis are not specific to hepatic fibrosis and may be increased when fibrosis of other organs occurs (Baranova et al. 2011). Some of these serum markers have been evaluated in dogs. Serum hyaluronic acid concentrations are increased in dogs with hepatic disease, especially cirrhosis and therefore this molecule holds some promise as a biomarker (Glinska-Suchocka et al. 2015; Kanemoto et al. 2009). Serum concentrations of TGFβ-1 (Neumann et al. 2008), the 7S fragment of type IV collagen (Glinska-Suchocka et al. 2016b), and procollagen type III N-terminal peptide (Glinska-Suchocka et al. 2016a) have also been found to be increased in dogs with hepatic fibrosis. Contradictorily, another study did not find a positive correlation between hepatic fibrosis and serum concentrations of hyaluronic acid, procollagen type III N-terminal peptide, or TIMP-1 (Lidbury et al. 2016). However, different assays were used in these studies, and in the latter study fewer dogs had advanced fibrosis. But, even in the studies that did detect a difference between groups of dogs, values from the advanced liver fibrosis groups either overlapped with those from dogs with milder fibrosis or there was only a separation of values for dogs with the most advanced stages of hepatic fibrosis.

Indirect markers are the measurement of parameters that indicate liver damage, liver function impairment, and portal hypertension, such as liver enzyme activities, albumin, bilirubin, and platelet counts or a combination of those. Two commonly used combinations in human medicine are the aspartate transaminase-to-platelet ratio index and FibroTest (FibroSURE in the Unites States). The latter combines age, gender, and results for serum haptoglobin, alpha 2-macroglobulin, apolipoprotein A1, gamma-glutamyltransferase, and bilirubin analyses into a single index (Imbert-Bismut et al. 2001; Rossi et al. 2003). Recently,

the FibroVet test (Echosens) was developed for use in dogs. This index combines patient age, gender, and several biochemical parameters in a proprietary algorithm to create a fibrosis score. In a study, reported as an abstract, this index had a negative predictive value for the diagnosis of moderate fibrosis of 90 – 100 % and distinguished dogs with significant fibrosis with a positive predictive value of 90 – 100 % (Lecoindre A 2015).

MicroRNAs are small non-coding RNAs that have a distinct expression profile depending on the liver disease (Arrese et al. 2015; Lidbury 2016). Liver levels of hepatocyte derived microRNAs seem to correlate with serum levels (Arrese et al. 2015; Murakami et al. 2012). In human patients with hepatic fibrosis, expression of miR-29 and miR-652 are decreased, while expression of miR-571 is increased (Roderburg et al. 2012; Roderburg et al. 2011). A recent study evaluated whether serum miRNA biomarkers hold promise for distinguishing between several hepatobiliary diseases in dogs. Two miRNAs were found to be increased in two groups of hepatobiliary disease; miR-200c in the hepatocellular carcinoma group (six dogs) and miR-126 in the CH group (six dogs) (Dirksen et al. 2016). It is possible that measurement of microRNAs in serum could be used to assess hepatic fibrosis in dogs and cats. However, further studies with greater sample sizes are needed to evaluate the sensitivity and specificity of these markers.

Elastography. Elastography is a medical imaging method to measure soft tissue elasticity (stiffness). Liver stiffness reflects the accumulation of ECM and has been shown to correlate with fibrosis stage. Transient elastography (FibroScan), real-time shear wave elastography and acoustic radiation force impulse are new ultrasound-based, reliable, and reproducible methods to assess liver fibrosis in humans (Friedman 2010; Sporea et al. 2013). These techniques are non-invasive and allow a large area of the hepatic parenchyma to be sampled, thus reducing sampling error. For example, transient elastography has been shown to sample a volume that is 100 times bigger than a typical needle biopsy specimen (Ferraioli et al. 2014). Methods such as shear wave elastography and acoustic radiation force impulse have also been shown useful in patients with ascites or in obese patients (Ferraioli et al. 2014; Sandrin et al. 2003). Magnetic resonance elastography measures quantitatively acoustic shear waves in liver tissue. This method also detects early fibrosis stages with a much higher sensitivity and specificity (98 % and 99 %) than transient elastography. A disadvantage of this methods are the higher costs compared to ultrasound based techniques (Baranova et al. 2011). The utility of elastography for the diagnosis of hepatic fibrosis in dogs or cats has not yet been evaluated.

2.2.5 Treatment

The optimal way to treat CH and resolve hepatic fibrosis is to identify and treat the underlying cause. This is applicable in human medicine, where the underlying cause for the chronic hepatic disease is known (e.g., abstinence in alcoholic liver disease or clearance of hepatitis B or hepatitis C virus in chronic viral hepatitis) (Friedman 2007). In human patients that were treated with direct-acting antiviral agents against hepatitis C, fibrosis resolved (Poelstra 2016).

Treatment of the underlying cause. In dogs with copper associated CH, it is often possible to address the underlying cause of hepatic fibrosis by a combination of chelation with D-penicillamine and feeding a low copper diet. Even if fibrosis does not resolve, chelation therapy is considered to be beneficial in these patients and has been shown to reduce copper accumulation effectively. However, the criteria for which patients to chelate are controversial (Dirksen and Fieten 2017; Fieten et al. 2013).

Antiinflammatory treatment. For dogs with idiopathic CH, treatment with prednisolone or another immunomodulatory drug is often initiated, especially if there is histological evidence of active inflammation. Glucocorticoids bind to glucocorticoid receptors in the cytoplasm. These complexes are translocated to the nucleus, where they act on glucocorticoid response elements and initiate the transcription of antiinflammatory and immunomodulatory protein coding genes (e.g., interleukin 10) (Barnes 1998). Inflammatory genes are under transcriptional control of nuclear factor-kappa B and activator protein-1. Glucocorticoids inhibit the effects of these transcription factors by reversion of histone acetylation at the site of gene transcription (Adcock et al. 2004; Kagoshima et al. 2003). The response of dogs with idiopathic CH to glucocorticoids seems to be quite variable. In a retrospective study of 20 dogs with idiopathic CH that were treated with prednisolone at a dose of 1 mg/kg PO q24 hours for at least six weeks, fibrosis resolved in five dogs, improved in four dogs, and worsened in five dogs, but a statistically significant difference in histological fibrosis scores before and after treatment was not found (Favier et al. 2013). However, in an older retrospective study that did not separate dogs with copper associated CH from those with idiopathic CH, prednisolone treatment was associated with longer median survival times (Strombeck et al. 1988). The effect of prednisolone on fibrosis was not evaluated in this study.

Antioxidant treatment. Antioxidant drugs have a cytoprotective effect by scavenging ROS or increasing tissue concentrations of antioxidant enzymes or proteins such as super

oxide dismutase, catalase, glutathione peroxidase, glutathione, or metallothionein (Webster and Cooper 2009). Oxidative stress occurs in a variety of liver diseases and contributes to the development of hepatic fibrosis in rodent models and humans. Antioxidants used to treat hepatobiliary disease in dogs and cats include S-adenosylmethionine, vitamin E, and silymarin (milk thistle extract). The latter may also inhibit hepatic fibrosis by reducing hepatic stellate cell DNA synthesis, proliferation and migration, and reducing hepatic collagen expression as well having antiinflammatory effects (Hackett et al. 2013; Manna et al. 1999; Trappoliere et al. 2009). Ursodeoxycholic acid is a non-toxic bile acid that has choleretic effects. It displaces hydrophobic bile acids from the circulating pool and is therefore used to treat cholestatic liver disease in dogs and cats (Meyer et al. 1997). There is evidence in other species that ursodeoxycholic acid may also have antiapoptotic properties (Honeckman 2003). The cytoprotective and antiapoptotic effects of ursodeoxycholic acid on hepatocytes have been proposed to be due to unspecific binding to steroid receptors and the upregulation of cellular antioxidant systems, such as glutathione and superoxide dismutase (Sola et al. 2006; Sola et al. 2005). As hepatocyte-derived apoptotic bodies are one mediator for HSC activation, ursodeoxycholic acid seems to be a reasonable treatment to inhibit fibrogenesis. Ursodeoxycholic acid is used to treat primary biliary cirrhosis in humans, although resolution of fibrosis does not consistently occur and other treatments may be needed for advanced disease (Corpechot 2016). Case reports describe the use of ursodeoxycholic acid in dogs with hepatobiliary disease but to our knowledge, there are no studies that critically evaluate its effectiveness in species (Bautista et al. 2015; McGrotty et al. 2003; Meyer et al. 1997; Osumi et al. 2011). Results of a retrospective study of cats with lymphocytic cholangitis showed that treatment with ursodeoxycholic acid was associated with shorter survival times than treatment with prednisolone (Otte et al. 2013). This study did not prove that ursodeoxycholic acid has no beneficial effects when treating this disease and some clinicians use this drug in combination with prednisolone. In this group of cats, treatment with neither medication resulted in an improvement of fibrosis score, although the inflammatory grade has been shown to improve more in cats treated with prednisolone (Otte et al. 2014).

Antifibrotic treatment. Colchicine, a plant extract from *Colchicum autumnale* that acts as a microtubule assembly inhibitor, has been shown to reduce hepatic fibrosis in rodent models (Rodriguez et al. 1998) and also in some human patients with hepatic fibrosis (Nikolaidis et al. 2006). The suggested mechanism is the inhibition of microtubule-associated transport of procollagen and the enhancement of collagenase activity (Muriel et al. 2005;

Rambaldi and Gluud 2005). However, there is insufficient evidence to support its use in humans with liver fibrosis or cirrhosis and it is commonly associated with side effects (Rambaldi and Gluud 2005). There are a few case reports describing its use in dogs (Boer et al. 1984; McAlister et al. 2014), but due to the lack of proven efficacy and relatively common occurrence of side effects (of the gastrointestinal tract and central nervous system), its use is not recommended (Ferguson 1952).

Novel treatment strategies for hepatic fibrosis. Therapeutic strategies, which target pathomechanisms of hepatic fibrosis can be divided into those that reduce myofibroblast activation, those that induce apoptosis of activated myofibroblasts, and those that induce ECM degradation (Friedman 1993). Pirfenidone and ACE inhibitors, for example, could reduce myofibroblast activation by inhibition of profibrogenic signals (e.g., TGFβ-1 or the RAS) (Flores-Contreras et al. 2014; Pereira et al. 2009). Modulation of the TIMP-1/MMP balance or targeting cell surface death receptors can induce apoptosis in HSCs (Iredale 2008). Degradation of the ECM could be achieved e.g., with transglutaminase inhibitors, which inhibit cross-linking of ECM components (Daneshpour et al. 2011; Nikolaidis et al. 2006). However, the testing of promising drugs is still at an experimental stage. Effectiveness has not been proven yet (Pinzani and Rombouts 2004) and currently, no antifibrotic drugs are available in human and veterinary medicine for clinical use.

3. Objectives

3.1 RNA Sequencing and Gene Expression Analysis

The RNA sequencing study aimed to determine differential gene expression in dogs with CH compared to healthy control dogs to elucidate the pathophysiology of chronic hepatic disease in dogs. Differentially expressed genes were characterized according to their associated biological pathways. Furthermore, quantitative polymerase chain reaction (qPCR) was performed to confirm the results of the RNA sequencing analysis for selected genes.

3.2 Immunohistochemistry

The immunohistochemistry study aimed to evaluate expression and distribution of three selected proteins (CYGB; Ki67; TIMP-1) in liver sections of dogs with CH and hepatic fibrosis compared to healthy control dogs. Expression and distribution of these tissue markers were compared to fibrosis scores, picrosirius red staining, and to αSMA expression.

4. Materials and Methods

4.1 RNA Extraction and Sequencing

4.1.1 Animals

Liver biopsy specimens were collected from two groups of dogs that presented to the Veterinary Medical Teaching Hospital at Texas A&M University between 2014 and 2016. The two groups consisted of 16 dogs with CH and 12 healthy control dogs. In the healthy group, a liver biopsy specimen was collected during ovariohysterectomy. For the sampling of liver biopsies informed owner consent was obtained. The study was approved by the Texas A&M University Institutional Animal Care and Use Committee (AUP #2014-0320 and #2015-0043). The diagnosis of CH was established by histopathological examination of a liver biopsy specimen. In the CH group, the hepatic copper content was quantified at Colorado State University by flame atomic absorption spectrometry. Fibrosis was scored by a board-certified veterinary pathologist using a 5-point staging scheme (score 0-4) and picrosirius red stain (Lidbury et al. 2017). Inclusion criteria for the healthy control dogs were the absence of clinically significant abnormalities on physical examination, serum biochemistry panel, complete blood count and urinalysis, no evidence of hepatic disease according to histopathological examination of the liver biopsy specimen, and adult age.

4.1.2 RNA Extraction

Liver biopsy specimens for RNA extraction were collected laparoscopically and stored in RNAlater solution (Ambion®) at -80°C until RNA extractions were performed. Total RNA was extracted using the RNeasy Plus Mini Kit (QIAGEN) according to the manufacturer's instructions. In brief, 15-30 mg of RNAlater-stabilized liver tissue was lysed and homogenized in 600 µl of lysis buffer. The lysate was applied to a gDNA Eliminator spin column to remove genomic DNA, 50 % ethanol was added to the flow through, and 700 µl of this mixture were used per RNeasy spin column. After three washing steps, two elution steps were performed with 50 µl RNAse-free water, which yielded in a total volume of 100 µl, containing the purified total RNA. RNA yield (ng/µl) and purity (OD 260/280, OD 260/230) were determined using the NanoDrop™ 1000 Spectrophotometer (Thermo Scientific) (**supplementary materials, Table S1**). The extracted RNA from each sample was divided

into separate aliquots for RNA sequencing and reverse transcription for qPCR, and stored at -80°C until analysis.

4.1.3 High-throughput RNA Sequencing and Data Analysis

RNA quality control, library preparation, and sequencing were performed by the Texas A&M Genomics Technology and Bioinformatics Services facility on a fee-for service basis. The quality control was done using the fragment analyzer resulting in RNA quality numbers (RQNs), equivalent to the usually reported RNA integrity numbers (RINs), between 6-8.5 (**Table S1**). RNA sequencing was performed with the Illumina HiSeq2500 platform (Illumina, San Diego, USA) using 50 single-end sequencing and four lanes. The reads were aligned against the dog reference genome (Canis lupus familiaris (Boxer) genome, NCBI) and analyzed using the CLC Genomics software (CLC bio, QIAGEN). Genes with an absolute fold change-value between groups >2.5 and a false discovery rate (FDR)-corrected *P*-value <0.05 were considered to be differentially expressed. Genes and transcripts that were differentially expressed and potentially related to the pathogenesis of hepatic fibrosis were selected and subcategorized using the genecards.org databases: GeneCards®, PathCards, and GeneAnalytics™ (Weizmann Institute of Sciences; LifeMap Sciences). Normalized expression values calculated by the CLC Genomics software were used and uploaded to the web-based software 'Morpheus' (https://software.broadinstitute.org/morpheus/) to generate heat maps.

4.1.4 Reverse Transcription and Quantitative Polymerase Chain Reaction

The High-Capacity cDNA Reverse Transcription Kit (Applied Biosystems) was used to generate cDNA. 2X Reverse Transcription Master Mix was prepared according to the manufacturer's instructions (10 µl/reaction). 10 µl of total RNA per reaction was added and reverse transcription was performed in the thermocycler 'Mastercycler® Gradient' (Eppendorf, Germany) using the following protocol: 10 min at 25°C, 120 min at 37°C, 5 min at 85°C, and ∞ at 4°C. For each sample, 20 µl of the obtained cDNA was diluted to a total volume of 100 µl and stored at -20°C until qPCR was performed. qPCRs were performed using Taqman-Probe detection chemistry. Genes were selected for confirmatory testing with qPCR based on significantly differential expression in dogs with chronic hepatitis according

to RNA sequencing and potential biological relevance. Primer and probe design was performed according to the recommendations for Taqman assays and synthesis was performed by Integrated DNA Technologies (IDT, Iowa, USA). Three reference genes (*RPL13A*, *RPL32*, and *HPRT1*) were used for normalization (Peters et al. 2007). Sequences of primers and probes are shown in **Table 3**. Reaction efficiencies (**Table 3**) were determined for each gene-specific primer/probe set with a serial dilution of plasmid DNA generated by cloning of dog liver cDNA in the pT7Blue vector (Perfectly Blunt® Cloning Kit, Novagen®). Cloning success was confirmed with sequencing (Eton Bioscience) to verify the insert. For all reactions, the following incubation protocol was applied: 3 min at 95°C, and 45 cycles of 95°C for 10 s and 52-62°C (depending on the optimal temperature for the primer set) for 15 s. The thermocycler CFX384 Touch™ (Bio-Rad Laboratories) was used for incubation and detection. All qPCRs were carried out in duplicate using '1X SsoAdvanced Universal Probes Supermix' (Bio-Rad Laboratories). The final concentrations in the reaction mix for primers and probes were 0.25 µM (each primer) and 0.15 µM (probe), respectively. 2 µl of a 1:100 dilution of sample cDNA was added to the reaction mix resulting in a final reaction volume of 10 µl. Analysis was carried out with the CFX Manager software (Bio-Rad Laboratories). The fold-change between groups was determined using relative quantification (Livak method) (Livak and Schmittgen 2001).

Table 3: Primer and Probe Sequences used for qPCR Analysis

Gene	Accession Numbers	Forward Primer (5'-3')	Reverse Primer (5'-3')	Probe (FAM 5'-3'ZEN™–Iowa Black® FQ)	Tm °C	E %	R^2
RPL13A	NC_006583.3, NM_001313766.1	GCCGGAAGGTTGTAGTCGT	GGAGGAAGGCCAGGTAATTC	TGTGAAGGCATCAACATTTCTGGCA	79.5	99.8	0.989
RPL32	NC_006602.3, NM_001252169.1	TGGTTACAGGAGCAACAAGAAA	GCACATCAGCAGCACTTCA	TGCTGCCCAGTGGCTTCTGG	82	102.3	0.99
HPRT1	NC_006621.3, NM_001003357.2	CACTGGGAAAACAATGCAGA	ACAAAGTCAGGTTTATAGCCAACA	TGCTGGTGAAAAGGACCCCTCG	80.5	102.6	0.994
TIMP1	NC_006621, NM_001003182	GACGGACACTTGCAGATCAA	GGGATGGATGAACAGGTAAACA	AAGACCTATGCTGCTGGCTGTGAG	86.5	95.9	0.989
CXCL10	NC_006614, NM_001010949	ACGCTGTACCTGTATCAAGATTAG	CATTGTGGCAATGATCTCAACAT	ATTCCTGCAAGTCCATCGTGTCCA	77.5	99.3	0.988
MKI67	NC_006610.3, XM_014108788	GCAGGAGGCGGTATTGTTTA	GATCACATCTCCGTGCTTTAGT	AACGGCTGTGCTATTGATGAGCCT	81	95.7	0.989
MATN3	NC_006599, XM_014120233	CCCACTTCCAACATCCCTAAG	CCCACAGCATACAGCTCAATA	ATCATTGTGACAGACGGGAGGCC	86	99	0.992
CCL5	NC_006591, NM_001003010	GGTCTCTAGGCTCTTGAGTTTC	GTCTTCTTCCCATCTTCGTCTC	TGCAGTCAGGAAGGAGATCAACAAGC	81.5	90	0.989
CHI3L1	NC_006589, NM_001177807.1	TGGAATGATGTCACGCTCTATG	TCTGGGTCTTGGAGGCTATT	ACACGCTGAACACACTCAAGAGCA	81.5	101.5	0.991
ADAMDEC1	NC_006607.3, XM_005635697.2	CTCACATACAACCAGGAGGAAC	TGGGCTATTGAGTGACCTAGA	AGAAATGTTGGCAGGAAGCAAGGC	80	92.4	0.992
CCL2	NC_006591.3, NM_001003297.1	CATGGCACACCTAGACAAGAA	GAGGGCATTTAGGGAAGGTTAG	CCAAACCCAAACTGCAAAGCCATGA	77	100	0.992

Tm: melting temperature (specific for PCR product); E: PCR efficiency (90-110 %); R^2: R square value (coefficient of correlation for standard curve), >0.98.

4.1.5 Statistical Analysis

RNA sequencing data analysis was performed with the CLC Genomics software (CLC bio, QIAGEN) and included empirical analysis of differential gene expression (Robinson and Smyth 2008), which uses the 'Exact Test' to determine significance between groups. The data were corrected for multiple comparisons by controlling the FDR (Benjamini and Hochberg 1995). A *P*-value <0.05 was considered statistically significant. The qPCR results are displayed as mean delta Cq ± SD. A two-tailed t-test was applied at the delta Cq level to determine statistical significance. Significance here was set at a *P*-value of <0.01.

4.2 Immunohistochemistry

4.2.1 Dog Liver Tissue for Immunohistochemistry

Liver biopsy specimens were obtained from dogs with CH and from healthy control dogs. Biopsies were obtained from the same client-owned dogs that participated in the RNA sequencing study and during the same procedure (for dog characteristics see **Table 5** in results section; dogs chosen for the immunohistochemistry study are marked with a red asterisk). Liver biopsy specimens for histopathological and immunohistochemical evaluation were fixed in 10 % neutral buffered formalin, embedded in paraffin, sectioned at a thickness of 4-5 µm, and transferred onto a slide. From the study group (**Table 5**), two CH-dogs of each fibrosis score (score 1-4) and two healthy control dogs (fibrosis score 0) were chosen. Slides with liver sections were stored at 4°C until processing.

4.2.2 Immunostaining of Dog Liver Tissue Sections

Liver sections were deparaffinized in Histosol (Electron Microscopy Sciences, Hatfield PA) and rehydrated in decreasing concentrations of ethanol. The following protocol was applied: Histosol: 3x 4 min, 100 % ethanol: 2x 1 min, 95 % ethanol: 1 min, 80 % ethanol: 1 min, 70 % ethanol: 1 min, and diH_2O: 2x 3 min. After deparaffinization and rehydration, slides were placed in a chamber with 1X DIVA-buffer (Biocare Medical, CA, USA), pH 6.2, and antigen retrieval was performed at a temperature of 121°C using the Antigen Retriever 2100 (Electron Microscopy Sciences, Hatfield PA). Slides were cooled to room temperature and rinsed with 1X PBS. All further steps were carried out at room temperature. For blocking of endogenous peroxidase, slides were incubated in 3 % H_2O_2 for 45 min. Protein blocking and detection was performed with the Vectastain® Universal Quick Kit (Vector Laboratories, CA, USA) in combination with DAB Quanto Chromogen and Substrate (Thermo Scientific, MA, USA). Slides were rinsed with 1X PBS and incubated with prediluted RTU blocking serum of the Vectastain® kit (normal horse serum) for 20 min. All dilutions of primary antibodies were made with the same blocking serum. **Table 4** lists the primary antibodies with applied dilutions and incubation times. After antibody incubation, slides were washed 3x for 5 min in a slide chamber with 1X PBS. Following this step, the prediluted biotinylated pan-specific universal secondary antibody of the Vectastain® Kit was applied for 10 min. Then, slides were again washed 3x for 5 min in a slide chamber with 1X PBS. RTU streptavidin/peroxidase complex reagent (Vectastain® Kit) was applied

for 5 min. Another washing step was performed (3x 5 min in 1X PBS), then DAB substrate with chromogen was prepared (1-drop chromogen in 1 ml of substrate) and the tissue sections were incubated until staining developed. Slides were washed in diH_2O (10 min) and counterstained with filtered Meyer's Hematoxylin (Electron Microscopy Sciences, Hatfield PA) and RTU Bluing Reagent (Thermo Scientific, MA, USA) (3 min hematoxylin; rinsed with diH_2O; 3 min bluing reagent). Dehydration and cleaning of the slides were performed in ascending alcohol concentrations (70 %; 80 %; 95 %; 100 %; 30 s each) and Histosol (4-20 min). The tissue sections were sealed with Cytoseal™60 (Thermo Scientific, MA, USA) and 24x60 mm Coverslips (VWR, Tx, USA). All samples were run in duplicate.

Table 4: Primary Antibodies for Immunostaining of Dog Liver Tissue

Primary Antibody	Species	Source	Dilution	Incubation Time
Anti-human αSMA	Mouse monoclonal	Dako (Clone 1A4)	1:400	45 min
Anti-dog TIMP-1	Rabbit polyclonal	Cloud Clone Corp.	1:400	1 h
Anti-human Ki-67	Mouse monoclonal	eBioscience™ (Clone 20Raj1)	1:400	1 h
Anti-human CYGB	Mouse monoclonal	Invitrogen (Clone 3A5-2D2)	1:200	1 h

αSMA: alpha-smooth muscle actin; min: minute; TIMP-1: tissue inhibitor of metalloproteinase-1; h: hour; Ki-67: antigen identified by monoclonal antibody Ki-67; CYGB: cytoglobin.

4.2.3 Analysis of Stained Sections

Sections were evaluated for location and distribution of staining and a semi-quantitative analysis was performed for the amount of staining present. Slides were scanned and digitalized with the NanoZoomer 2.0 HT (Hamamatsu Photonics, Japan) at 40x magnification and images were taken with the NDP.view 2 software (Hamamatsu Photonics, Japan). For every slide, 10 fields were evaluated at a magnification of 10x for measurement of the stained area in % (picrosirius red; αSMA), and at a magnification of 20x for cell counting (TIMP-1; Ki-67; CYGB). Analysis was performed with the free software ImageJ (https://imagej.nih.gov/ij/index.html).

4.2.4 Statistical Analysis

To determine significance between groups of samples a student's t-test was applied. Significance was set at a *P*-value <0.05. Either the Pearson or the Spearman correlation coefficient was calculated to assess each stain in relation to the fibrosis scores.

5. Results

5.1 RNA Extraction and Sequencing

5.1.1 Dog Characteristics

The 16 CH-dogs included five Labrador retrievers, two Doberman pinschers, one Viszla, one German shepherd, one Labradoodle, one Toy poodle, one German shorthaired pointer, one Rat terrier, one American cocker spaniel, one Bichon frise, and one Rottweiler. Ages ranged from 3-14 years with a median age of 7.5 years. The group included seven spayed-females, two intact females, four neutered males, and three intact males. Seven of the CH-dogs had copper levels higher than 700 ppm (median: 818.5 ppm; range: 701–1,540 ppm; normal: < 400 ppm) and in five of these dogs, copper was also evident in the histopathological examination (rhodanine stain). Fibrosis scores ranged from 0-4 (absent; mild; moderate; marked; very marked) (**Table 5**). Only six of the original twelve healthy control dogs were included in the comparison to make the age ranges of the groups closer (healthy dogs <1 year of age were excluded). The six healthy female dogs included one Flat coated retriever, one Border collie, one Greyhound, one American Staffordshire terrier, one Treeing walker coonhound, and one Chihuahua. Ages of the six included dogs ranged from one year to six years with a median of 4 years. Fibrosis was not observed in samples from the control dogs (score 0). Characteristics of the dogs are summarized in **Table 5**.

Table 5: Dog Characteristics

Dog (CH)	Breed	Age (years)	Sex (F/FS/M/CM)	Fibrosis Score (0-4)	Copper Level (ppm)	Dog (H)	Breed	Age	Sex
1*	Labrador retriever	11	FS	1	normal	1*	Crossbreed	6 months	F
2*	Viszla	3	F	4	normal	2	Labrador retriever	8 months	F
3	Labrador retriever	11	FS	3	407	3*	Flat Coated retriever	5 years	F
4	German shepherd	7	FS	3	1530	4	Australian shepherd	6 months	F
5*	Labrador retriever	7	CM	1	1540	5	Crossbreed	8 months	F
6	Labrador retriever	8	M	2	777	6*	Border collie	2 years	F
7*	Labradoodle	11	FS	2	1230	7*	Greyhound	6 years	F
8	Toy poodle	3	M	0	normal	8*	American Staffordshire terrier	5 years	F
9	Labrador retriever	13	FS	2	716	9*	Treeing walker coonhound	3 years	F
10	German shorthaired pointer	4	FS	1	701	10	Catahoula hog dog	6 months	F
11*	Doberman pinscher	6	CM	3	normal	11*	Chihuahua	>1 year	F
12*	Rat terrier	14	CM	3	normal	12*	Crossbreed	6 months	F
13*	Doberman pinscher	5	M	2	normal				
14	American cocker spaniel	4	CM	2	860				
15	Bichon frise	10	F	3	normal				
16*	Rottweiler	9	FS	4	normal				

CH = chronic hepatitis; H = healthy; F = female; FS = female spayed; M = male; CM = castrated male; ppm = parts per million; *included in RNA sequencing study. All control dogs had a fibrosis score of 0. Copper concentration was considered normal when < 400 ppm. *included in immunohistochemistry study.

5.1.2 RNA Sequencing Data Analysis

Genome-wide analysis of RNA sequencing data revealed that 651 genes (and 1,136 transcripts) were significantly differentially expressed in dogs with chronic hepatitis compared to the control group. The expression profiles for all 651 genes and the transcriptional profiles for all 1,136 transcripts can be found in the supplementary material (**supplementary materials, Table S2 & S3**). According to the analysis with the genecard.org databases, 190 of these genes are associated with mechanisms involved in fibrosis. A heat map presentation for the 190 genes and each individual sample is shown in **Figure 4** and a list of these genes with their expression profiles and transcripts is given in **Table 6.** The 190 fibrosis-related genes were further subgrouped according to the five pathway categories they are involved in: i) hepatic stellate cell (HSC) activation; ii) ECM organization; iii) ECM degradation; iv) apoptosis- or NF-κB-related pathways, and v) detoxification of ROS (**Table 6**). One-hundred-and-sixty-five (86.8 %) of these genes were upregulated and 25 (13.2 %) were downregulated. **Figure 5** gives an overview of the percentages of genes that were assigned to each group (HSC activation: 46 %; ECM organization: 25 %; ECM degradation: 10 %; apoptosis: 18 %, and detoxification of ROS: 1 %). Some genes could be assigned to more than one group.

Significant differentially expressed genes that could be assigned to HSC activation pathways are, for example, genes for growth factors: *PDGFD* (FC +4.2), *VEGFA* (FC -3.2), *CTGF* (FC +2.6), genes for chemokines: *CXCL10* (FC +19.1), *CCL5* (FC +13.8), *CCL2* (FC +8.4), *CCL21* (FC +3.1), genes for chemokine receptors: *CX3CR1* (FC +7.1), *CCR1* (FC +3.9), *CCR5* (FC +3.8), the gene for the proliferation marker *MKI67* (FC +10.0), and the gene for renin *REN* (FC -4.9). Upregulated genes that demonstrate ECM remodeling are the collagen genes: *COL1A1* (FC +5.7), *COL16A1* (FC +3.7), *COL6A1* (FC +3.6), *COL6A2* (FC +3.4), *COL2A1* (FC +3.1), *COL12A1* (FC +3.0*), COL15A1* (FC +3.0), *COL23A1* (FC +3.0), *COL3A1* (FC +3.0), *COL8A1* (FC +3.0), *COL1A2* (FC +2.6), the genes for chitinase 3 like 1 and matrilin 3, *CHI3L1* (FC +35.9) and *MATN3* (FC +10.7), and the genes for matrix remodeling enzymes or the inhibitors of those: *ADAMDEC1* (FC +45.7), *TIMP1* (FC +11.8), *MMP9* (FC +9.9), *MMP*2 (FC +7.2), *FAP* (FC +8.1), *ADAM28* (FC +3.7), *ADAMTS12* (FC +2.5). Genes for proteins involved in the NF-kB pathway can influence HSC survival. Apoptosis of hepatocytes and generation of apoptotic bodies contribute to the HSC activation

process. Genes possibly connected to apoptotic mechanisms and with altered expression in this analysis were e.g., *NFKBIZ* (FC -2.9), *MAPK8IP3* (FC -3.5), *GSN* (FC +3.2), or *IL33* (FC -2.9). Cytoglobin is an interesting protein involved in ROS scavenging and detoxification in HSCs (Yoshizato et al. 2016). The *CYGB* gene was upregulated (FC +3.4) in dogs with CH. Eight of these genes (*ADAMDEC1; CHI3L1*; *CXCL10*; *CCL5*; *TIMP1*; *MATN3*, *MKI67*, and *CCL2*) were selected for further confirmatory testing by qPCR.

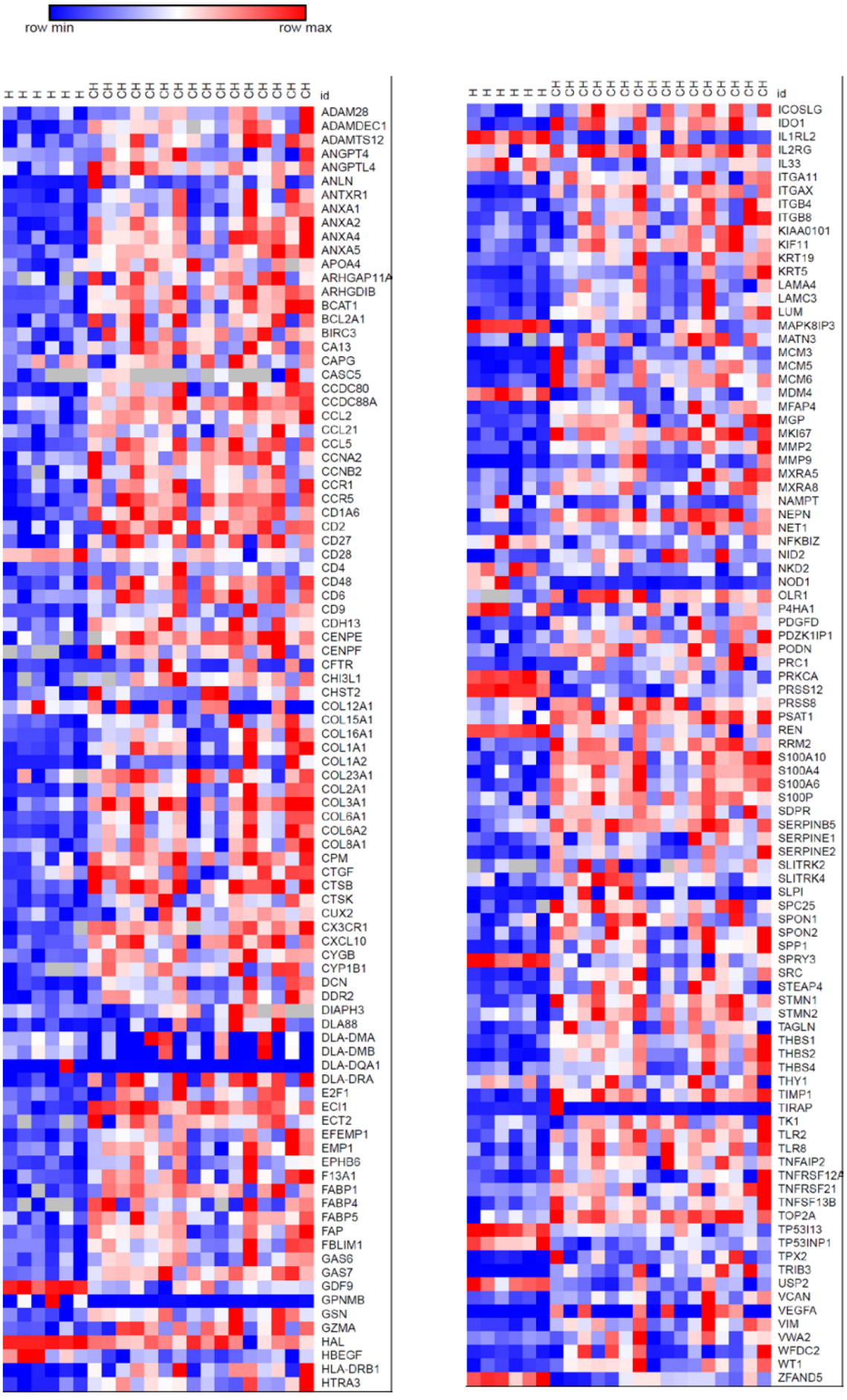
row min
row max
H H H H H H CH CH CH CH CH CH CH CH CH CH CH CH CH CH
id
ADAM28
ADAMDEC1
ADAMTS12
ANGPT4
ANGPTL4
ANLN
ANTXR1
ANXA1
ANXA2
ANXA4
ANXA5
APOA4
ARHGAP11A
ARHGDIB
BCAT1
BCL2A1
BIRC3
CA13
CAPG
CASC5
CCDC80
CCDC88A
CCL2
CCL21
CCL5
CCNA2
CCNB2
CCR1
CCR5
CD1A6
CD2
CD27
CD28
CD4
CD48
CD6
CD9
CDH13
CENPE
CENPF
CFTR
CHI3L1
CHST2
COL12A1
COL15A1
COL16A1
COL1A1
COL1A2
COL23A1
COL2A1
COL3A1
COL6A1
COL6A2
COL8A1
CPM
CTGF
CTSB
CTSK
CUX2
CX3CR1
CXCL10
CYGB
CYP1B1
DCN
DDR2
DIAPH3
DLA88
DLA-DMA
DLA-DMB
DLA-DQA1
DLA-DRA
E2F1
ECI1
ECT2
EFEMP1
EMP1
EPHB6
F13A1
FABP1
FABP4
FABP5
FAP
FBLIM1
GAS6
GAS7
GDF9
GPNMB
GSN
GZMA
HAL
HBEGF
HLA-DRB1
HTRA3
H H H H H H CH CH CH CH CH CH CH CH CH CH CH CH CH CH
id
ICOSLG
IDO1
IL1RL2
IL2RG
IL33
ITGA11
ITGAX
ITGB4
ITGB8
KIAA0101
KIF11
KRT19
KRT5
LAMA4
LAMC3
LUM
MAPK8IP3
MATN3
MCM3
MCM5
MCM6
MDM4
MFAP4
MGP
MKI67
MMP2
MMP9
MXRA5
MXRA8
NAMPT
NEPN
NET1
NFKBIZ
NID2
NKD2
NOD1
OLR1
P4HA1
PDGFD
PDZK1IP1
PODN
PRC1
PRKCA
PRSS12
PRSS8
PSAT1
REN
RRM2
S100A10
S100A4
S100A6
S100P
SDPR
SERPINB5
SERPINE1
SERPINE2
SLITRK2
SLITRK4
SLPI
SPC25
SPON1
SPON2
SPP1
SPRY3
SRC
STEAP4
STMN1
STMN2
TAGLN
THBS1
THBS2
THBS4
THY1
TIMP1
TIRAP
TK1
TLR2
TLR8
TNFAIP2
TNFRSF12A
TNFRSF21
TNFSF13B
TOP2A
TP53I13
TP53INP1
TPX2
TRIB3
USP2
VCAN
VEGFA
VIM
VWA2
WFDC2
WT1
ZFAND5

Figure 4: Heat Map Presentation of Fibrosis-Related Significantly Differentially Expressed Genes in Dogs with CH. Rows represent the normalized expression values of each gene, standardized across all samples. Columns show the values of individual dogs. High expression levels are marked in red, low expression levels are marked in blue, neutral expression levels are marked in white. The first six columns represent the six healthy control dogs that were included in the comparison according to their age (age >1 year). FDR-adjusted *P*-value for all genes <0.05. H = healthy; CH = chronic hepatitis.

Table 6: Significantly Differentially Expressed Genes in Dogs with Chronic Hepatitis

Gene	Name	Chromosome	Fold Change	FDR-adjusted *P*-value	Function	Transcript(s)
ADAM28	ADAM Metallopeptidase Domain 28	25	3.67	5.26E-03	ECM degradation, ECM organization	ADAM28_1
*ADAMDEC1**	ADAM-Like, Decysin 1	25	45.72	3.28E-07	ECM degradation, ECM organization	ADAMDEC1_1
ADAMTS12	ADAM Metallopeptidase With Thrombospondin Type 1 Motif 12	4	2.52	1.36E-03	ECM degradation, ECM organization	ADAMTS12_1
ANGPT4	Angiopoietin 4	24	2.52	8.98E-03	HSC activation pathways	ANGPT4_2
ANGPTL4	Angiopoietin Like 4	20	2.56	2.34E-04	HSC activation pathways	ANGPTL4_1
ANLN	Anillin Actin Binding Protein	14	7.09	2.87E-05	HSC activation pathways	ANLN_1; 3
ANTXR1	Anthrax Toxin Receptor 1	10	2.51	1.35E-03	ECM organization	ANTXR1_1
ANXA1	Annexin A1	1	2.58	3.94E-15	HSC activation pathways	ANXA1_1
ANXA2	Annexin A2	30	6.69	5.48E-31	HSC activation pathways	ANXA2_1
ANXA4	Annexin A3	10	3.97	5.64E-08	HSC activation pathways	ANXA4_1
ANXA5	Annexin A5	19	2.73	1.05E-06	HSC activation pathways	ANXA5_1
APOA4	Apolipoprotein A4	5	12.51	4.66E-09	HSC activation pathways	APOA4_1
ARHGAP11A	Rho GTPase Activating Protein 11A	30	5.53	2.08E-13	Apoptosis/NFκB	ARHGAP11A_1
ARHGDIB	Rho GDP Dissociation Inhibitor Beta	27	2.63	6.40E-07	Apoptosis/NFκB	ARHGDIB_1
BCAT1	Branched Chain Amino Acid Transaminase 1	27	6.85	2.34E-05	HSC activation pathways	Not detected
BCL2A1	BCL2 Related Protein A1	3	2.5	3.28E-03	HSC activation pathways, Apoptosis/NFκB	BCL2A1_1
BIRC3	Baculoviral IAP Repeat Containing 3	5	3.36	4.47E-14	Apoptosis/NFκB	Not detected
CA13	Carbonic Anhydrase 13	29	3.71	3.24E-04	HSC activation pathways	CA13_1
CAPG	Capping Actin Protein, Gelsolin Like	17	4.2	1.18E-29	HSC activation pathways	CAPG_3
CASC5	Cancer Susceptibility Candidate 5	20	5.59	6.12E-15	HSC activation pathways	Not detected
CCDC80	Coiled-Coil Domain Containing 80	33	3.67	2.89E-05	HSC activation pathways	CCDC80_1

CCDC88A	Coiled-Coil Domain Containing 88A	10	2.94	1.89E-06	HSC activation pathways	CCDC88A_1; 2
*CCL2**	C-C Motif Chemokine Ligand 2	9	8.39	1.94E-21	HSC activation pathways	CCL2_1
CCL21	C-C Motif Chemokine Ligand 21	11	3.1	2.25E-06	HSC activation pathways	CCL21_1
*CCL5**	C-C Motif Chemokine Ligand 5	9	13.75	1.39E-27	HSC activation pathways	CCL5_1
CCNA2	Cyclin A2	19	3.93	1.57E-03	HSC activation pathways	CCNA2_1
CCNB2	Cyclin B2	30	2.59	6.58E-13	HSC activation pathways	CCNB2_1
CCR1	C-C Motif Chemokine Receptor 1	20	3.89	1.42E-05	HSC activation pathways	CCR1_2
CCR5	C-C Motif Chemokine Receptor 5	20	3.76	5.69E-07	HSC activation pathways	Not detected
CD1A6	CD1A6 Protein	38	7.33	2.88E-08	Apoptosis/NFκB	CD1A6_1
CD2	CD2 Molecule	17	3.88	5.00E-21	HSC activation pathways	CD2_1
CD27	CD27 Molecule	27	4.25	6.64E-04	Apoptosis/NFκB	CD27_1
CD28	CD28 Molecule	37	-2.92	7.10E-04	Apoptosis/NFκB	CD28_1
CD4	CD4 Molecule	27	2.96	0.01	Apoptosis/NFκB	CD4_1
CD48	CD48 Molecule	38	3.8	1.76E-05	Apoptosis/NFκB	CD48_1
CD6	CD6 Molecule	18	5.91	2.09E-04	HSC activation pathways	CD6_1
CD9	CD9 Molecule	27	2.56	1.03E-03	HSC activation pathways	CD9_1
CDH13	Cadherin 13	5	4.27	2.93E-10	ECM degradation, ECM organization, HSC activation pathway, Detoxification of ROS	CDH13_1
CENPE	Centromere Protein E	32	7.07	5.19E-07	HSC activation pathways	CENPE_1; 2
CENPF	Centromere Protein F	7	11.41	2.84E-21	HSC activation pathways	CENPF_1
CFTR	Cystic Fibrosis Transmembrane Conductance Regulator	14	3.41	0.01	HSC activation pathways	CFTR_1
*CHI3L1**	Chitinase 3 Like 1	7	35.92	2.50E-25	ECM organization	CHI3L1_2
CHST2	Carbohydrate Sulfotransferase 2	23	5.35	7.40E-08	HSC activation pathways	CHST2_1
COL12A1	Collagen Type XII Alpha 1	12	3.03	2.11E-03	ECM degradation, ECM organization	COL12A1_3
COL15A1	Collagen Type XV Alpha 1	11	3.03	3.75E-10	ECM degradation, ECM organization	COL15A1_1; 2; 3

COL16A1	Collagen Type XVI Alpha 1	2	3.68	1.25E-03	ECM degradation, ECM organization	COL16A1_1
COL1A1	Collagen Type I Alpha 1	9	5.69	5.38E-22	ECM organization	COL1A1_1
COL1A2	Collagen Type I Alpha 2	14	2.59	1.94E-03	ECM organization	COL1A2_1
COL23A1	Collagen Type XXIII Alpha 1	11	2.98	1.73E-08	ECM degradation, ECM organization	COL23A1_1
COL2A1	Collagen Type II Alpha 1	27	3.13	2.80E-04	ECM organization	COL2A1_1; 2; 3
COL3A1	Collagen Type III Alpha 1	36	2.98	3.95E-04	ECM organization	COL3A1_1
COL6A1	Collagen Type VI Alpha 1	31	3.58	1.52E-04	ECM organization	COL6A1_1
COL6A2	Collagen Type VI Alpha 2	31	3.42	5.28E-05	ECM organization	COL6A2_1
COL8A1	Collagen Type VIII Alpha 1	33	2.95	2.32E-03	ECM organization	COL8A1_1
CPM	Carboxypeptidase M	10	4.84	2.89E-05	HSC activation pathways	CPM_1
CTGF	Connective Tissue Growth Factor	1	2.62	1.03E-06	HSC activation pathways	CTGF_1
CTSB	Cathepsin B	25	2.53	1.77E-04	ECM degradation, ECM organization	CTSB_1
CTSK	Cathepsin K	17	4.59	6.60E-18	ECM degradation, ECM organization	CTSK_1
CUX2	Cut Like Homeobox 2	26	6.09	1.06E-03	HSC activation pathways	CUX2_1; 2
CX3CR1	C-X3-C Motif Chemokine Receptor 1	23	7.06	5.40E-29	HSC activation pathways	Not detected
*CXCL10**	C-X-C Motif Chemokine Ligand 10	32	19.05	1.69E-06	HSC activation pathways	CXCL10_1
CYGB	Cytoglobin, Stellate Cell Activation-Associated Protein	9	3.43	1.52E-18	Detoxification of ROS	CYGB_1
CYP1B1	Cytochrome P450 Family 1 Subfamily B Member 1	17	5.82	5.14E-14	Detoxification of ROS	CYP1B1_1
DCN	Decorin	15	3.05	5.93E-04	ECM degradation, ECM organization	DCN_1; 3; 4
DDR2	Discoidin Domain Receptor Tyrosine Kinase 2	38	4.59	1.30E-04	ECM organization	DDR2_3; 4; 6
DIAPH3	Diaphanous Related Formin 3	22	6.62	9.92E-07	ECM organization	Not detected
DLA88	Major Histocompatibility Complex, Class I, B	12	2.96	0.01	Apoptosis/NFκB	DLA88_1
DLA-DMA	Major Histocompatibility Complex, Class II, DM Alpha	12	3.03	9.60E-06	Apoptosis/NFκB	DLA-DMA_1; 2; 3; 4; 5
DLA-DMB	Major Histocompatibility Complex, Class II, DM Beta	12	3.23	1.27E-06	Apoptosis/NFκB	DLA-DMB_1

DLA-DRA	Major Histocompatibility Complex, Class II, DR Alpha	12	3.13	2.95E-06	Apoptosis/NFκB	DLA-DRA_2
E2F1	E2F Transcription Factor 1	24	3.03	1.03E-03	HSC activation pathways	Not detected
ECI1	Enoyl-CoA Delta Isomerase 2	6	3.84	3.57E-18	HSC activation pathways	Not detected
ECT2	Epithelial Cell Transforming 2	34	5.89	2.30E-21	HSC activation pathways	Not detected
EFEMP1	EGF Containing Fibulin-Like Extracellular Matrix Protein 1	10	4.73	5.14E-04	ECM organization	EFEMP1_2; 3
EMP1	Epithelial Membrane Protein 1	27	6.62	1.57E-04	HSC activation pathways	Not detected
EPHB6	EPH Receptor B6	16	3.55	4.44E-03	HSC activation pathways	EPHB6_1
F13A1	Coagulation Factor XIII A Chain	35	5.3	5.38E-04	HSC activation pathways	F13A1_1
FABP1	Fatty Acid Binding Protein 1	17	17.24	1.02E-28	HSC activation pathways	FABP1_1
FABP4	Fatty Acid Binding Protein 4	29	15.57	1.05E-03	HSC activation pathways	FABP4_1
FABP5	Fatty Acid Binding Protein 5	29	4.42	3.24E-04	HSC activation pathways	FABP5_1
FAP	Fibroblast Activation Protein Alpha	36	8.06	1.40E-04	ECM degradation	FAP_1; 2; 3; 4
FBLIM1	Filamin Binding LIM Protein 1	2	2.65	1.77E-03	ECM organization	FBLIM1_1
GAS6	Growth Arrest Specific 6	22	3.03	4.17E-03	HSC activation pathways, Apoptosis/NFκB	GAS6_1
GAS7	Growth Arrest Specific 7	5	2.92	1.05E-20	HSC activation pathways, Apoptosis/NFκB	Not detected
GDF9	Growth Differentiation Factor 9	11	-3.47	2.68E-68	ECM organization, HSC activation pathway	GDF9_1
GPNMB	Glycoprotein Nmb	14	11.97	1.66E-06	HSC activation pathways	GPNMB_1
GSN	Gelsolin	11	3.83	4.64E-18	Apoptosis/NFκB	GSN_1
GZMA	Granzyme A	2	5.13	1.37E-04	HSC activation pathways	GZMA_1
HAL	Histidine Ammonia-Lyase	15	-2.88	3.76E-04	HSC activation pathways	HAL_1
HBEGF	Heparin Binding EGF Like Growth Factor	2	-3.06	3.74E-07	HSC activation pathways	HBEGF_2
HLA-DRB1	Major Histocompatibility Complex, Class II, DR	12	3.67	2.35E-07	Apoptosis/NFκB	HLA-DRB1_1

	Beta 1					
HTRA3	HtrA Serine Peptidase 3	3	2.74	4.99E-04	ECM degradation, ECM organization, Apoptosis/NFκB	HTRA3_1
ICOSLG	Inducible T-Cell Co-Stimulator Ligand	31	2.77	9.68E-04	HSC activation pathways	ICOSLG_1
IDO1	Indoleamine 2,3-Dioxygenase 1	16	9.01	5.30E-06	HSC activation pathways	IDO1_1
IL1RL2	Interleukin 1 Receptor Like 2	10	-5.61	<0.001	Apoptosis/NFκB	IL1RL2_1; 2; 3; 4; 5; 6
IL2RG	Interleukin 2 Receptor Subunit Gamma	X	5.9	7.16E-23	Apoptosis/NFκB	IL2RG_1; 2
IL33	Interleukin 33	11	-2.9	<0.001	Apoptosis/NFκB	IL33_2
INTS6	Integrator Complex Subunit 6	22	-2.55	7.79E-11	HSC activation pathways	INTS6_2
IRG1	Immune-Responsive Gene 1 Protein	22	8.39	8.30E-04	Apoptosis/NFκB	IRG1_1; 2
ITGA11	Integrin Subunit Alpha 11	30	3.01	9.24E-09	ECM organization, HSC activation pathways	ITGA11_1
ITGAX	Integrin Subunit Alpha X	6	9.62	1.37E-11	ECM organization, HSC activation pathways	ITGAX_1
ITGB4	Integrin Subunit Beta 8	9	2.55	8.64E-08	ECM organization, HSC activation pathways	ITGB4_1
ITGB8	Integrin Subunit Beta 5	14	2.55	0.01	ECM organization, HSC activation pathways	ITGB8_4
KIAA0101	KIAA0101	30	4.98	4.21E-13	HSC activation pathways	KIAA0101_2
KIF11	Kinesin Family Member 11	28	8.67	2.50E-07	HSC activation pathways	KIF11_1
KRT19	Keratin 19	9	2.92	2.10E-11	Apoptosis/NFκB	KRT19_1
KRT5	Keratin 5	27	5.26	9.72E-04	Apoptosis/NFκB	KRT5_1
LAMA4	Laminin Subunit Alpha 4	12	4.56	1.27E-04	ECM degradation, ECM organization	LAMA4_1
LAMC3	Laminin Subunit Gamma 3	9	3.15	8.33E-11	ECM degradation, ECM organization	LAMC3_1
LUM	Lumican	15	7.02	1.22E-05	ECM organization	LUM_1
MAPK8IP3	Mitogen-Activated Protein Kinase 8 Interacting Protein 3	6	-3.49	5.23E-12	HSC activation pathways, Apoptosis/NFκB	MAPK8IP3_1
*MATN3**	Matrilin 3	17	10.68	5.32E-14	ECM organization	MATN3_1
MCM3	Minichromosome Maintenance Complex Component 3	12	2.54	8.79E-05	HSC activation pathways	MCM3_1

MCM5	Minichromosome Maintenance Complex Component 5	10	3.62	1.37E-05	HSC activation pathways	MCM5_1
MCM6	Minichromosome Maintenance Complex Component 6	19	3.3	1.05E-06	HSC activation pathways	MCM6_1
MDM4	MDM4, P53 Regulator	38	-2.54	6.84E-09	HSC activation pathways	MDM4_1; 4
MFAP4	Microfibrillar Associated Protein 4	5	7.28	4.84E-31	ECM organization	MFAP4_1
MGP	Matrix Gla Protein	27	4.73	7.39E-05	HSC activation pathways	Not detected
*MKI67**	Marker Of Proliferation Ki-67	28	10.04	2.45E-08	HSC activation pathways	MKI67_1
MMP2	Matrix Metallopeptidase 2	2	7.22	3.31E-05	ECM degradation, ECM organization, HSC activation pathways	MMP2_1
MMP9	Matrix Metallopeptidase 9	24	9.73	5.11E-06	ECM degradation, ECM organization, HSC activation pathways	MMP9_1
MXRA5	Matrix-Remodelling Associated 5	X	4.39	1.60E-12	ECM organization	MXRA5_1
MXRA8	Matrix-Remodelling Associated 8	5	2.78	7.18E-12	ECM organization	MXRA8_1
NAMPT	Nicotinamide Phosphoribosyl-transferase	18	-2.83	9.93E-04	HSC activation pathways	NAMPT_1
NEPN	Nephrocan	1	3.7	2.58E-22	HSC activation pathways	NEPN_1
NET1	Neuroepithelial Cell Transforming 1	2	2.67	4.23E-04	HSC activation pathways	NET1_1
NFKBIZ	NFKB Inhibitor Zeta	33	-2.9	2.89E-05	Apoptosis/NFκB	NFKBIZ_1
NID2	Nidogen 2	8	3.81	8.59E-04	ECM degradation, ECM organization	NID2_1
NKD2	Naked Cuticle Homolog 2	34	-5.06	6.23E-21	HSC activation pathways	NKD2_1
NOD1	Nucleotide Binding Oligomerization Domain Containing 1	14	-3.45	1.16E-09	Apoptosis/NFκB	NOD1_2; 3; 4
OLR1	Oxidized Low Density Lipoprotein Receptor 1	27	9.7	1.77E-04	HSC activation pathways	OLR1_2
P4HA1	Prolyl 4-Hydroxylase Subunit Alpha 1	4	-2.77	2.95E-04	ECM organization	P4HA1_2
PDGFD	Platelet Derived Growth Factor D	5	4.24	8.19E-16	ECM organization, HSC activation pathways	PDGFD_1
PDZK1IP1	PDZK1 Interacting	15	4.2	1.25E-03	HSC activation	PDZK1IP1_3

	Protein 1				pathways	
PODN	Podocan	5	3.31	9.54E-15	ECM organization	Not detected
PRC1	Protein Regulator Of Cytokinesis 1	3	4.26	9.42E-04	HSC activation pathways	PRC1_1
PRKCA	Protein Kinase C Alpha	9	-3.42	<0.001	ECM organization, Apoptosis/NFκB	PRKCA_1; 2
PRSS12	Protease, Serine 12	32	-5.23	1.44E-16	ECM degradation, ECM organization	PRSS12_1
PRSS8	Protease, Serine 8	6	2.53	8.75E-03	ECM degradation, ECM organization	PRSS8_1
PSAT1	Phosphoserine Aminotransferase 1	1	5.56	3.59E-18	HSC activation pathways	PSAT1_1
REN	Renin	38	-4.93	1.54E-05	HSC activation pathways	REN_1; 3
RRM2	Ribonucleotide Reductase Regulatory Subunit M2	17	11.97	5.32E-30	HSC activation pathways	RRM2_1
S100A10	S100 Calcium Binding Protein A10	17	3.53	1.96E-24	HSC activation pathways	S100A10_1
S100A4	S100 Calcium Binding Protein A4	7	7.77	2.09E-27	HSC activation pathways	S100A4_1; 2
S100A6	S100 Calcium Binding Protein A6	7	5.21	1.33E-28	HSC activation pathways	S100A6_1
S100P	S100 Calcium Binding Protein P	3	4.47	1.66E-03	HSC activation pathways	S100P_1
SDPR	Serum Deprivation Response	37	2.64	2.66E-04	HSC activation pathways	SDPR_1
SERPINB5	Serpin Family B Member 5	1	4.68	3.00E-19	ECM organization	SERPINB5_3
SERPINE1	Serpin Family E Member 1	6	2.97	0.02	ECM organization	Not detected
SERPINE2	Serpin Family E Member 2	37	13.71	1.01E-06	ECM organization	SERPINE2_1
SLITRK2	SLIT And NTRK Like Family Member 2	X	9.5	5.02E-09	HSC activation pathways	Not detected
SLITRK4	SLIT And NTRK Like Family Member 4	X	2.51	1.76E-06	HSC activation pathways	Not detected
SLITRK6	SLIT And NTRK Like Family Member 6	22	3.92	0.01	HSC activation pathways	Not detected
SLPI	Secretory Leukocyte Peptidase Inhibitor	24	69.78	9.87E-07	Apoptosis/NFκB	SLPI_1
SPC25	SPC25, NDC80 Kinetochore Complex Component	36	9.34	1.57E-04	HSC activation pathways	SPC25_1
SPON1	Spondin 1	21	3.44	3.05E-11	HSC activation pathways	SPON1_1

SPON2	Spondin 2	3	5.26	3.48E-03	HSC activation pathways	SPON2_1
SPP1	Secreted Phosphoprotein 1	32	5.88	5.19E-07	ECM degradation, ECM organization	SPP1_1; 2
SPRY3	Sprouty RTK Signaling Antagonist 3	X	-5.94	2.79E-79	HSC activation pathways	SPRY3_1; 2; 3; 4
SRC	SRC Proto-Oncogene, Non-Receptor Tyrosine Kinase	24	2.59	2.66E-08	HSC activation pathways	SRC_4
STEAP4	STEAP4 Metalloreductase	14	9.44	2.43E-05	HSC activation pathways	STEAP4_1; 2
STMN1	Stathmin 1	2	4.36	3.13E-07	HSC activation pathways	STMN1_1; 2; 3
STMN2	Stathmin 2	29	3.35	6.69E-03	HSC activation pathways	STMN2_1
TAGLN	Transgelin	5	3.69	4.90E-18	HSC activation pathways	TAGLN_1
THBS1	Thrombospondin 1	30	2.97	4.36E-31	ECM organization, HSC activation pathways	THBS1_1
THBS2	Thrombospondin 2	1	3.76	4.62E-22	ECM organization, HSC activation pathways	THBS2_1
THBS4	Thrombospondin 4	3	9.28	5.93E-03	ECM organization, HSC activation pathways	THBS4_1
THY1	Thy-1 Cell Surface Antigen	5	4.89	1.27E-28	HSC activation pathways	Not detected
*TIMP1**	TIMP Metallopeptidase Inhibitor 1	X	11.81	1.62E-30	ECM degradation, ECM organization, HSC activation pathways	TIMP1_1
TIRAP	Toll-Interleukin 1 Receptor (TIR) Domain Containing Adaptor Protein	5	-4.8	1.55E-62	Apoptosis/NFκB	Not detected
TK1	Thymidine Kinase 1	9	2.59	3.25E-11	HSC activation pathways	TK1_1
TLR2	Toll Like Receptor 2	15	3.29	9.21E-06	Apoptosis/NFκB	TLR2_1
TLR8	Toll Like Receptor 8	X	2.89	4.79E-13	Apoptosis/NFκB	TLR8_2
TNFAIP2	TNF Alpha Induced Protein 2	8	2.88	1.16E-04	Apoptosis/NFκB	TNFAIP2_1
TNFRSF12A	Tumor Necrosis Factor Receptor Superfamily Member 12A	6	3.1	2.10E-03	Apoptosis/NFκB	TNFRSF12A_1
TNFRSF21	Tumor Necrosis Factor Receptor Superfamily Member 21	12	2.51	7.26E-06	Apoptosis/NFκB	TNFRSF21_1
TNFSF13B	Tumor Necrosis Factor Superfamily Member	22	4.44	4.00E-04	Apoptosis/NFκB	TNFSF13B_1

	13b					
TOP2A	Topoisomerase (DNA) II Alpha	9	4.85	2.72E-27	HSC activation pathways	Not detected
TP53I13	Tumor Protein P53 Inducible Protein 13	9	-4.38	<0.001	HSC activation pathways	TP53I13_1; 2
TP53INP1	Tumor Protein P53 Inducible Nuclear Protein 1	29	-3.67	5.19E-12	HSC activation pathways	TP53INP1_1; 4
TPX2	TPX2, Microtubule Nucleation Factor	24	6.25	1.10E-06	HSC activation pathways	TPX2_4
TRIB3	Tribbles Pseudokinase 3	24	-5.91	6.17E-10	Apoptosis/NFκB	TRIB3_2
USP2	Ubiquitin Specific Peptidase 2	5	-2.84	1.48E-14	Apoptosis/NFκB	Not detected
VCAN	Versican	3	3.97	4.53E-03	ECM organization	VCAN_1; 2; 3
VEGFA	Vascular Endothelial Growth Factor A	12	-3.2	<0.001	HSC activation pathways	VEGFA_1
VIM	Vimentin	2	2.73	4.91E-05	Apoptosis/NFκB	VIM_1
VWA2	Von Willebrand Factor A Domain Containing 2	28	2.51	0.02	ECM organization	VWA2_1
WFDC2	WAP Four-Disulfide Core Domain 2	24	15.5	8.51E-05	ECM organization	WFDC2_1
WT1	Wilms Tumor 1	18	3.86	5.21E-04	HSC activation pathways	WT1_1
ZFAND5	Zinc Finger AN1-Type Containing 5	1	-2.85	<0.001	Apoptosis/NFκB	ZFAND5_2

Expression profiles of 190 genes (and transcripts), significantly up- or down-regulated in dogs with chronic hepatitis. RNA sequencing was performed on liver samples of 16 dogs with chronic hepatitis compared to six healthy control dogs. Positive fold change values represent upregulation, negative fold change values represent down-regulation. The *P*-value was adjusted for multiple comparisons and significance was set at an FDR-adjusted *P*-value of <0.05. Genes marked with a '*' were selected for confirmation with qPCR. 'Not detected': selection criteria (absolute fold change-value >2.5; FDR corrected *P*-value <0.05) not fulfilled.

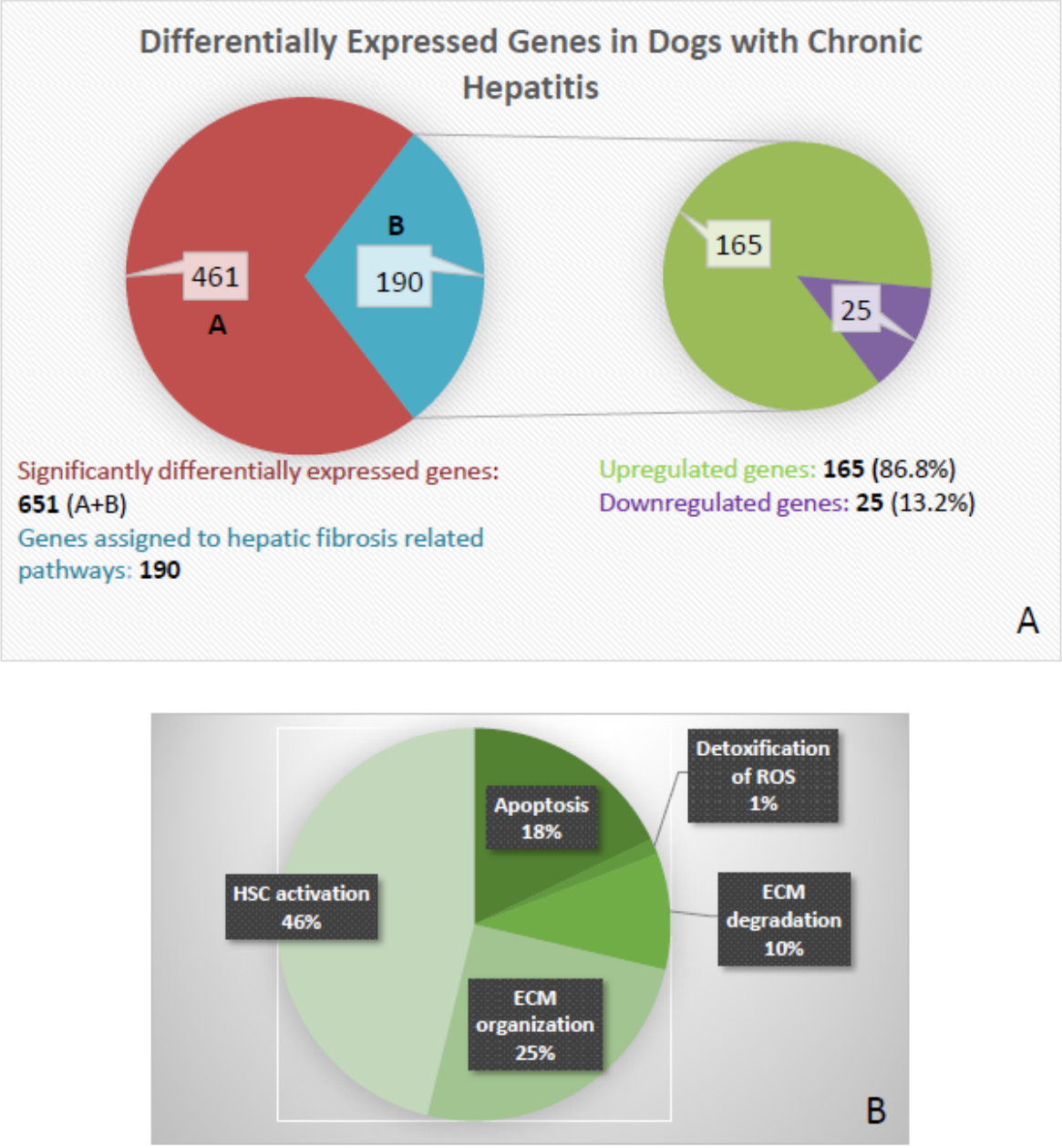

Figure 5: Absolute Numbers and Percentages of Differentially Expressed Genes in Dogs with Chronic Hepatitis. A) overview and B) subcategorization with pathway analysis. HSC = hepatic stellate cell; ECM = extracellular matrix; ROS = reactive oxygen species.

5.1.3 Quantitative Polymerase Chain Reactions

Quantitative polymerase chain reactions confirmed a significant upregulation of the mRNA expression of all selected genes in dogs with CH compared to healthy dogs. Results of the qPCR analysis at the delta Cq (quantification cycle) level before calculation of the fold change values are shown in **Figure 6**. Displayed is the mean delta Cq ± SD for each gene for dogs with CH followed by healthy control dogs. For each gene, the CH samples showed statistically significant relative higher mRNA expression compared to samples of the healthy dogs (*P*-value <0.01). Quantitative polymerase chain reaction analysis confirmed the upregulation in mRNA expression for all evaluated fibrosis related genes. Fold change estimations (FC ± SE) with the Livak method were as follows: 4.3 – 14.4 (± 0.1 – 3.4): *CCL2* (14.4 ± 1.5), *TIMP-1* (12.5 ± 0.1), *MATN3* (9.4 ± 3.4), *CHI3L1* (7.8 ± 1.4), *CCL5* (8.3 ± 0.2), *ADAMDEC1* (6.4 ± 2), *CXCL10* (5.3 ± 0.4), and *MKI67* (4.6 ± 0.6).

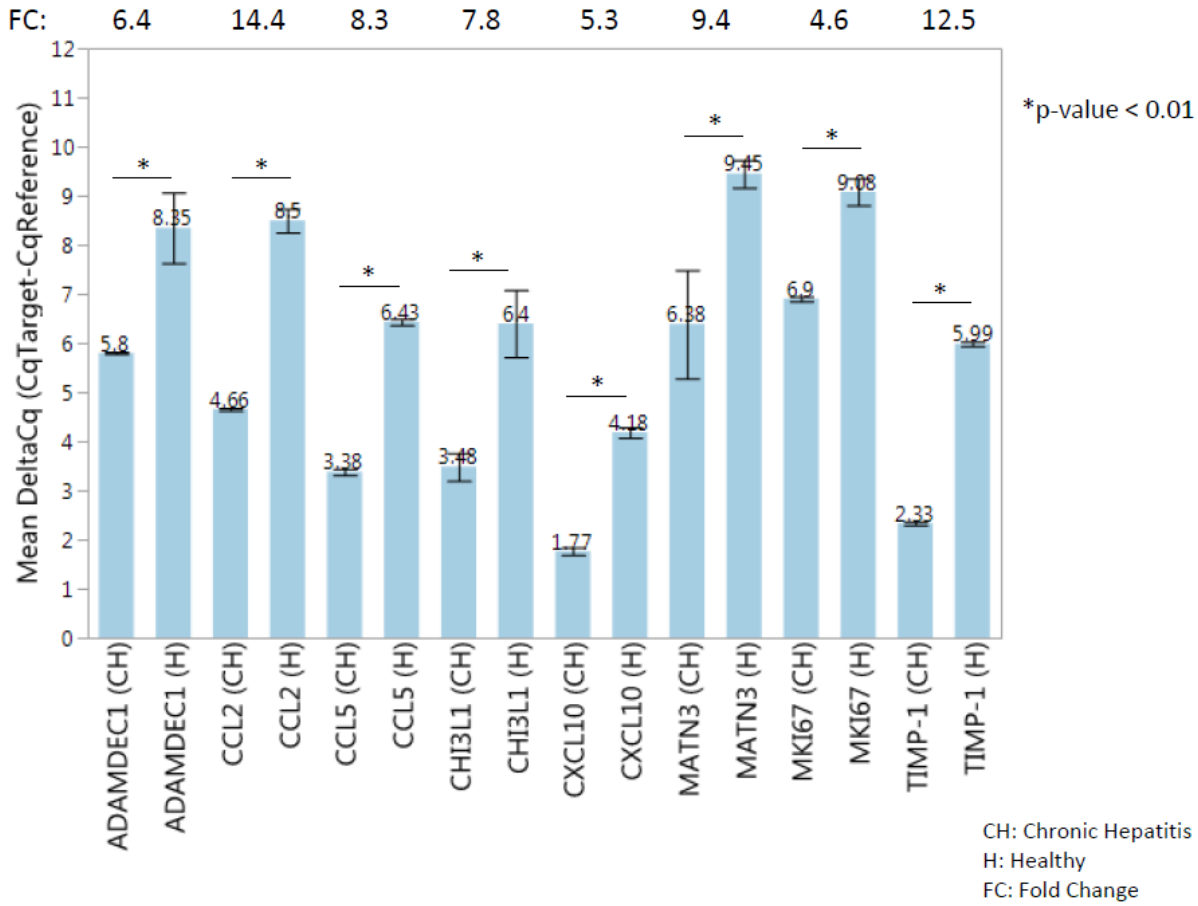

Figure 6: Quantitative PCR Confirmatory Testing of 8 Selected Genes. Data is expressed as mean delta Cq (CqTarget - CqReference) for dogs with chronic hepatitis (CH) followed by healthy control dogs (H) for each of the eight genes. Lower delta Cq values indicate increased expression. The expression of all eight genes was upregulated in dogs with CH compared to healthy control dogs ($p<0.01$ for each comparison). Fold changes (FC) were calculated with the Livak method (FC ± SE). *ADAMDEC1* (FC: 6.4 ± 2); *CCL2* (FC: 14.4 ± 1.5); *CCL5* (FC: 8.3 ± 0.2); *CHI3L1* (FC: 7.8 ± 1.4); *CXCL10* (FC: 5.3 ± 0.4); *MATN3* (FC: 9.4 ± 3.4); *MKI67* (FC: 4.6 ± 0.6), and *TIMP-1* (FC: 12.5 ± 0.1). Cq = quantification cycle.

5.2 Immunohistochemistry

5.2.1 Specificity of the Primary Antibody

The antibody for αSMA was previously assessed and used for staining of αSMA in canine tissue at a Texas A&M laboratory (Veterinary Histopathology Lab). The antibody for canine TIMP-1 was validated by the manufacturer (Cloud Clone Corp., Tx, USA) for the canine antigen and was previously used for detecting TIMP-1 in serum of dogs in an ELISA procedure at the author's laboratory (Lidbury et al. 2016). The antibodies for Ki67 and CYGB detect the human antigens and were, to the author's knowledge, not previously evaluated for use with canine liver tissue. Canine tissues with known expression of the proteins were used as positive controls (i.e., lymph node for Ki67, small intestine for CYGB and TIMP-1). Negative controls (liver tissue) without primary antibody to exclude non-specific staining and artefacts were included in each procedure (**Figure 7**). The location of the staining for αSMA, Ki67, and TIMP-1 was as expected. In liver tissue, αSMA cytoplasmatic staining was detected perisinusoidally and in fibrotic septa. Ki67 nuclear staining was detected in proliferating cells. TIMP-1 staining was found in the cytoplasm of perisinusoidal cells. Although CYGB cytoplasmatic staining was found in the positive control in glandular cells, no staining was detected in any of the study's liver samples. Therefore, CYGB could not be evaluated.

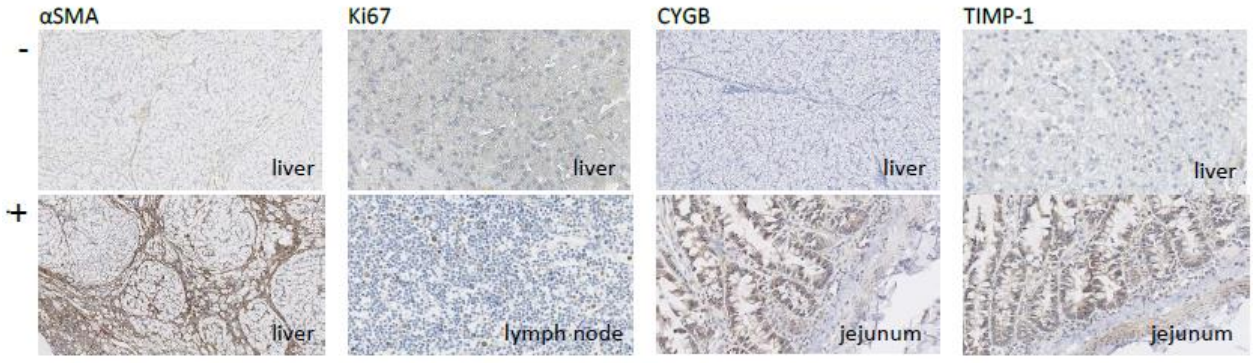

Figure 7: Positive (+) and Negative (-) Controls for the Primary Antibodies. αSMA: liver tissue; strong cytoplasmatic staining perisinusoidal and in fibrotic septa. Ki67: lymph node; strong nuclear staining in several cells. CYGB: jejunum; moderate cytoplasmatic staining in glandular cells. TIMP-1: jejunum; moderate cytoplasmatic staining in glandular cells. Negative controls show no background or artefacts.

5.2.2 Immunostaining of Dog Liver Sections

5.2.2.1 αSMA

In liver sections of healthy dogs with fibrosis score 0, αSMA was detected in the cytoplasm of perisinusoidal cells and of cells around the portal tracts. Measurements of the stained area ranged from 3.3-13.6 % (mean: 6.9 %; SD: 2.6). In liver sections of dogs with CH and fibrosis, the staining increased with the amount of fibrosis and could be detected perisinusoidal and in fibrotic areas (**Figure 8**). The percentage of stained area ranged from 3.5-13.9 % (mean: 7.4 %; SD: 2.5) for fibrosis score 1, from 2.8-17.2 % (mean: 9.2 %; SD: 3.5) for fibrosis score 2, from 2.3-22.8 % (mean: 10.5 %; SD: 4.2) for fibrosis score 3, and from 2.5-27.2 % (mean: 14.8 %; SD: 6.3) for fibrosis score 4. A moderate correlation was found for the percentage of stained area and the fibrosis score (ρ: 0.54; *P*-value: <0.0001). Except for the comparisons of fibrosis score 3 with 2 and 1 with 0, for all other pairings a significant difference in αSMA expression was detected (*P*-value: <0.05). **Figure 9** shows a box plot presentation for αSMA expression in association with the fibrotic stage (**A**) and the distribution of the measurements for each sample (**B**).

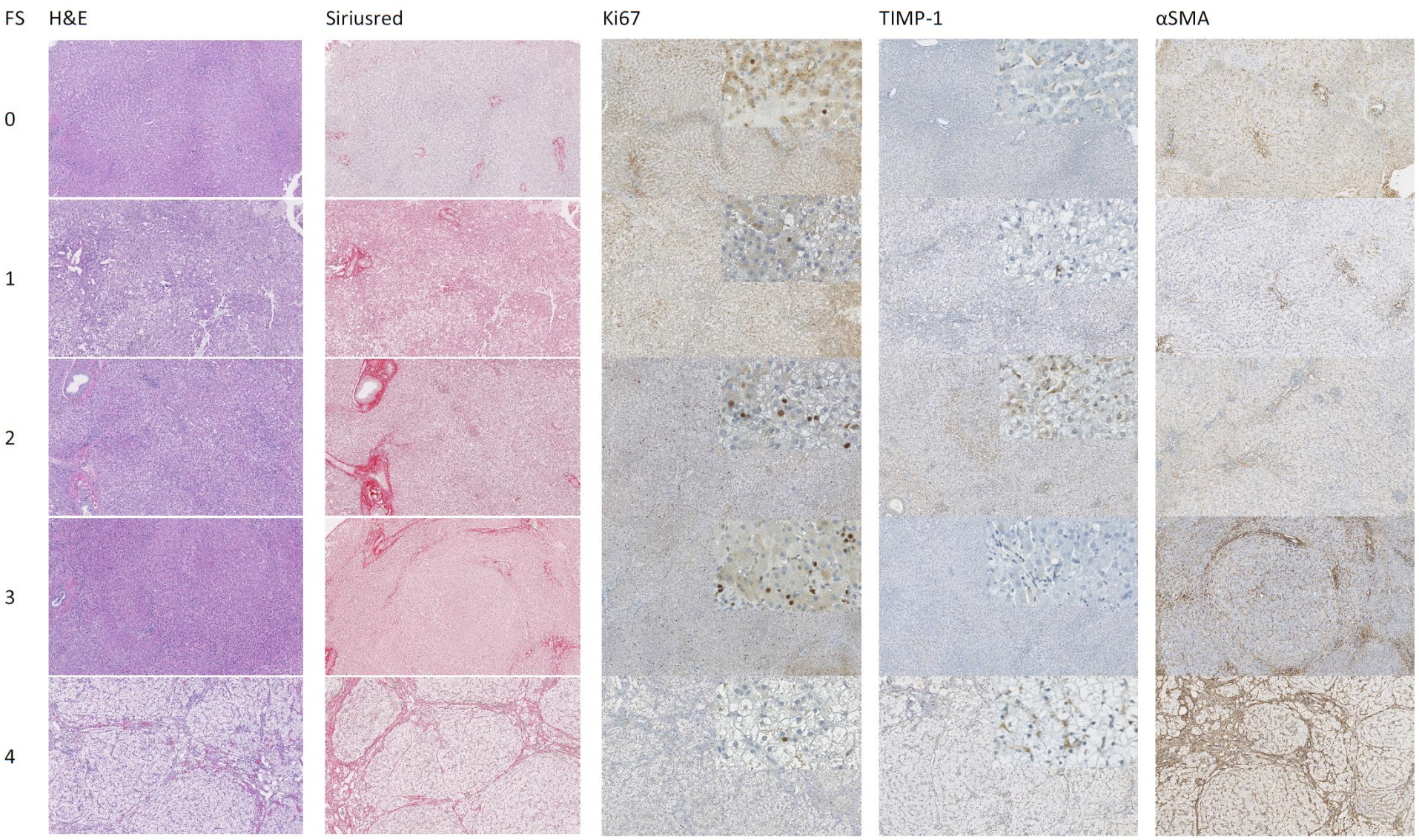
FS
H&E
Siriusred
Ki67
TIMP-1
αSMA
0
1
2
3
4

Figure 8: Immunostaining of Canine Liver Sections with Ki67, TIMP-1, and αSMA. The figure shows the staining for Ki67, TIMP-1, and αSMA in dogs with different stages of fibrosis (FS = fibrosis score). The dog with fibrosis score 0 was a healthy dog of the control group. All other dogs were diagnosed with CH. The hematoxylin & eosin and the picrosirius red stains were included for each fibrosis score and are displayed in the first two columns. (Figure 8 on previous page). Insets show magnified views.

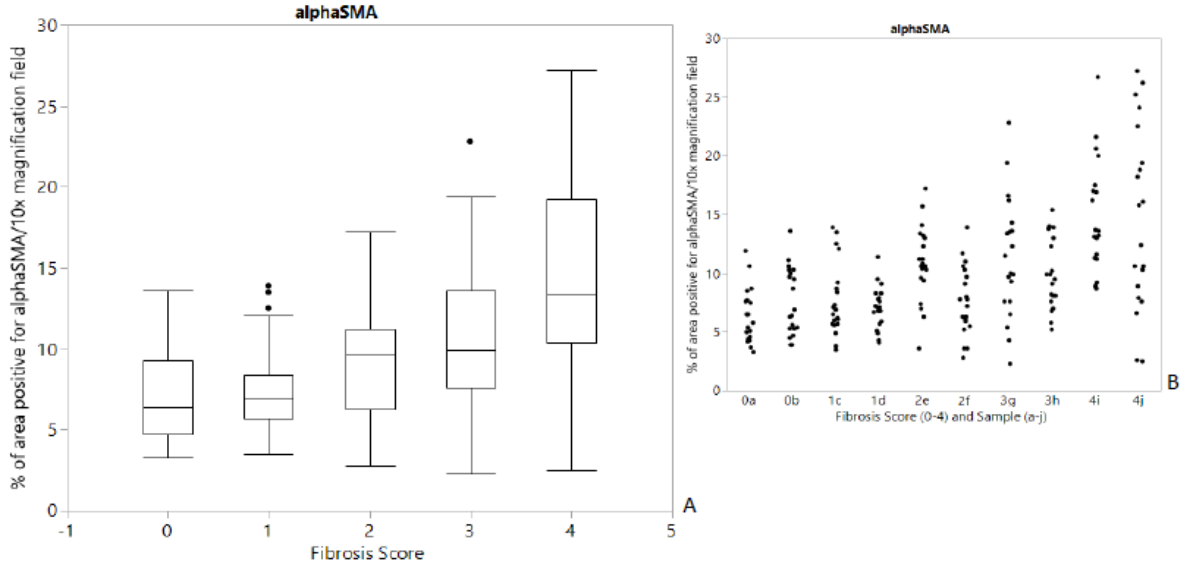

Figure 9: Percentage of αSMA Stained Area and Fibrosis Score. (A) An outliner box plot for each fibrosis score (0-4) is shown with mean bar and standard deviation. **(B)** Part B shows the distribution of the measurements for each sample (a-j).

5.2.2.2 Ki67

In liver sections of healthy dogs with fibrosis score 0 and in liver sections of CH dogs with fibrosis, Ki67 was detected in the nuclei of proliferating liver cells (**Figure 8**). The amount of stained nuclei increased with mild and moderate fibrosis and decreased with marked and very marked fibrosis (**Figure 8**). The numbers of stained nuclei per 20x magnification field ranged from 1-8 (mean: 3.5; SD: 1.9) for healthy dogs with fibrosis score 0, from 1-58 (mean: 12.4; SD: 13.6) for CH-dogs and fibrosis score 1, from 4-103 (mean: 21.2; SD: 17.2) for CH-dogs with fibrosis score 2, from 4-40 (mean: 17.1; SD: 9.6) for CH-dogs with fibrosis score 3, and from 0-6 (mean: 1.9; SD: 1.7) for CH-dogs with fibrosis score 4. No correlation was present for Ki67 expression and the fibrotic stage. Except for the comparisons of fibrosis score 2 with 3 and 0 with 4, for all other pairings a significant

difference was detected (*P*-value: <0.05). **Figure 10** shows a box plot presentation for Ki67 expression in association with the fibrotic stage (**A**) and the distribution of the measurements for each sample (**B**).

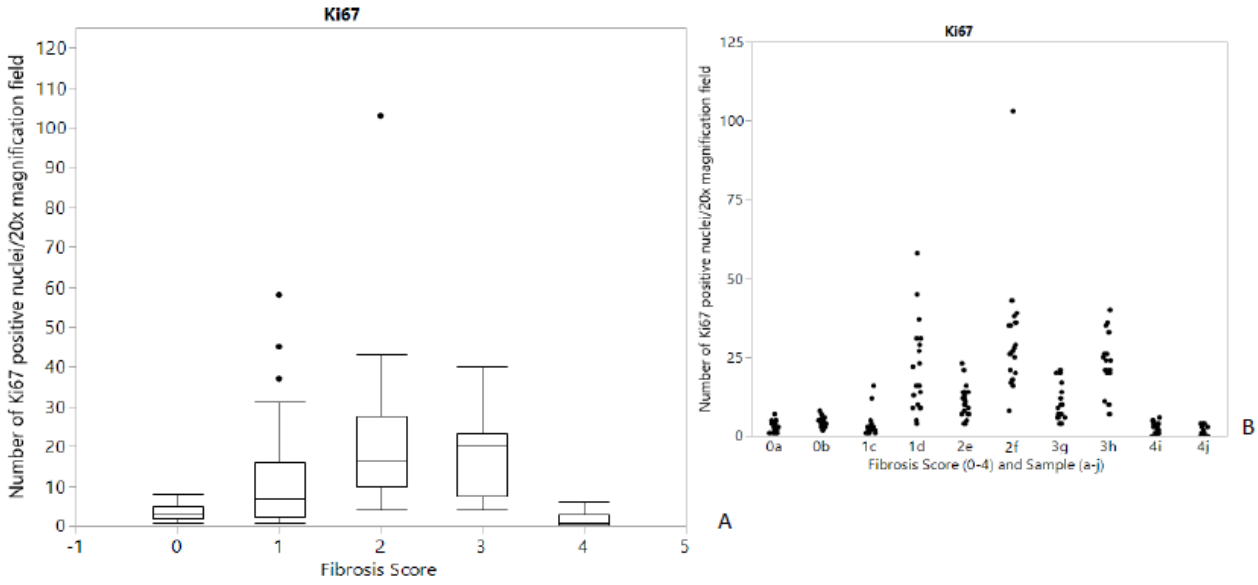

Figure 10: Number of Ki67 Positive Nuclei and Fibrosis Score. (A) An outliner box plot for each fibrosis score (0-4) is shown with mean bar and standard deviation. **(B)** Part B shows the distribution of the measurements for each sample (a-j).

5.2.2.3 TIMP-1

In liver sections of healthy dogs with fibrosis score 0 and in liver sections of dogs with CH and fibrosis, TIMP-1 staining could be detected in the cytoplasm of perisinusoidal cells (**Figure 8**). The number of stained cells did not show any relation to the amount of fibrosis present in the sections. Instead, the staining seemed to be dependent on the individual sample (dog). The numbers of stained cells per 20x magnification field ranged from 0-13 (mean: 3.3; SD: 3.9) for healthy dogs with fibrosis score 0, from 0-3 (mean: 0.2; SD: 0.6) for CH-dogs and fibrosis score 1, from 0-4 (mean: 0.6; SD: 1.1) for CH-dogs with fibrosis score 2, and from 0-10 (mean: 1.1; SD: 1.9) for CH-dogs with fibrosis score 4. In the samples with fibrosis score 3 no stained cells could be detected in the evaluated fields. Nonetheless, a weak negative correlation (ρ: -0.17; *P*-value: 0.0168) for the number of stained cells and the fibrosis score was found. Also, for fibrosis score 0 compared to all other fibrosis scores and for fibrosis score 4 compared to fibrosis score 3 and 1, a significant difference could be

detected (*P*-value: <0.05). **Figure 11** shows a box plot presentation for TIMP-1 expression in association with the fibrotic stage (**A**) and the distribution of the measurements (**B**).

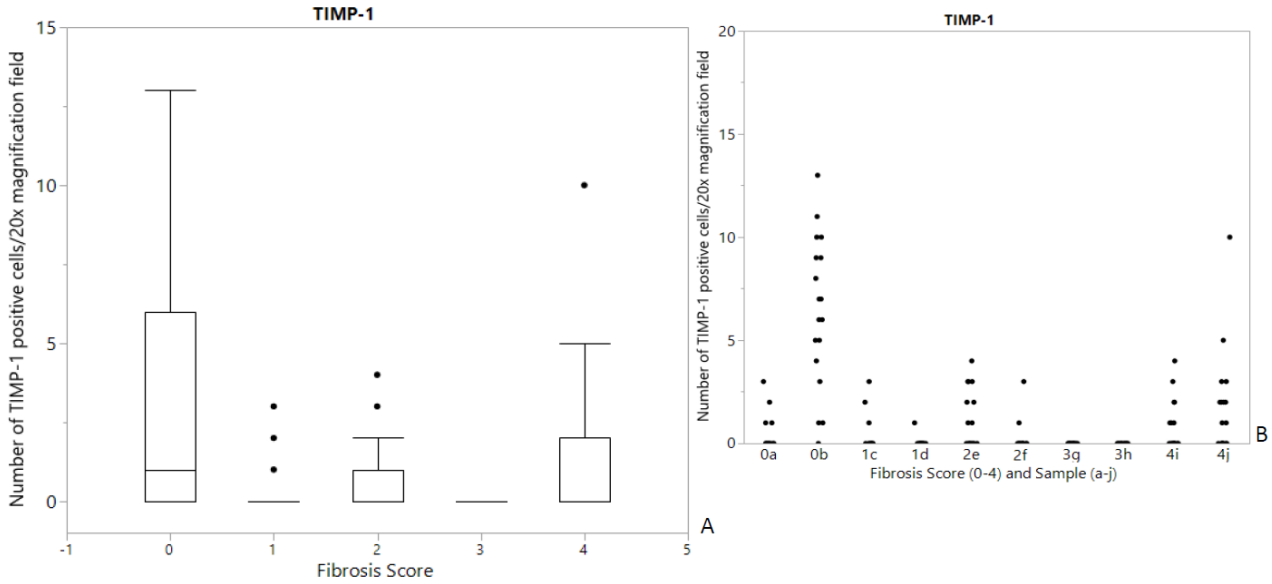

Figure 11: Number of TIMP-1 Positive Cells and Fibrosis Score. (A) An outliner box plot for each fibrosis score (0-4) is shown with mean bar and standard deviation. **(B)** Part B shows the distribution of the measurements for each sample (a-j). In the samples of fibrotic stage 3 no stained cells were detected.

5.2.2.4 αSMA and Picrosirius Red

In addition to the evaluation of the picrosirius red stained sections by a board certified veterinary pathobiologist to determine the fibrosis stage, the amount of fibrosis was assessed by image analysis (ImageJ). Ten to twenty images for each fibrosis score were analyzed. For healthy dogs with fibrosis score 0 the fibrotic proportion (area staining positively for collagen/total stained area x 100) of each 10x magnification field ranged from 0.9-3.5 % (mean: 2.0 %; SD: 1.0). For dogs with CH and fibrosis the percentage of stained area ranged from 0.4-6.0 % (mean: 2.9 %; SD: 1.5) for fibrosis score 1, from 1.4-8.1 % (mean: 4.4 %; SD: 1.9) for fibrosis score 2, from 1.7-7.7 % (mean: 4.0 %; SD: 1.6) for fibrosis score 3, and from 9.2-53.2 % (mean: 21.1 %; SD: 13.4) for fibrosis score 4. A strong positive correlation (ρ: 0.79; *P*-value: 0.0001) between fibrosis score and fibrotic proportion of each section was

found. However, a significant difference could be detected only for fibrosis score 4 compared to all other fibrosis scores (*P*-value: <0.0001), but not between lower fibrosis scores. Additionally, the comparison of the fibrotic proportion and the area of myofibroblast activation (αSMA) showed a moderate positive correlation (ρ: 0.43; *P*-value*:* 0.0002). **Figure 8** shows the picrosirius red stain for different fibrosis scores. **Figure 12** shows a box plot presentation for picrosirius red in association with the fibrotic stage (**A**) and the distribution of the measurements for the evaluated samples (**B**).

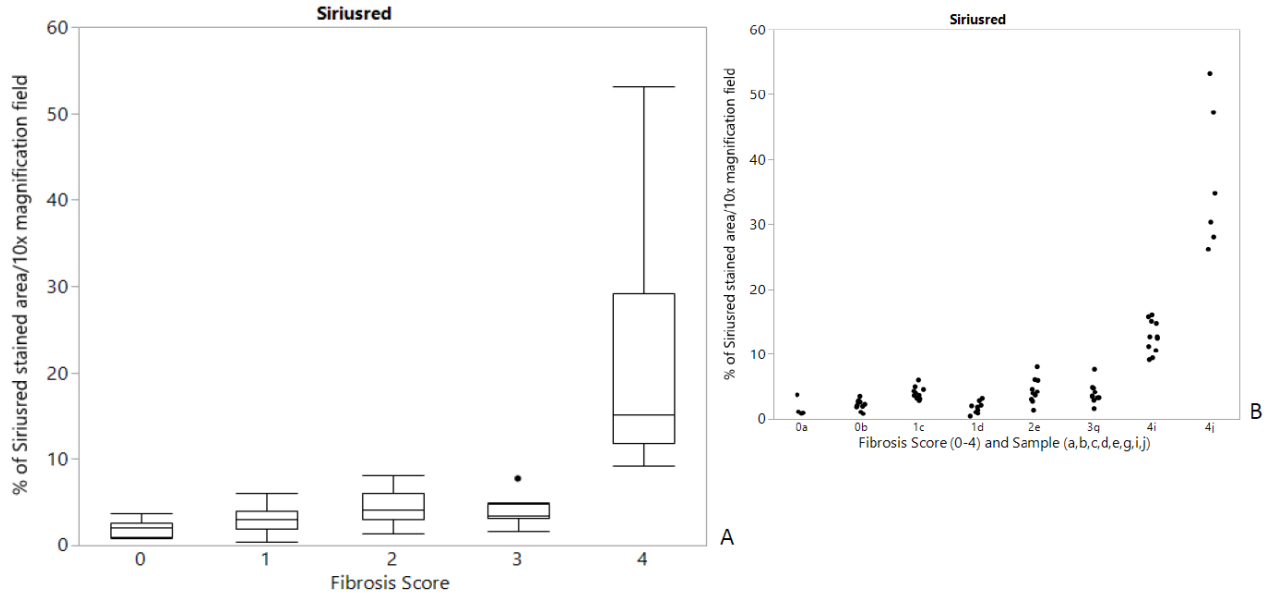

Figure 12: Percentage of Picrosirius Red Stained Area and Fibrosis Score. (A) An outliner box plot for each fibrosis score (0-4) is shown with mean bar and standard deviation. **(B)** Part B shows the distribution of the measurements for each sample (a,b,c,d,e,g,i,j). For fibrosis score 2 and 3 only one sample was available for the picrosirius red stain.

6. Discussion

6.1 RNA Sequencing and Gene Expression Analysis

This study determined the gene expression profile in liver samples of dogs with CH compared to healthy control dogs. Total RNA extraction and RNA sequencing were performed, as well as qPCRs to confirm the results. The study revealed that 651 genes were significantly differentially expressed in dogs with CH and that 190 could be assigned to hepatic fibrosis related pathways. The greatest percentage of the hepatic fibrosis-related genes were associated with hepatic stellate cell activation pathways (46 %). mRNA for PDGF and CTGF was upregulated in the RNA sequencing study with fold changes of +4.2 and +2.6, respectively. These growth factors are important mediators of HSC activation. Platelet derived growth factor initiates proliferation and migration, and promotes the survival of HSCs (Friedman 2008; Pinzani and Marra 2001). Connective tissue growth factor (CTGF) expression has been shown to be increased in human fibrotic livers and in animal models of hepatic fibrosis. In addition, serum levels of CTGF have been shown to be higher in human patients with advanced disease (Kovalenko et al. 2009). One study exists, where gene expression of fibrosis-related genes was evaluated by qPCR, that demonstrated a strong positive correlation for the upregulation of PDGF and the degree of fibrosis in dogs with CH (Kanemoto et al. 2011), but to the author's knowledge, CTGF has not been evaluated in dogs with CH and hepatic fibrosis before. mRNA for the chemokines CXCL10 (+19.1), CCL5 (+13.8), CCL2 (+8.4), CCL21 (+3.1), as well as mRNA for the chemokine receptors CX3CR1 (+7.1), CCR1 (+3.9), CCR5 (+3.8) was upregulated in this study. The chemokine (C-C motif) ligand 2 (CCL2) recruits HSCs and infiltrating macrophages to the site of liver injury and promotes functional changes, not only in HSCs, but also in portal fibroblasts, another source of ECM production during hepatic fibrosis (Ehling et al. 2014; Friedman 2008; Kruglov et al. 2006). Chemokine (C-C motif) ligand 5 (or RANTES), which is produced by the immune cells of the liver, is associated with progression of fibrosis in human patients and murine models (Berres et al. 2010; Ramm 2011). Suppression of CCL5 or treatment with antagonists for its receptors, C-C chemokine receptor type 5 (CCR5) or type 1 (CCR1) could attenuate liver fibrosis (Berres et al. 2010; Seki et al. 2009). The chemokine (C-X-C motif) ligand 10 (CXCL10), which triggers a Th1-dependent inflammatory response, has been shown to promote liver fibrosis by suppression of natural killer cells (NK cells), which are a key factor in the apoptosis of HSCs (Hintermann et al. 2010; Puche et al. 2013).

Hepatic stellate cells express the C-X-C motif chemokine receptor 3 (CXCR3), which is a receptor for both, CXCL10 and CXCL9. While CXCL10 acts in a profibrogenic way as described above, CXCL9 seems to have anti-fibrotic effects (Wasmuth et al. 2009). Chemokine (C-X-C motif) ligand 9 signaling through CXCR3 on HSCs induces CXCL1 secretion, which has been shown to affect the infiltration of immune cells, but also to promote the survival of hepatocytes. This results in a reduced activation of HSCs (Saiman and Friedman 2012; Scholten et al. 2012). The upregulation of CCL2, CCL5, and CXCL10 was confirmed by qPCR. To the author's knowledge no previous studies exist that investigate the expression of CCL2, CCL5 or CXCL10 in dogs with hepatic fibrosis.

In total, 35 % of the hepatic fibrosis-related genes were assigned to ECM remodeling, which includes ECM deposition and organization, but also ECM degradation. In a fibrotic liver the collagen content is 3-10 fold higher compared to a healthy liver, with increases in fibrillary collagens and non-fibrillary collagens (Friedman 2007). Correspondingly, in this study, in dogs with CH, which is associated with hepatic fibrosis, mRNA for many collagen types (e.g., collagen types I, III, and VI) were upregulated (fold changes: COL1A1 (+5.7), COL6A1 (+3.6), COL6A2 (+3.4), COL3A1 (+3.0)). Additionally, the measurement of the fibrotic portion in the picrosirius red stained sections in this study confirmed the increase in the amount of collagen from fibrotic score 0 to fibrotic score 4. In addition, mRNA for Chitinase 3 like 1 (CHI3L1) was upregulated in the RNA sequencing study (fold change +35.9). The CHI3L1 protein (also known as YKL-40) has a role in inflammation and tissue remodeling. Elevated serum levels of CHI3L1 have been proposed as non-invasive biomarker for hepatic fibrosis in humans (Berres et al. 2009; Kumagai et al. 2016; Schiavon et al. 2008; Tao et al. 2014) but have not been evaluated in dogs. Matrix metalloproteinases play important roles in degradation and remodeling of the ECM, but they also act on cytokines and chemokines and regulate inflammation and immunity (Duarte et al. 2015; Parks et al. 2004). Tissue inhibitors of metalloproteinases regulate the activity of MMPs, and the balance between MMPs and TIMPs seems to be a major factor in fibrosis progression or resolution (Ramachandran and Iredale 2012). In our study, gene expression for the gelatinases MMP2 and MMP9 was upregulated in dogs with CH (fold changes +7.2 and +9.9). Matrix metalloproteinase 2 (MMP2) has been shown to be increased during the process of fibrosis and decreased during recovery in rat livers (Watanabe et al. 2001). It reduces the collagen amount and can regulate the activity of tumor necrosis factor alpha, which influences apoptotic mechanisms in HSCs (Giannandrea and Parks 2014; Osawa et al. 2013; Saile et al.

1999). Overexpression of MMP9 in rodent models of hepatic fibrosis has been shown to reduce fibrosis (Osawa et al. 2013). Tissue inhibitor of metalloproteinase 1, a counter-regulator of ECM degradation and able to inhibit both, MMP2 and MMP9 (Vaillant et al. 2001), showed increased expression in dogs with CH and fibrosis in this study (+11.8). Expression of TIMP-1 has been shown to correlate with the development of fibrosis and has been evaluated as non-invasive biomarker in human patients and in dogs with chronic liver disease (Boeker et al. 2002; Lidbury et al. 2016; Rath et al. 2012). While TIMP-1 seems to be a useful biomarker in advanced fibrosis/cirrhosis in humans, it was not possible to demonstrate an association between hepatic fibrosis and TIMP-1 serum levels in a dog study (Lidbury et al. 2016). In addition to its role as inhibitor of metalloproteinase, TIMP-1 is anti-apoptotic for HSCs and supports the survival of theses cells (Vaillant et al. 2001). ADAM like decysin1 (ADAMDEC1) is a member of the disintegrin metalloproteinases family, which is not inhibited by TIMP-1 (Lund et al. 2015). The upregulation of CHI3L1 and TIMP-1 was confirmed by qPCR in this study. However, no correlation was found for the tissue expression of TIMP-1 in dogs with CH and fibrosis and the fibrosis score with immunohistochemistry.

In addition, 18 % of the hepatic fibrosis-related genes in our study could be assigned to apoptosis-related pathways (e.g., *NFKBIZ, MAPK8IP3*, *GSN*, *IL33*). Apoptosis pathways are relevant in both, fibrosis progression and fibrosis resolution. Hepatocytes that undergo apoptosis promote the activation of HSCs and fibrosis, whereas apoptosis of HSCs is important for fibrosis resolution (Wang 2014; Wang 2015). The downregulation (fold change -2.9) of NF-κB inhibitor zeta (NFKBIZ*)* in this study may support the inhibition of apoptotic pathways. During fibrogenesis, in rodent studies, HSCs have been shown to demonstrate high levels of NF-κB, which is an important transcription factor for HSC survival (Elsharkawy et al. 1999; He et al. 2014).

Only 1% of the differentially expressed genes were involved in detoxification or ROS scavenging (*CYGB*, *CYP1B1*). Reactive oxygen species (ROS) play a role in the activation of HSCs. mRNA for CYGB was upregulated in dogs with CH and fibrosis in this study (fold change +3.4). Cytoglobin is a ROS scavenger and able to suppress the activation of HSCs. Cell culture experiments showed that even extracellular treatment with cytoglobin could reduce alpha-smooth muscle actin mRNA and protein levels in HSCs (Yoshizato et al. 2016). In rodent and human liver, cytoglobin is expressed in quiescent HSCs and its expression increases with the transdifferentiation into activated myofibroblasts, as possible protection

mechanism (Kawada 2015). Unfortunately, in this study, it was not possible to evaluate CYGB expression with immunohistochemistry, probably due to the lack of antibody specificity for the canine antigen.

Few studies exist that evaluate the gene expression in dogs with CH and fibrosis. Kanemoto et al. investigated nine fibrosis-related genes (*PDGFB*, *PDGFD*, *MMP2*, *TIMP-1*, *THBS1*, *COL1A1*, *COL3A1*, *TGFB1*, and *TGFB2*) by qPCR and demonstrated a positive correlation with the degree of fibrosis for all of the genes (Kanemoto et al. 2011). Dirksen et al. investigated the gene expression in canine copper-associated chronic hepatitis in a population of Labrador retrievers using a commercially available gene expression microarray. Similiarly to this study they found that differentially expressed genes in the CH group frequently belonged to ECM remodeling pathways and include genes for collagens, metalloendopeptidases (ADAMs) or TIMPs (Dirksen et al. 2017). The results reported in these papers support the findings of the RNA sequencing study.

Interestingly, one of the study dogs (CH sample 9 from the left; **Figure 4**) was diagnosed with CH but fibrosis was not evident on histopathological examination (fibrosis score 0). It is possible that the fibrosis score of 0 occurred due to sampling error. Probably fibrosis was present in the liver of this dog but not in the obtained liver biopsy specimen and thus could not be detected on histopathological examination. Regardless, the expression profile of this dog is not consistent with the expression profiles of the healthy control dogs: some genes that showed upregulation in all of the control samples, showed decreased expression in this dog (e.g., *SPRY3*, *REN, MDM4*, or *IL3;* **Figure 4**). It is possible, that the expression profile of this dog with CH (but where fibrosis was not observed) reflects an early stage of the disease, whereas the expression profiles of all other dogs reflect the later stages of the disease. Unfortunately, as there was only one dog without apparent fibrosis (score 0) among the CH dogs, a verification or comparison to another sample could not take place.

Limitations of the study were the small size of the control group (n=6) and that it consisted exclusively of female dogs as liver biopsies were sampled during ovariohysterectomy of the dogs. Although all dogs younger than one year of age were excluded from the control group for the gene expression study, the median age of the control group (4 years) was still statistically significant lower (*P*-value = 0.014) than the median age of the dogs with CH (7.5 years). Thus, it cannot be completely excluded that some of the gene expression differences between groups were due to age and not disease status. However,

it is difficult to obtain liver samples from healthy dogs and the author does not consider the acquisition of liver tissue from dogs that are not already undergoing an abdominal surgery to be ethical. In addition, in this study, whole liver biopsies were evaluated, which means that the expression profile of individual cells (e.g., expression by HSCs) could not be assessed. Future studies could concentrate on a specific cell population. Also, mRNA expression does not necessarily reflect expression at the protein level and further studies (e.g., immunohistochemistry or ELISA studies) need to be performed to evaluate tissue expression or serum levels of the proteins of interesting genes.

6.2 Immunohistochemistry

In the transcriptomics study above, an increased gene expression was demonstrated for Ki67, TIMP-1, and CYGB. To investigate the expression at the protein level, immunohistochemistry was performed with liver sections of a subset of the same samples used for the sequencing study. Staining was successful for Ki67 and TIMP-1, but not for CYGB. To the author's knowledge this CYGB antibody had not been used for studies on dog tissue before. Although, the positive control (canine tissue, jejunum) demonstrated positive staining similar to CYGB-stained human tissue sections (cytoplasmatic staining of glandular cells), no staining could be detected in any of the liver samples. Prior to the processing of the study samples, several protocols were tested to define optimal staining conditions. It was expected to see staining in perisinusoidal HSCs (similar to the TIMP-1 stain) in healthy dogs and in dogs with CH, with an increased expression in advanced disease stages. However, gene expression does not necessarily reflect expression at the protein level. Also, in dogs, expression and tissue distribution may be different to what is described for humans or rodent models. Based on the absence of staining, it is probable that CYGB is not expressed in the canine liver samples. Another possibility is that the positive control showed false positive results. The antibody might have bound to some granules in the cells and might not be useful for detecting CYGB in formalin-fixed paraffin embedded canine tissue. Even if the sequence of the human immunogen and the canine amino acid sequence of CYGB are similar, this is not a guaranty for the utility of the antibody on canine tissue (secondary structures may play a role as well).

TIMP-1 was inconsistently detected in the cytoplasm of perisinusoidal cells (possibly HSCs). The staining seemed to be dependent on the individual sample and in some samples (i.e., in the samples for fibrosis score 3) no stained cells were observed. As in the study

group, TIMP-1 expression did not seem to be associated with the stage of fibrosis, but was different in each individual sample, it would have been interesting to screen a greater number of dogs. Despite of the strong increase in mRNA expression, TIMP-1 protein expression was not found to be upregulated in CH-dogs with fibrosis compared to healthy, non-fibrotic dogs. Therefore, TIMP-1 does not seem to be a reliable marker for HSCs in dogs. Several human studies reported, that TIMP-1 expression (mRNA and protein) was increased in liver samples with advanced fibrosis compared to the normal liver (Benyon et al. 1996; Herbst et al. 1997; Joo et al. 2000). In addition, TIMP-1 protein expression has been observed in several cell types (e.g., hepatocytes and bile duct cells) (Joo et al. 2000). The reason for the difference in expression between species is not known.

Ki67 was detected in the nuclei of proliferating liver cells (hepatocytes). The amount of stained nuclei increased with mild and moderate fibrosis and then decreased with marked and very marked fibrosis in this study. Ki67 expression has been evaluated in dogs with hepatic fibrosis before (Neumann S 2012; Sridharan et al. 2015). One of these studies reported immunohistochemical Ki67 expression in all stages of fibrosis and a positive correlation was found between Ki67 expression and the fibrotic stage, which is contradictory to the present study, where Ki67 expression was decreased in advanced hepatic fibrosis. The other study used Ki67 immunostaining to calculate the hepatocellular growth fraction as a measurement of hepatic regeneration, which seemed to be quite variable across the fibrosis scores of the evaluated samples. But, as another fibrosis scoring scale was applied in this study, a direct comparison to the present study is not possible. In the present study high Ki67 expression was found for fibrosis scores 2 and 3, where proliferation and hepatocellular remodeling is predominant. But as cellularity decreases with advanced fibrosis, a decrease in Ki67 expression can be expected. Ki67 expression for fibrosis stages 2 and 3 differed significantly from lower or higher fibrosis scores, which means Ki67 could be a useful tissue marker for medium fibrotic stages. In the RNA sequencing study, which included CH dogs of all fibrosis scores, Ki67 mRNA expression was upregulated (+10.0) compared to healthy dogs. The upregulation was confirmed by qPCR.

In the healthy canine liver, αSMA expression can be found in perisinusoidal HSCs, as well as in myofibroblasts and vascular smooth muscle cells within the portal tracts. In dogs with chronic liver disease, an increase in αSMA expression, perisinusoidally as well as in fibrotic septa, has been demonstrated in some studies, and was positively correlated with the stage of fibrosis. In other studies no significant difference or a weak negative correlation has

been reported (Boisclair et al. 2001; Mekonnen et al. 2007; Neumann et al. 2012; Vince et al. 2016). Here, an increase of αSMA was positively correlated with the stage of fibrosis. In addition, αSMA showed a moderate positive correlation with fibrotic proportion of picrosirius red stained liver sections. The picrosirius red stain is used for the histopathological evaluation and scoring of fibrosis. Interestingly, although a strong positive correlation between fibrosis scoring and image analysis was found, with image analysis, only for the last fibrosis stage (fibrosis score 4) compared to all other fibrotic stages, a significant difference in the amount of collagen was detected. Image analysis may not be reliable enough to distinguish between lower fibrosis stages. Instead, an accurate and well-accepted staging scheme with defined criteria for each fibrotic stage is needed.

Limitations of the study were the small sample size for each fibrosis score and the restricted availability of validated antibodies for formalin-fixed paraffin embedded canine tissue. Although the immunogenic sequence detected by the human CYGB antibody is similar to the amino acid sequence of the canine CYGB protein, this is not a guaranty for the usefulness of an antibody in canine tissue. Other human antibodies may exists that can detect canine CYGB, but the testing of antibodies is expensive. However, future studies could concentrate on evaluating those antibodies and, in addition, evaluate antibodies for other fibrogenic mediators to confirm the results of the sequencing study.

7. Conclusion

Transcriptome profiling by RNA sequencing analysis and confirmatory testing with a targeted gene approach by qPCRs are novel and useful methods for evaluating differential gene expression. The differential expression of fibrosis related genes and pathways in dogs with CH demonstrates that the development of hepatic fibrosis is a major event in the progression of canine chronic hepatitis. The study suggests that the same mechanisms, which are described for the pathophysiology of hepatic fibrosis in human patients (e.g., HSC activation and ECM remodeling by MMPs and TIMPs), regulate hepatic fibrosis in dogs. However, further studies with greater sample sizes and with a more targeted approach are needed – for example, by concentrating on a single cell population. Evaluation of gene expression can provide insight into the pathophysiology of CH and hepatic fibrosis and help to define possible new biomarkers for the disease. Some tissue markers of fibrogenesis investigated in this study (Ki67, αSMA), are differentially expressed in dogs with different fibrosis stages. Evaluating other fibrotic markers could be interesting and help to elucidate the mechanisms of canine hepatic fibrosis at the protein level. However, the availability of validated antibodies is restricted. Additionally, an internationally accepted staging scheme for canine hepatic fibrosis is necessary to compare different studies with each other.

8. Summary

Chronic hepatitis is a well-recognized cause for hepatic fibrosis in dogs. For the majority of chronic hepatitis cases an etiology cannot be determined and the pathophysiology of chronic hepatitis and hepatic fibrosis is still not fully understood. Evaluation of gene expression can provide insight into disease mechanisms and lead to the identification of candidate biomarkers. The aim of the RNA sequencing study was to identify differential gene expression in dogs with chronic hepatitis compared to healthy control dogs. Additionally, tissue expression of selected markers was investigated by immunohistochemistry.

The first part of this study analyzed the transcriptome of liver samples of dogs with chronic hepatitis and fibrosis compared to healthy dogs. Six-hundred-and-fifty-one genes were significantly differentially expressed in dogs with chronic hepatitis. Pathway analysis revealed a connection to pathways involved in hepatic fibrosis: genes for growth factors (e.g., *CTGF, PDGFD*), chemokines and chemokine receptors (e.g., *CCL2, CCL5, CXCL10, CCR5, CXCR3),* matrix collagens (e.g., *Col1A1, Col3A1*), and genes for ECM remodeling (e.g., *TIMP-1, MATN3, ADAMDEC1, CHI3L1, MMP9, MMP2*) are upregulated in dogs with hepatic fibrosis. These genes also play important roles in the pathophysiology of hepatic fibrosis in humans.

The second part of the study investigated the tissue distribution and expression of cytoglobin, tissue inhibitor of metalloproteinase 1, proliferation marker Ki67, and alpha-smooth muscle actin with immunohistochemistry. Expression was evaluated in association with the fibrotic stage. Neither cytoglobin nor tissue inhibitor of metalloproteinase 1 were shown to be specific markers for hepatic stellate cells or were able to distinguish between quiescent and activated hepatic stellate cells. However, Ki67 and alpha-smooth muscle actin were differentially expressed between dogs with different stages of hepatic fibrosis.

RNA-Sequenzierung, Genexpressionsanalyse und immunhistochemische Studien bei Hunden mit chronischer Hepatitis und hepatischer Fibrose

9. Zusammenfassung

Die chronische Hepatitis des Hundes ist eine häufige Ursache für Leberfibrose. Die Ursache für die chronische Hepatitis kann allerdings in den meisten Fällen nicht festgestellt werden und auch die Pathophysiologie ist noch nicht vollständig geklärt. Die Analyse der Genexpression kann Einblick geben in die beteiligten Mechanismen und Hinweise zulassen auf potentielle neue Biomarker. Das Ziel der Studie war die Untersuchung der Genexpression bei Hunden mit chronischer Hepatitis im Vergleich zu gesunden Hunden mit Hilfe von RNA-Sequenzierung. Zusätzlich wurde die Gewebeexpression ausgewählter Marker immunhistochemisch untersucht.

Der erste Teil der Arbeit befasst sich mit der Transkriptomanalyse aus Leberbiopsien von Hunden mit chronischer Hepatitis und Fibrose im Vergleich zu gesunden Hunden. Bei Hunden mit chronischer Hepatitis konnte für über 600 Gene eine signifikant veränderte Expression festgestellt werden. Eine Pathwayanalyse ergab Verbindungen zu Signalwegen, die eine wichtige Rolle bei hepatischer Fibrose spielen. Gene für Wachstumsfaktoren (z.B., *CTGF, PDGFD*), Gene für Chemokine und Chemokinrezeptoren (z.B., *CCL2, CCL5, CXCL10, CCR5, CXCR3),* Gene für Matrixkollagene (z.B., *Col1A1, Col3A1*) und Gene für Faktoren für den Umbau der extrazellulären Matrix (z.B., *TIMP-1, MATN3, ADAMDEC1, CHI3L1, MMP9, MMP2*) zeigen erhöhte Expression während chronischer Hepatitis und Fibrogenese bei Hunden. Von dem, was aus Human- und Nagerstudien bekannt ist, spielen die Genprodukte aller genannten Gene eine wichtige Rolle in der Pathophysiologie der Leberfibrose.

Der zweite Teil der Arbeit untersuchte die Gewebeverteilung und -expression von Cytoglobin, Tissue Inhibitor of Metalloproteinase 1, Proliferationsmarker Ki67 und von Alpha Smooth Muscle Actin mittels Immunhistochemie. Die Expression der Marker wurde in Relation zum Fibrosestadium betrachtet. Weder Cytoglobin noch Tissue Inhibitor of Metalloproteinase 1 ist ein spezifischer Marker für hepatische Sternzellen des Hundes. Ebensowenig ist es möglich, mit diesen Markern zwischen ruhenden und aktivierten hepatischen Sternzellen zu unterscheiden. Jedoch zeigten Ki67 und Alpha Smooth Muscle Actin differentielle Expression bei Hunden mit unterschiedlichen Fibrosestadien.

10. References

Adamus, C., Buggin-Daubie, M., Izembart, A., Sonrier-Pierre, C., Guigand, L., Masson, M. T., Andre-Fontaine, G., and Wyers, M. (1997). "Chronic hepatitis associated with leptospiral infection in vaccinated beagles." *J Comp Pathol*, 117(4), 311-28.

Adcock, I. M., Ito, K., and Barnes, P. J. (2004). "Glucocorticoids: effects on gene transcription." *Proc Am Thorac Soc*, 1(3), 247-54.

Alfadda, A. A., and Sallam, R. M. (2012). "Reactive oxygen species in health and disease." *J Biomed Biotechnol*, 2012, 936486.

Andersson, M., and Sevelius, E. (1991). "Breed, Sex and Age Distribution in Dogs with Chronic Liver-Disease - a Demographic-Study." *J Small Anim Pract*, 32(1), 1-5.

Arrese, M., Eguchi, A., and Feldstein, A. E. (2015). "Circulating microRNAs: emerging biomarkers of liver disease." *Semin Liver Dis*, 35(1), 43-54.

Banks, W. J. (1993). *Applied Veterinary Histology*, 3rd ed., St. Louis: Mosby-Year Book.

Baranova, A., Lal, P., Birerdinc, A., and Younossi, Z. M. (2011). "Non-invasive markers for hepatic fibrosis." *BMC Gastroenterol*, 11, 91.

Barnes, P. J. (1998). "Anti-inflammatory actions of glucocorticoids: molecular mechanisms." *Clin Sci (Lond)*, 94(6), 557-72.

Bataller, R., Sancho-Bru, P., Gines, P., Lora, J. M., Al-Garawi, A., Sole, M., Colmenero, J., Nicolas, J. M., Jimenez, W., Weich, N., Gutierrez-Ramos, J. C., Arroyo, V., and Rodes, J. (2003). "Activated human hepatic stellate cells express the renin-angiotensin system and synthesize angiotensin II." *Gastroenterology*, 125(1), 117-25.

Bautista, A. C., Moore, C. E., Lin, Y., Cline, M. G., Benitah, N., and Puschner, B. (2015). "Hepatopathy following consumption of a commercially available blue-green algae dietary supplement in a dog." *BMC Vet Res*, 11, 136.

Bedossa, P., Dargere, D., and Paradis, V. (2003). "Sampling variability of liver fibrosis in chronic hepatitis C." *Hepatology*, 38(6), 1449-57.

Bedossa, P., and Poynard, T. (1996). "An algorithm for the grading of activity in chronic hepatitis C. The METAVIR Cooperative Study Group." *Hepatology*, 24(2), 289-93.

Benjamini, Y., and Hochberg, Y. (1995). "Controlling the False Discovery Rate - a Practical and Powerful Approach to Multiple Testing." *J R Stat Soc Series B Stat Methodol*, 57(1), 289-300.

Benyon, R. C., Iredale, J. P., Goddard, S., Winwood, P. J., and Arthur, M. J. (1996). "Expression of tissue inhibitor of metalloproteinases 1 and 2 is increased in fibrotic human liver." *Gastroenterology*, 110(3), 821-31.

Berres, M. L., Koenen, R. R., Rueland, A., Zaldivar, M. M., Heinrichs, D., Sahin, H., Schmitz, P., Streetz, K. L., Berg, T., Gassler, N., Weiskirchen, R., Proudfoot, A., Weber, C., Trautwein, C., and Wasmuth, H. E. (2010). "Antagonism of the chemokine Ccl5 ameliorates experimental liver fibrosis in mice." *J Clin Invest*, 120(11), 4129-40.

Berres, M. L., Papen, S., Pauels, K., Schmitz, P., Zaldivar, M. M., Hellerbrand, C., Mueller, T., Berg, T., Weiskirchen, R., Trautwein, C., and Wasmuth, H. E. (2009). "A functional variation in CHI3L1 is associated with severity of liver fibrosis and YKL-40 serum levels in chronic hepatitis C infection." *J Hepatol*, 50(2), 370-6.

Bettaieb, A., Jiang, J. X., Sasaki, Y., Chao, T. I., Kiss, Z., Chen, X., Tian, J., Katsuyama, M., Yabe-Nishimura, C., Xi, Y., Szyndralewiez, C., Schroder, K., Shah, A., Brandes, R. P., Haj, F. G., and Torok, N. J. (2015). "Hepatocyte Nicotinamide Adenine Dinucleotide Phosphate Reduced Oxidase 4 Regulates Stress Signaling, Fibrosis, and Insulin Sensitivity During Development of Steatohepatitis in Mice." *Gastroenterology*, 149(2), 468-80 e10.

Bexfield, N. (2017). "Canine Idiopathic Chronic Hepatitis." *Vet Clin North Am Small Anim Pract*, 47(3), 645-663.

Bexfield, N. H., Buxton, R. J., Vicek, T. J., Day, M. J., Bailey, S. M., Haugland, S. P., Morrison, L. R., Else, R. W., Constantino-Casas, F., and Watson, P. J. (2012). "Breed, age and gender distribution of dogs with chronic hepatitis in the United Kingdom." *Vet J*, 193(1), 124-8.

Bigge, L. A., Brown, D. J., and Penninck, D. G. (2001). "Correlation between coagulation profile findings and bleeding complications after ultrasound-guided biopsies: 434 cases (1993-1996)." *J Am Anim Hosp Assoc*, 37(3), 228-33.

Bircher, J. (1999). *Oxford Textbook of Clinical Hepatology*, 2nd ed., Oxford ; New York: Oxford University Press.

Bishop, L., Strandberg, J. D., Adams, R. J., Brownstein, D. G., and Patterson, R. (1979). "Chronic active hepatitis in dogs associated with leptospires." *Am J Vet Res*, 40(6), 839-44.

Blom, I. E., Goldschmeding, R., and Leask, A. (2002). "Gene regulation of connective tissue growth factor: new targets for antifibrotic therapy?" *Matrix Biol*, 21(6), 473-82.

Boeker, K. H., Haberkorn, C. I., Michels, D., Flemming, P., Manns, M. P., and Lichtinghagen, R. (2002). "Diagnostic potential of circulating TIMP-1 and MMP-2 as markers of liver fibrosis in patients with chronic hepatitis C." *Clin Chim Acta*, 316(1-2), 71-81.

Boer, H. H., Nelson, R. W., and Long, G. G. (1984). "Colchicine therapy for hepatic fibrosis in a dog." *J Am Vet Med Assoc*, 185(3), 303-5.

Boisclair, J., Dore, M., Beauchamp, G., Chouinard, L., and Girard, C. (2001). "Characterization of the inflammatory infiltrate in canine chronic hepatitis." *Vet Pathol*, 38(6), 628-35.

Boomkens, S. Y., Penning, L. C., Egberink, H. F., van den Ingh, T. S., and Rothuizen, J. (2004). "Hepatitis with special reference to dogs. A review on the pathogenesis and infectious etiologies, including unpublished results of recent own studies." *Vet Q*, 26(3), 107-14.

Boomkens, S. Y., Slump, E., Egberink, H. F., Rothuizen, J., and Penning, L. C. (2005). "PCR screening for candidate etiological agents of canine hepatitis." *Vet Microbiol*, 108(1-2), 49-55.

Borkham-Kamphorst, E., van Roeyen, C. R., Ostendorf, T., Floege, J., Gressner, A. M., and Weiskirchen, R. (2007). "Pro-fibrogenic potential of PDGF-D in liver fibrosis." *J Hepatol*, 46(6), 1064-74.

Borkham-Kamphorst, E., and Weiskirchen, R. (2016). "The PDGF system and its antagonists in liver fibrosis." *Cytokine Growth Factor Rev*, 28, 53-61.

Brown, D. L., Van Winkle, T., Cecere, T., Rushton, S., Brachelente, C., and Cullen, J. M. (2010). "Congenital hepatic fibrosis in 5 dogs." *Vet Pathol*, 47(1), 102-7.

Bunch, S. E., Castleman, W. L., Hornbuckle, W. E., and Tennant, B. C. (1982). "Hepatic cirrhosis associated with long-term anticonvulsant drug therapy in dogs." *J Am Vet Med Assoc*, 181(4), 357-62.

Buob, S., Johnston, A. N., and Webster, C. R. (2011). "Portal hypertension: pathophysiology, diagnosis, and treatment." *J Vet Intern Med*, 25(2), 169-86.

Center, S. A., Warner, K. L., and Erb, H. N. (2002). "Liver glutathione concentrations in dogs and cats with naturally occurring liver disease." *Am J Vet Res*, 63(8), 1187-97.

Cerquetella, M., Giuliano, V., Rossi, G., Corsi, S., Laus, F., Spaterna, A., Villanacci, V., and Bassotti, G. (2012). "Chronic hepatitis in man and in dog: a comparative update." *Rev Esp Enferm Dig*, 104(4), 203-9.

Chaffee, V. W., Edds, G. T., Himes, J. A., and Neal, F. C. (1969). "Aflatoxicosis in dogs." *Am J Vet Res*, 30(10), 1737-49.

Chapman, B. L., Hendrick, M. J., and Washabau, R. J. (1993). "Granulomatous hepatitis in dogs: nine cases (1987-1990)." *J Am Vet Med Assoc*, 203(5), 680-4.

Chevallier, M., Guerret, S., Chossegros, P., Gerard, F., and Grimaud, J. A. (1994). "A histological semiquantitative scoring system for evaluation of hepatic fibrosis in needle liver biopsy specimens: comparison with morphometric studies." *Hepatology*, 20(2), 349-55.

Choi, S. S., Omenetti, A., Syn, W. K., and Diehl, A. M. (2011). "The role of Hedgehog signaling in fibrogenic liver repair." *Int J Biochem Cell Biol*, 43(2), 238-44.

Cholongitas, E., Senzolo, M., Standish, R., Marelli, L., Quaglia, A., Patch, D., Dhillon, A. P., and Burroughs, A. K. (2006). "A systematic review of the quality of liver biopsy specimens." *Am J Clin Pathol*, 125(5), 710-21.

Chouinard, L., Martineau, D., Forget, C., and Girard, C. (1998). "Use of polymerase chain reaction and immunohistochemistry for detection of canine adenovirus type 1 in formalin-fixed, paraffin-embedded liver of dogs with chronic hepatitis or cirrhosis." *J Vet Diagn Invest*, 10(4), 320-5.

Chu, A. S., Diaz, R., Hui, J. J., Yanger, K., Zong, Y., Alpini, G., Stanger, B. Z., and Wells, R. G. (2011). "Lineage tracing demonstrates no evidence of cholangiocyte epithelial-to-mesenchymal transition in murine models of hepatic fibrosis." *Hepatology*, 53(5), 1685-95.

Colloredo, G., Guido, M., Sonzogni, A., and Leandro, G. (2003). "Impact of liver biopsy size on histological evaluation of chronic viral hepatitis: the smaller the sample, the milder the disease." *J Hepatol*, 39(2), 239-44.

Cook, S., Priestnall, S. L., Blake, D., and Meeson, R. L. (2015). "Angiostrongylus vasorum Causing Severe Granulomatous Hepatitis with Concurrent Multiple Acquired PSS." *J Am Anim Hosp Assoc*, 51(5), 320-4.

Corapi, W. V., Ajithdoss, D. K., Snowden, K. F., and Spaulding, K. A. (2011). "Multi-organ involvement of Heterobilharzia americana infection in a dog presented for systemic mineralization." *J Vet Diagn Invest*, 23(4), 826-31.

Coronado, V. A., O'Neill, B., Nanji, M., and Cox, D. W. (2008). "Polymorphisms in canine ATP7B: candidate modifier of copper toxicosis in the Bedlington terrier." *Vet J*, 177(2), 293-6.

Corpechot, C. (2016). "Primary Biliary Cirrhosis Beyond Ursodeoxycholic Acid." *Semin Liver Dis*, 36(1), 15-26.

Crosas-Molist, E., and Fabregat, I. (2015). "Role of NADPH oxidases in the redox biology of liver fibrosis." *Redox Biol*, 6, 106-11.

Cullen, J. (2015). "Liver and Biliary System", in G. Maxie, (ed.), *Jubb, Kennedy & Palmer's Pathology of Domestic Animals*. Saunders Elsevier.

Cullen, J. M. (2009). "Summary of the World Small Animal Veterinary Association standardization committee guide to classification of liver disease in dogs and cats." *Vet Clin North Am Small Anim Pract*, 39(3), 395-418.

Czaja, A. J. (2014). "Hepatic inflammation and progressive liver fibrosis in chronic liver disease." *World J Gastroenterol*, 20(10), 2515-32.

Daneshpour, N., Griffin, M., Collighan, R., and Perrie, Y. (2011). "Targeted delivery of a novel group of site-directed transglutaminase inhibitors to the liver using liposomes: a new approach for the potential treatment of liver fibrosis." *J Drug Target*, 19(8), 624-31.

Dayrell-Hart, B., Steinberg, S. A., VanWinkle, T. J., and Farnbach, G. C. (1991). "Hepatotoxicity of phenobarbital in dogs: 18 cases (1985-1989)." *J Am Vet Med Assoc*, 199(8), 1060-6.

De Minicis, S., and Brenner, D. A. (2007). "NOX in liver fibrosis." *Arch Biochem Biophys*, 462(2), 266-72.

Dellmann, H.-D., and Brown, E. M. (1987). *Textbook of Veterinary Histology*, 3rd. ed., Philadelphia: Lea & Febiger.

Dendooven, A., Gerritsen, K. G., Nguyen, T. Q., Kok, R. J., and Goldschmeding, R. (2011). "Connective tissue growth factor (CTGF/CCN2) ELISA: a novel tool for monitoring fibrosis." *Biomarkers*, 16(4), 289-301.

Dirksen, K., and Fieten, H. (2017). "Canine Copper-Associated Hepatitis." *Vet Clin North Am Small Anim Pract*., 47(3), 631-644.

Dirksen, K., Spee, B., Penning, L. C., van den Ingh, T., Burgener, I. A., Watson, A. L., Groot Koerkamp, M., Rothuizen, J., van Steenbeek, F. G., and Fieten, H. (2017). "Gene expression patterns in the progression of canine copper-associated chronic hepatitis." *PLoS One*, 12(5), e0176826.

Dirksen, K., Verzijl, T., Grinwis, G. C., Favier, R. P., Penning, L. C., Burgener, I. A., van der Laan, L. J., Fieten, H., and Spee, B. (2016). "Use of Serum MicroRNAs as Biomarker for Hepatobiliary Diseases in Dogs." *J Vet Intern Med*, 30(6), 1816-1823.

Duarte, S., Baber, J., Fujii, T., and Coito, A. J. (2015). "Matrix metalloproteinases in liver injury, repair and fibrosis." *Matrix Biol*, 44-46, 147-56.

Dundar, H. Z., and Yilmazlar, T. (2015). "Management of hepatorenal syndrome." *World J Nephrol*, 4(2), 277-86.

Ehling, J., Bartneck, M., Wei, X., Gremse, F., Fech, V., Mockel, D., Baeck, C., Hittatiya, K., Eulberg, D., Luedde, T., Kiessling, F., Trautwein, C., Lammers, T., and Tacke, F. (2014). "CCL2-dependent infiltrating macrophages promote angiogenesis in progressive liver fibrosis." *Gut*, 63(12), 1960-71.

El Serafy, M. A., Kassem, A. M., Omar, H., Mahfouz, M. S., and El Said El Raziky, M. (2017). "APRI test and hyaluronic acid as non-invasive diagnostic tools for post HCV liver fibrosis: Systematic review and meta-analysis." *Arab J Gastroenterol*, 18(2), 51-57.

Elsharkawy, A. M., Wright, M. C., Hay, R. T., Arthur, M. J., Hughes, T., Bahr, M. J., Degitz, K., and Mann, D. A. (1999). "Persistent activation of nuclear factor-kappaB in cultured rat hepatic stellate cells involves the induction of potentially novel Rel-like factors and prolonged changes in the expression of IkappaB family proteins." *Hepatology*, 30(3), 761-9.

Ettinger, S. J., Feldman, E. C., and Côté, E. (2017). "Section XIX: Hepatobiliary Disease", 1611-1680, in: *Textbook of Veterinary Internal Medicine*, 8th ed., St. Louis, Missouri: Elsevier.

Evans, H. E., and Miller, M. E. (2013). *Miller's Anatomy of the Dog*, St. Louis, Missouri: Elsevier.

Favier, R. P. (2009). "Idiopathic hepatitis and cirrhosis in dogs." *Vet Clin North Am Small Anim Pract*, 39(3), 481-8.

Favier, R. P., Poldervaart, J. H., van den Ingh, T. S., Penning, L. C., and Rothuizen, J. (2013). "A retrospective study of oral prednisolone treatment in canine chronic hepatitis." *Vet Q*, 33(3), 113-20.

Ferguson, F. C., Jr. (1952). "Colchicine. I. General pharmacology." *J Pharmacol Exp Ther*, 106(3), 261-70.

Ferraioli, G., Parekh, P., Levitov, A. B., and Filice, C. (2014). "Shear wave elastography for evaluation of liver fibrosis." *J Ultrasound Med*, 33(2), 197-203.

Fieten, H., Biourge, V. C., Watson, A. L., Leegwater, P. A., van den Ingh, T. S., and Rothuizen, J. (2014). "Nutritional management of inherited copper-associated hepatitis in the Labrador retriever." *Vet J*, 199(3), 429-33.

Fieten, H., Dirksen, K., van den Ingh, T. S., Winter, E. A., Watson, A. L., Leegwater, P. A., and Rothuizen, J. (2013). "D-penicillamine treatment of copper-associated hepatitis in Labrador retrievers." *Vet J*, 196(3), 522-7.

Fieten, H., Gill, Y., Martin, A. J., Concilli, M., Dirksen, K., van Steenbeek, F. G., Spee, B., van den Ingh, T. S., Martens, E. C., Festa, P., Chesi, G., van de Sluis, B., Houwen, R. H., Watson, A. L., Aulchenko, Y. S., Hodgkinson, V. L., Zhu, S., Petris, M. J., Polishchuk, R. S., Leegwater, P. A., and Rothuizen, J. (2016). "The Menkes and Wilson disease genes counteract in copper toxicosis in Labrador retrievers: a new canine model for copper-metabolism disorders." *Dis Model Mech*, 9(1), 25-38.

Flores-Contreras, L., Sandoval-Rodriguez, A. S., Mena-Enriquez, M. G., Lucano-Landeros, S., Arellano-Olivera, I., Alvarez-Alvarez, A., Sanchez-Parada, M. G., and Armendariz-Borunda, J. (2014). "Treatment with pirfenidone for two years decreases fibrosis, cytokine levels and enhances CB2 gene expression in patients with chronic hepatitis C." *BMC Gastroenterol*, 14, 131.

Friedman, S. L. (1993). "Seminars in medicine of the Beth Israel Hospital, Boston. The cellular basis of hepatic fibrosis. Mechanisms and treatment strategies." *N Engl J Med*, 328(25), 1828-35.

Friedman, S. L. (2008). "Hepatic stellate cells: protean, multifunctional, and enigmatic cells of the liver." *Physiol Rev*, 88(1), 125-72.

Friedman, S. L. (2010). "Evolving challenges in hepatic fibrosis." *Nat Rev Gastroenterol Hepatol*, 7(8), 425-36.

Friedman, S. L. (2007). "Hepatic fibrosis", in: Schiff, E. R., Sorrell, M. F., and Maddrey, W. C., *Schiff's Diseases of the Liver*, Philadelphia: Lippincott Williams & Wilkins.

Fry, W., Lester, C., Etedali, N. M., Shaw, S., DeLaforcade, A., and Webster, C. R. (2017). "Thromboelastography in Dogs with Chronic Hepatopathies." *J Vet Intern Med*, 31(2), 419-426.

Gabriel, A., van den Ingh, T. S., Clercx, C., and Peeters, D. (2006). "Suspected drug-induced destructive cholangitis in a young dog." *J Small Anim Pract*, 47(6), 344-8.

Gao, R., and Brigstock, D. R. (2004). "Connective tissue growth factor (CCN2) induces adhesion of rat activated hepatic stellate cells by binding of its C-terminal domain to integrin alpha(v)beta(3) and heparan sulfate proteoglycan." *J Biol Chem*, 279(10), 8848-55.

Giannandrea, M., and Parks, W. C. (2014). "Diverse functions of matrix metalloproteinases during fibrosis." *Dis Model Mech*, 7(2), 193-203.

Glinska-Suchocka, K., Orlowska, A., Jankowski, M., Kubiak, K., and Spuzak, J. (2016a). "Serum concentrations of PIIINP aminopeptide in dogs with liver fibrosis." *Pol J Vet Sci*, 19(2), 365-9.

Glinska-Suchocka, K., Orlowska, A., Kubiak, K., Spuzak, J., and Jankowski, M. (2016b). "7S Fragment of Type IV Collagen as a Serum Marker of Canine Liver Fibrosis." *Pol J Vet Sci*, 19(3), 647-649.

Glinska-Suchocka, K., Orlowska, A., Spuzak, J., Jankowski, M., and Kubiak, K. (2015). "Suitability of using serum hialuronic acid concentrations in the diagnosis of canine liver fibrosis." *Pol J Vet Sci*, 18(4), 873-8.

Gocke, D. J., Preisig, R., Morris, T. Q., McKay, D. G., and Bradley, S. E. (1967). "Experimental viral hepatitis in the dog: production of persistent disease in partially immune animals." *J Clin Invest*, 46(9), 1506-17.

Goodman, Z. D. (2007). "Grading and staging systems for inflammation and fibrosis in chronic liver diseases." *J Hepatol*, 47(4), 598-607.

Grenard, P., Bresson-Hadni, S., El Alaoui, S., Chevallier, M., Vuitton, D. A., and Ricard-Blum, S. (2001). "Transglutaminase-mediated cross-linking is involved in the stabilization of extracellular matrix in human liver fibrosis." *J Hepatol*, 35(3), 367-75.

Gressner, O. A., Rizk, M. S., Kovalenko, E., Weiskirchen, R., and Gressner, A. M. (2008). "Changing the pathogenetic roadmap of liver fibrosis? Where did it start; where will it go?" *J Gastroenterol Hepatol*, 23(7 Pt 1), 1024-35.

Hackett, E. S., Twedt, D. C., and Gustafson, D. L. (2013). "Milk thistle and its derivative compounds: a review of opportunities for treatment of liver disease." *J Vet Intern Med*, 27(1), 10-6.

Hall, J. E., and Guyton, A. C. (2015). "Unit XII: Gastrointestinal Physiology", 771-824, in: *Guyton and Hall Textbook of Medical Physiology*, 13th ed., Philadelphia, Pa.: Saunders/Elsevier.

He, X., Pu, G., Tang, R., Zhang, D., and Pan, W. (2014). "Activation of nuclear factor kappa B in the hepatic stellate cells of mice with schistosomiasis japonica." *PLoS One*, 9(8), e104323.

Herbst, H., Wege, T., Milani, S., Pellegrini, G., Orzechowski, H. D., Bechstein, W. O., Neuhaus, P., Gressner, A. M., and Schuppan, D. (1997). "Tissue inhibitor of metalloproteinase-1 and -2 RNA expression in rat and human liver fibrosis." *Am J Pathol*, 150(5), 1647-59.

Hintermann, E., Bayer, M., Pfeilschifter, J. M., Luster, A. D., and Christen, U. (2010). "CXCL10 promotes liver fibrosis by prevention of NK cell mediated hepatic stellate cell inactivation." *J Autoimmun*, 35(4), 424-35.

Honeckman, A. (2003). "Current concepts in the treatment of canine chronic hepatitis." *Clin Tech Small Anim Pract*, 18(4), 239-44.

Hyttel, P. (2010). *Essentials of Domestic Animal Embryology*, Edinburgh ; New York: Saunders/Elsevier.

Imbert-Bismut, F., Ratziu, V., Pieroni, L., Charlotte, F., Benhamou, Y., Poynard, T., and Group, M. (2001). "Biochemical markers of liver fibrosis in patients with hepatitis C virus infection: a prospective study." *Lancet*, 357(9262), 1069-75.

Inagaki, Y., and Okazaki, I. (2007). "Emerging insights into Transforming growth factor beta Smad signal in hepatic fibrogenesis." *Gut*, 56(2), 284-92.

Iredale, J. (2008). "Defining therapeutic targets for liver fibrosis: exploiting the biology of inflammation and repair." *Pharmacol Res*, 58(2), 129-36.

Iredale, J. P. (2007). "Models of liver fibrosis: exploring the dynamic nature of inflammation and repair in a solid organ." *J Clin Invest*, 117(3), 539-48.

Iredale, J. P., Benyon, R. C., Arthur, M. J., Ferris, W. F., Alcolado, R., Winwood, P. J., Clark, N., and Murphy, G. (1996). "Tissue inhibitor of metalloproteinase-1 messenger RNA expression is enhanced relative to interstitial collagenase messenger RNA in experimental liver injury and fibrosis." *Hepatology*, 24(1), 176-84.

Iredale, J. P., Murphy, G., Hembry, R. M., Friedman, S. L., and Arthur, M. J. (1992). "Human hepatic lipocytes synthesize tissue inhibitor of metalloproteinases-1. Implications for regulation of matrix degradation in liver." *J Clin Invest*, 90(1), 282-7.

Ishak, K., Baptista, A., Bianchi, L., Callea, F., De Groote, J., Gudat, F., Denk, H., Desmet, V., Korb, G., MacSween, R. N., and et al. (1995). "Histological grading and staging of chronic hepatitis." *J Hepatol*, 22(6), 696-9.

Issa, R., Zhou, X., Constandinou, C. M., Fallowfield, J., Millward-Sadler, H., Gaca, M. D., Sands, E., Suliman, I., Trim, N., Knorr, A., Arthur, M. J., Benyon, R. C., and Iredale, J. P. (2004). "Spontaneous recovery from micronodular cirrhosis: evidence for incomplete resolution associated with matrix cross-linking." *Gastroenterology*, 126(7), 1795-808.

Iwaisako, K., Jiang, C., Zhang, M., Cong, M., Moore-Morris, T. J., Park, T. J., Liu, X., Xu, J., Wang, P., Paik, Y. H., Meng, F., Asagiri, M., Murray, L. A., Hofmann, A. F., Iida, T., Glass, C. K., Brenner, D. A., and Kisseleva, T. (2014). "Origin of myofibroblasts in the fibrotic liver in mice." *Proc Natl Acad Sci U S A*, 111(32), E3297-305.

Jonsson, J. R., Clouston, A. D., Ando, Y., Kelemen, L. I., Horn, M. J., Adamson, M. D., Purdie, D. M., and Powell, E. E. (2001). "Angiotensin-converting enzyme inhibition attenuates the progression of rat hepatic fibrosis." *Gastroenterology*, 121(1), 148-55.

Joo, Y. E., Seo, Y. H., Lee, W. S., Kim, H. S., Choi, S. K., Rew, J. S., Park, C. S., and Kim, S. J. (2000). "Expression of tissue inhibitors of metalloproteinases (TIMPs) in hepatocellular carcinoma." *Korean J Intern Med*, 15(3), 171-8.

Kagoshima, M., Ito, K., Cosio, B., and Adcock, I. M. (2003). "Glucocorticoid suppression of nuclear factor-kappa B: a role for histone modifications." *Biochem Soc Trans*, 31(Pt 1), 60-5.

Kalluri, R., and Weinberg, R. A. (2009). "The basics of epithelial-mesenchymal transition." *J Clin Invest*, 119(6), 1420-8.

Kaneko, Y., Torisu, S., Hagio, M., Yamaguchi, R., Mizutani, S., and Naganobu, K. (2016). "A case report of suspected hepatopulmonary syndrome secondary to ductal plate malformation with chronic active hepatitis in a dog." *J Vet Med Sci*, 78(3), 493-7.

Kanemoto, H., Ohno, K., Sakai, M., Nakashima, K., Takahashi, M., Fujino, Y., and Tsujimoto, H. (2009). "Blood hyaluronic acid as a marker for canine cirrhosis." *J Vet Med Sci*, 71(9), 1251-4.

Kanemoto, H., Ohno, K., Sakai, M., Nakashima, K., Takahashi, M., Fujino, Y., and Tsujimoto, H. (2011). "Expression of fibrosis-related genes in canine chronic hepatitis." *Vet Pathol*, 48(4), 839-45.

Karin, D., Koyama, Y., Brenner, D., and Kisseleva, T. (2016). "The characteristics of activated portal fibroblasts/myofibroblasts in liver fibrosis." *Differentiation*, 92(3), 84-92.

Kawada, N. (2015). "Cytoglobin as a Marker of Hepatic Stellate Cell-derived Myofibroblasts." *Front Physiol*, 6, 329.

Kemp, S. D., Zimmerman, K. L., Panciera, D. L., Monroe, W. E., and Leib, M. S. (2015). "Histopathologic Variation between Liver Lobes in Dogs." *J Vet Intern Med*, 29(1), 58-62.

Kemp, T. J., Aggeli, I. K., Sugden, P. H., and Clerk, A. (2004). "Phenylephrine and endothelin-1 upregulate connective tissue growth factor in neonatal rat cardiac myocytes." *J Mol Cell Cardiol*, 37(2), 603-6.

Kiryu, M., Niwano, S., Niwano, H., Kishihara, J., Aoyama, Y., Fukaya, H., Masaki, Y., and Izumi, T. (2012). "Angiotensin II-mediated up-regulation of connective tissue growth factor promotes atrial tissue fibrosis in the canine atrial fibrillation model." *Europace*, 14(8), 1206-14.

Kordes, C., Sawitza, I., Gotze, S., and Haussinger, D. (2013). "Hepatic stellate cells support hematopoiesis and are liver-resident mesenchymal stem cells." *Cell Physiol Biochem*, 31(2-3), 290-304.

Kovalenko, E., Tacke, F., Gressner, O. A., Zimmermann, H. W., Lahme, B., Janetzko, A., Wiederholt, T., Berg, T., Muller, T., Trautwein, C., Gressner, A. M., and Weiskirchen, R. (2009). "Validation of connective tissue growth factor (CTGF/CCN2) and its gene polymorphisms as noninvasive biomarkers for the assessment of liver fibrosis." *J Viral Hepat*, 16(9), 612-20.

Kruglov, E. A., Nathanson, R. A., Nguyen, T., and Dranoff, J. A. (2006). "Secretion of MCP-1/CCL2 by bile duct epithelia induces myofibroblastic transdifferentiation of portal fibroblasts." *Am J Physiol Gastrointest Liver Physiol*, 290(4), G765-71.

Kumagai, E., Mano, Y., Yoshio, S., Shoji, H., Sugiyama, M., Korenaga, M., Ishida, T., Arai, T., Itokawa, N., Atsukawa, M., Hyogo, H., Chayama, K., Ohashi, T., Ito, K., Yoneda, M., Kawaguchi, T., Torimura, T., Nozaki, Y., Watanabe, S., Mizokami, M., and Kanto, T. (2016). "Serum YKL-40 as a marker of liver fibrosis in patients with non-alcoholic fatty liver disease." *Sci Rep*, 6, 35282.

Kumar, M. S. A. (2013). *Clinically Oriented Anatomy of the Dog & Cat*, Ronkonkoma, NY 11779: Linus Learning.

Kurikawa, N., Suga, M., Kuroda, S., Yamada, K., and Ishikawa, H. (2003). "An angiotensin II type 1 receptor antagonist, olmesartan medoxomil, improves experimental liver fibrosis by suppression of proliferation and collagen synthesis in activated hepatic stellate cells." *Br J Pharmacol*, 139(6), 1085-94.

Kvitko-White, H. L., Sayre, R. S., Corapi, W. V., and Spaulding, K. A. (2011). "Imaging diagnosis-heterobilharzia americana infection in a dog." *Vet Radiol Ultrasound*, 52(5), 538-41.

Lan, T., Kisseleva, T., and Brenner, D. A. (2015). "Deficiency of NOX1 or NOX4 Prevents Liver Inflammation and Fibrosis in Mice through Inhibition of Hepatic Stellate Cell Activation." *PLoS One*, 10(7), e0129743.

Latshaw, W. K., and Latshaw, J. L. K. (1987). *Veterinary Developmental Anatomy : a clinically oriented approach*, Toronto, Philadelphia; Saint Louis, Mo.: B.C. Decker ; C.V. Mosby Co. distributor.

Lechuga, C. G., Hernandez-Nazara, Z. H., Hernandez, E., Bustamante, M., Desierto, G., Cotty, A., Dharker, N., Choe, M., and Rojkind, M. (2006). "PI3K is involved in PDGF-beta receptor upregulation post-PDGF-BB treatment in mouse HSC." *Am J Physiol Gastrointest Liver Physiol*, 291(6), G1051-61.

Lecoindre A, L. P., Chevallier M, et al. (2015). "A new combination of blood parameters for accurate non-invasive diagnosis of liver fibrosis in dogs."*J Vet Intern Med*. City, pp. 1197.

Lee, H. S. J. (2000). *Dates in Gastroenterology*, New York: Parthenon Pub. Group.

Lemoinne, S., Cadoret, A., Rautou, P. E., El Mourabit, H., Ratziu, V., Corpechot, C., Rey, C., Bosselut, N., Barbu, V., Wendum, D., Feldmann, G., Boulanger, C., Henegar, C., Housset, C., and Thabut, D. (2015). "Portal Myofibroblasts Promote Vascular Remodeling Underlying Cirrhosis Formation Through the Release of Microparticles." *Hepatology*, 61(3), 1041-1055.

Lemoinne, S., Thabut, D., and Housset, C. (2016). "Portal myofibroblasts connect angiogenesis and fibrosis in liver." *Cell and Tissue Research*, 365(3), 583-589.

Li, P., Robertson, T. A., Zhang, Q., Fletcher, L. M., Crawford, D. H., Weiss, M., and Roberts, M. S. (2012). "Hepatocellular necrosis, fibrosis and microsomal activity determine the hepatic pharmacokinetics of basic drugs in right-heart-failure-induced liver damage." *Pharm Res*, 29(6), 1658-69.

Liang, S., Kisseleva, T., and Brenner, D. A. (2016). "The Role of NADPH Oxidases (NOXs) in Liver Fibrosis and the Activation of Myofibroblasts." *Front Physiol*, 7, 17.

Lidbury, J. A. (2016). "Potential of circulating microRNAs as biomarkers in veterinary medicine." *Vet J*, 212, 78-9.

Lidbury, J. A. (2017). "Getting the Most Out of Liver Biopsy." *Vet Clin North Am Small Anim Pract*, 47(3), 569-583.

Lidbury, J. A., Cook, A. K., and Steiner, J. M. (2016). "Hepatic encephalopathy in dogs and cats." *J Vet Emerg Crit Care,* 26(4), 471-87.

Lidbury, J. A., Hoffmann, A. R., Fry, J. K., Suchodolski, J. S., and Steiner, J. M. (2016). "Evaluation of hyaluronic acid, procollagen type III N-terminal peptide, and tissue inhibitor of matrix metalloproteinase-1 as serum markers of canine hepatic fibrosis." *Can J Vet Res*, 80(4), 302-308.

Lidbury, J. A., Rodrigues Hoffmann, A., Ivanek, R., Cullen, J. M., Porter, B. F., Oliveira, F., Van Winkle, T. J., Grinwis, G. C., Sucholdolski, J. S., and Steiner, J. M. (2017). "Interobserver Agreement Using Histological Scoring of the Canine Liver." *J Vet Intern Med*, 31(3), 778-783.

Liu, J., Gong, H., Zhang, Z. T., and Wang, Y. (2008). "Effect of angiotensin II and angiotensin II type 1 receptor antagonist on the proliferation, contraction and collagen synthesis in rat hepatic stellate cells." *Chin Med J (Engl)*, 121(2), 161-5.

Livak, K. J., and Schmittgen, T. D. (2001). "Analysis of relative gene expression data using real-time quantitative PCR and the 2(-Delta Delta C(T)) Method." *Methods*, 25(4), 402-8.

Lua, I., Li, Y., Zagory, J. A., Wang, K. S., French, S. W., Sevigny, J., and Asahina, K. (2016). "Characterization of hepatic stellate cells, portal fibroblasts, and mesothelial cells in normal and fibrotic livers." *J Hepatol*, 64(5), 1137-46.

Lubel, J. S., Herath, C. B., Burrell, L. M., and Angus, P. W. (2008). "Liver disease and the renin-angiotensin system: recent discoveries and clinical implications." *J Gastroenterol Hepatol*, 23(9), 1327-38.

Lubel, J. S., Herath, C. B., Tchongue, J., Grace, J., Jia, Z., Spencer, K., Casley, D., Crowley, P., Sievert, W., Burrell, L. M., and Angus, P. W. (2009). "Angiotensin-(1-7), an alternative metabolite of the renin-angiotensin system, is up-regulated in human liver disease and has antifibrotic activity in the bile-duct-ligated rat." *Clin Sci (Lond)*, 117(11), 375-86.

Lund, J., Troeberg, L., Kjeldal, H., Olsen, O. H., Nagase, H., Sorensen, E. S., Stennicke, H. R., Petersen, H. H., and Overgaard, M. T. (2015). "Evidence for restricted reactivity of ADAMDEC1 with protein substrates and endogenous inhibitors." *J Biol Chem*, 290(10), 6620-9.

Ma, J. Q., Ding, J., Zhang, L., and Liu, C. M. (2015). "Protective effects of ursolic acid in an experimental model of liver fibrosis through Nrf2/ARE pathway." *Clin Res Hepatol Gastroenterol*, 39(2), 188-97.

Mallat, A., and Lotersztajn, S. (2013). "Cellular mechanisms of tissue fibrosis. 5. Novel insights into liver fibrosis." *Am J Physiol Cell Physiol*, 305(8), C789-99.

Mani, N. (1959). *Die historischen Grundlagen der Leberforschung*, Basel,: B. Schwabe.

Manna, S. K., Mukhopadhyay, A., Van, N. T., and Aggarwal, B. B. (1999). "Silymarin suppresses TNF-induced activation of NF-kappa B, c-Jun N-terminal kinase, and apoptosis." *J Immunol*, 163(12), 6800-9.

McAlister, A., Center, S. A., Bender, H., and McDonough, S. P. (2014). "Adverse interaction between colchicine and ketoconazole in a Chinese shar pei." *J Am Anim Hosp Assoc*, 50(6), 417-23.

McGrotty, Y. L., Ramsey, I. K., and Knottenbelt, C. M. (2003). "Diagnosis and management of hepatic copper accumulation in a Skye terrier." *J Small Anim Pract*, 44(2), 85-9.

Mekonnen, G. A., Ijzer, J., and Nederbragt, H. (2007). "Tenascin-C in chronic canine hepatitis: immunohistochemical localization and correlation with necro-inflammatory activity, fibrotic stage, and expression of alpha-smooth muscle actin, cytokeratin 7, and CD3+ cells." *Vet Pathol*, 44(6), 803-13.

Meyer, D. J., Thompson, M. B., and Senior, D. F. (1997). "Use of ursodeoxycholic acids in a dog with chronic hepatitis: effects on serum hepatic tests and endogenous bile acid composition." *J Vet Intern Med*, 11(3), 195-7.

Mizooku, H., Kagawa, Y., Matsuda, K., Okamoto, M., and Taniyama, H. (2013). "Histological and immunohistochemical evaluations of lobular dissecting hepatitis in American cocker spaniel dogs." *J Vet Med Sci*, 75(5), 597-603.

Murakami, Y., Toyoda, H., Tanahashi, T., Tanaka, J., Kumada, T., Yoshioka, Y., Kosaka, N., Ochiya, T., and Taguchi, Y. H. (2012). "Comprehensive miRNA expression analysis in peripheral blood can diagnose liver disease." *PLoS One*, 7(10), e48366.

Muriel, P., Moreno, M. G., Hernandez Mdel, C., Chavez, E., and Alcantar, L. K. (2005). "Resolution of liver fibrosis in chronic CCl4 administration in the rat after discontinuation of treatment: effect of silymarin, silibinin, colchicine and trimethylcolchicinic acid." *Basic Clin Pharmacol Toxicol*, 96(5), 375-80.

Neumann, S., Kaup, F. J., and Beardi, B. (2008). "Plasma concentration of transforming growth factor-beta1 and hepatic fibrosis in dogs." *Can J Vet Res*, 72(5), 428-31.

Neumann S, K. F. (2012). "α-SMA and Ki-67 Immunohistochemistry as Indicators for the Fibrotic Remodeling Process in the Liver of Dogs." *J Adv Vet Res, 2, 42-47.*

Newberne, P. M. (1973). "Chronic aflatoxicosis." *J Am Vet Med Assoc*, 163(11), 1262-7.

Nikolaidis, N., Kountouras, J., Giouleme, O., Tzarou, V., Chatzizisi, O., Patsiaoura, K., Papageorgiou, A., Leontsini, M., Eugenidis, N., and Zamboulis, C. (2006). "Colchicine treatment of liver fibrosis." *Hepatogastroenterology*, 53(68), 281-5.

Oakley, F., Teoh, V., Ching, A. S. G., Bataller, R., Colmenero, J., Jonsson, J. R., Eliopoulos, A. G., Watson, M. R., Manas, D., and Mann, D. A. (2009). "Angiotensin II activates I kappaB kinase phosphorylation of RelA at Ser 536 to promote myofibroblast survival and liver fibrosis." *Gastroenterology*, 136(7), 2334-2344 e1.

Omenetti, A., Choi, S., Michelotti, G., and Diehl, A. M. (2011). "Hedgehog signaling in the liver." *J Hepatol*, 54(2), 366-73.

Omenetti, A., and Diehl, A. M. (2011). "Hedgehog signaling in cholangiocytes." *Curr Opin Gastroenterol*, 27(3), 268-75.

Osawa, Y., Hoshi, M., Yasuda, I., Saibara, T., Moriwaki, H., and Kozawa, O. (2013). "Tumor necrosis factor-alpha promotes cholestasis-induced liver fibrosis in the mouse through tissue inhibitor of metalloproteinase-1 production in hepatic stellate cells." *PLoS One*, 8(6), e65251.

Osumi, T., Ohno, K., Kanemoto, H., Nakashima, K., Uchida, K., Karasawa, A., Fujino, Y., and Tsujimoto, H. (2011). "A case of recovery from canine destructive cholangitis in a Miniature Dachshund." *J Vet Med Sci*, 73(7), 937-9.

Otte, C. M., Penning, L. C., Rothuizen, J., and Favier, R. P. (2013). "Retrospective comparison of prednisolone and ursodeoxycholic acid for the treatment of feline lymphocytic cholangitis." *Vet J*, 195(2), 205-9.

Otte, C. M., Rothuizen, J., Favier, R. P., Penning, L. C., and Vreman, S. (2014). "A morphological and immunohistochemical study of the effects of prednisolone or ursodeoxycholic acid on liver histology in feline lymphocytic cholangitis." *J Feline Med Surg*, 16(10), 796-804.

Parks, W. C., Wilson, C. L., and Lopez-Boado, Y. S. (2004). "Matrix metalloproteinases as modulators of inflammation and innate immunity." *Nat Rev Immunol*, 4(8), 617-29.

Pellicoro, A., Ramachandran, P., and Iredale, J. P. (2012). "Reversibility of liver fibrosis." *Fibrogenesis Tissue Repair*, 5(Suppl 1), S26.

Pereira, R. M., dos Santos, R. A., da Costa Dias, F. L., Teixeira, M. M., and Simoes e Silva, A. C. (2009). "Renin-angiotensin system in the pathogenesis of liver fibrosis." *World J Gastroenterol*, 15(21), 2579-86.

Pereira, R. M., Dos Santos, R. A., Teixeira, M. M., Leite, V. H., Costa, L. P., da Costa Dias, F. L., Barcelos, L. S., Collares, G. B., and Simoes e Silva, A. C. (2007). "The renin-angiotensin system in a rat model of hepatic fibrosis: evidence for a protective role of Angiotensin-(1-7)." *J Hepatol*, 46(4), 674-81.

Pereira, T. N., Lewindon, P. J., Smith, J. L., Murphy, T. L., Lincoln, D. J., Shepherd, R. W., and Ramm, G. A. (2004). "Serum markers of hepatic fibrogenesis in cystic fibrosis liver disease." *J Hepatol*, 41(4), 576-83.

Perepelyuk, M., Terajima, M., Wang, A. Y., Georges, P. C., Janmey, P. A., Yamauchi, M., and Wells, R. G. (2013). "Hepatic stellate cells and portal fibroblasts are the major cellular sources of

collagens and lysyl oxidases in normal liver and early after injury." *Am J Physiol Gastrointest Liver Physiol*, 304(6), G605-14.

Peters, I. R., Peeters, D., Helps, C. R., and Day, M. J. (2007). "Development and application of multiple internal reference (housekeeper) gene assays for accurate normalisation of canine gene expression studies." *Vet Immunol Immunopathol*, 117(1-2), 55-66.

Pilette, C., Rousselet, M. C., Bedossa, P., Chappard, D., Oberti, F., Rifflet, H., Maiga, M. Y., Gallois, Y., and Cales, P. (1998). "Histopathological evaluation of liver fibrosis: quantitative image analysis vs semi-quantitative scores. Comparison with serum markers." *J Hepatol*, 28(3), 439-46.

Pillai, S., Center, S. A., McDonough, S. P., Demarco, J., Pintar, J., Henderson, A. K., Cooper, J., Bolton, T., Sharpe, K., Hill, S., Benedict, A. G., and Haviland, R. (2016). "Ductal Plate Malformation in the Liver of Boxer Dogs: Clinical and Histological Features." *Vet Pathol*, 53(3), 602-13.

Pinzani, M., and Marra, F. (2001). "Cytokine receptors and signaling in hepatic stellate cells." *Semin Liver Dis*, 21(3), 397-416.

Pinzani, M., Milani, S., De Franco, R., Grappone, C., Caligiuri, A., Gentilini, A., Tosti-Guerra, C., Maggi, M., Failli, P., Ruocco, C., and Gentilini, P. (1996). "Endothelin 1 is overexpressed in human cirrhotic liver and exerts multiple effects on activated hepatic stellate cells." *Gastroenterology*, 110(2), 534-48.

Pinzani, M., and Rombouts, K. (2004). "Liver fibrosis: from the bench to clinical targets." *Dig Liver Dis*, 36(4), 231-42.

Plebani, M., and Basso, D. (2007). "Non-invasive assessment of chronic liver and gastric diseases." *Clin Chim Acta*, 381(1), 39-49.

Poelstra, K. (2016). "Liver fibrosis in 2015: Crucial steps towards an effective treatment." *Nat Rev Gastroenterol Hepatol*, 13(2), 67-8.

Poffenbarger, E. M., and Hardy, R. M. (1985). "Hepatic cirrhosis associated with long-term primidone therapy in a dog." *J Am Vet Med Assoc*, 186(9), 978-80.

Poldervaart, J. H., Favier, R. P., Penning, L. C., van den Ingh, T. S., and Rothuizen, J. (2009). "Primary hepatitis in dogs: a retrospective review (2002-2006)." *J Vet Intern Med*, 23(1), 72-80.

Prins, M., Schellens, C. J., van Leeuwen, M. W., Rothuizen, J., and Teske, E. (2010). "Coagulation disorders in dogs with hepatic disease." *Vet J*, 185(2), 163-8.

Puche, J. E., Saiman, Y., and Friedman, S. L. (2013). "Hepatic stellate cells and liver fibrosis." *Compr Physiol*, 3(4), 1473-92.

Rakich, P. M., Prasse, K. W., Lukert, P. D., and Cornelius, L. M. (1986). "Immunohistochemical detection of canine adenovirus in paraffin sections of liver." *Vet Pathol*, 23(4), 478-84.

Rallis, T., Day, M. J., Saridomichelakis, M. N., Adamama-Moraitou, K. K., Papazoglou, L., Fytianou, A., and Koutinas, A. F. (2005). "Chronic hepatitis associated with canine leishmaniosis (Leishmania infantum): a clinicopathological study of 26 cases." *J Comp Pathol*, 132(2-3), 145-52.

Ramachandran, P., and Iredale, J. P. (2012). "Liver fibrosis: a bidirectional model of fibrogenesis and resolution." *QJM*, 105(9), 813-7.

Ramachandran, P., Iredale, J. P., and Fallowfield, J. A. (2015). "Resolution of liver fibrosis: basic mechanisms and clinical relevance." *Semin Liver Dis*, 35(2), 119-31.

Rambaldi, A., and Gluud, C. (2005). "Colchicine for alcoholic and non-alcoholic liver fibrosis and cirrhosis." *Cochrane Database Syst Rev*(2), CD002148.

Ramm, G. A. (2011). "Anti-chemokine therapy for the treatment of hepatic fibrosis: an attractive approach." *Hepatology*, 54(1), 354-8.

Rath, T., Menendez, K. M., Kugler, M., Hage, L., Wenzel, C., Schulz, R., Graf, J., Nahrlich, L., Roeb, E., and Roderfeld, M. (2012). "TIMP-1/-2 and transient elastography allow non invasive diagnosis of cystic fibrosis associated liver disease." *Dig Liver Dis*, 44(9), 780-7.

Respess, M., O'Toole, T. E., Taeymans, O., Rogers, C. L., Johnston, A., and Webster, C. R. (2012). "Portal vein thrombosis in 33 dogs: 1998-2011." *J Vet Intern Med*, 26(2), 230-7.

Robinson, M. D., and Smyth, G. K. (2008). "Small-sample estimation of negative binomial dispersion, with applications to SAGE data." *Biostatistics*, 9(2), 321-32.

Rockey, D. C., Fouassier, L., Chung, J. J., Carayon, A., Vallee, P., Rey, C., and Housset, C. (1998). "Cellular localization of endothelin-1 and increased production in liver injury in the rat: potential for autocrine and paracrine effects on stellate cells." *Hepatology*, 27(2), 472-80.

Roderburg, C., Mollnow, T., Bongaerts, B., Elfimova, N., Vargas Cardenas, D., Berger, K., Zimmermann, H., Koch, A., Vucur, M., Luedde, M., Hellerbrand, C., Odenthal, M., Trautwein, C., Tacke, F., and Luedde, T. (2012). "Micro-RNA profiling in human serum reveals compartment-specific roles of miR-571 and miR-652 in liver cirrhosis." *PLoS One*, 7(3), e32999.

Roderburg, C., Urban, G. W., Bettermann, K., Vucur, M., Zimmermann, H., Schmidt, S., Janssen, J., Koppe, C., Knolle, P., Castoldi, M., Tacke, F., Trautwein, C., and Luedde, T. (2011). "Micro-RNA profiling reveals a role for miR-29 in human and murine liver fibrosis." *Hepatology*, 53(1), 209-18.

Rodriguez, J. Y., Lewis, B. C., and Snowden, K. F. (2014). "Distribution and characterization of Heterobilharzia americana in dogs in Texas." *Vet Parasitol*, 203(1-2), 35-42.

Rodriguez, L., Cerbon-Ambriz, J., and Munoz, M. L. (1998). "Effects of colchicine and colchiceine in a biochemical model of liver injury and fibrosis." *Arch Med Res*, 29(2), 109-16.

Rolfe, D. S., and Twedt, D. C. (1995). "Copper-associated hepatopathies in dogs." *Vet Clin North Am Small Anim Pract*, 25(2), 399-417.

Rossi, E., Adams, L., Prins, A., Bulsara, M., de Boer, B., Garas, G., MacQuillan, G., Speers, D., and Jeffrey, G. (2003). "Validation of the FibroTest biochemical markers score in assessing liver fibrosis in hepatitis C patients." *Clin Chem*, 49(3), 450-4.

Rothuizen, J., and Twedt, D. C. (2009). "Liver biopsy techniques." *Vet Clin North Am Small Anim Pract*, 39(3), 469-80.

Rothuizen, J. (2008): “Liver”, 254–255, in: Steiner JM (Hrsg.), *Small Animal Gastroenterology*. Schlütersche, Hannover.

Saile, B., Matthes, N., Knittel, T., and Ramadori, G. (1999). "Transforming growth factor beta and tumor necrosis factor alpha inhibit both apoptosis and proliferation of activated rat hepatic stellate cells." *Hepatology*, 30(1), 196-202.

Saiman, Y., and Friedman, S. L. (2012). "The role of chemokines in acute liver injury." *Front Physiol*, 3, 213.

Samuelson, D. A. (2007). *Textbook of Veterinary Histology*, St. Louis, Mo.: Saunders-Elsevier.

Sancho, P., Mainez, J., Crosas-Molist, E., Roncero, C., Fernandez-Rodriguez, C. M., Pinedo, F., Huber, H., Eferl, R., Mikulits, W., and Fabregat, I. (2012). "NADPH oxidase NOX4 mediates stellate cell activation and hepatocyte cell death during liver fibrosis development." *PLoS One*, 7(9), e45285.

Sandrin, L., Fourquet, B., Hasquenoph, J. M., Yon, S., Fournier, C., Mal, F., Christidis, C., Ziol, M., Poulet, B., Kazemi, F., Beaugrand, M., and Palau, R. (2003). "Transient elastography: a new noninvasive method for assessment of hepatic fibrosis." *Ultrasound Med Biol*, 29(12), 1705-13.

Santos, R. A., Ferreira, A. J., Verano-Braga, T., and Bader, M. (2013). "Angiotensin-converting enzyme 2, angiotensin-(1-7) and Mas: new players of the renin-angiotensin system." *J Endocrinol*, 216(2), R1-R17.

Sanyal, A. J., Bosch, J., Blei, A., and Arroyo, V. (2008). "Portal hypertension and its complications." *Gastroenterology*, 134(6), 1715-28.

Schiavon, L. L., Narciso-Schiavon, J. L., Carvalho Filho, R. J., Sampaio, J. P., Medina-Pestana, J. O., Lanzoni, V. P., Silva, A. E., and Ferraz, M. L. (2008). "Serum levels of YKL-40 and hyaluronic acid as noninvasive markers of liver fibrosis in haemodialysis patients with chronic hepatitis C virus infection." *J Viral Hepat*, 15(9), 666-74.

Schmidt, S., Vet, M., Suter, P. F., and Vet, M. (1980). "Indirect and Direct Determination of the Portal Vein Pressure in Normal and Abnormal Dogs and Normal Cats1." *Vet Radiol*, 21(6), 246-259.

Scholten, D., Samman, M. A., Sahin, H., Trautwein, C., and Wasmuth, H. E. (2012). "CXCR3 Ligands induce Expression of CXCL1 (KC/murine IL8 homolog) in Mouse Hepatic Stellate Cells." *J Cell Sci Ther*, 5.

Seki, E., De Minicis, S., Gwak, G. Y., Kluwe, J., Inokuchi, S., Bursill, C. A., Llovet, J. M., Brenner, D. A., and Schwabe, R. F. (2009). "CCR1 and CCR5 promote hepatic fibrosis in mice." *J Clin Invest*, 119(7), 1858-70.

Seppa, H., Grotendorst, G., Seppa, S., Schiffmann, E., and Martin, G. R. (1982). "Platelet-derived growth factor in chemotactic for fibroblasts." *J Cell Biol*, 92(2), 584-8.

Sferra, R., Vetuschi, A., Pompili, S., Gaudio, E., Speca, S., and Latella, G. (2017). "Expression of pro-fibrotic and anti-fibrotic molecules in dimethylnitrosamine-induced hepatic fibrosis." *Pathol Res Pract*, 213(1), 58-65.

Shih, J. L., Keating, J. H., Freeman, L. M., and Webster, C. R. (2007). "Chronic hepatitis in Labrador Retrievers: clinical presentation and prognostic factors." *J Vet Intern Med*, 21(1), 33-9.

Sola, S., Amaral, J. D., Aranha, M. M., Steer, C. J., and Rodrigues, C. M. (2006). "Modulation of hepatocyte apoptosis: cross-talk between bile acids and nuclear steroid receptors." *Curr Med Chem*, 13(25), 3039-51.

Sola, S., Amaral, J. D., Castro, R. E., Ramalho, R. M., Borralho, P. M., Kren, B. T., Tanaka, H., Steer, C. J., and Rodrigues, C. M. (2005). "Nuclear translocation of UDCA by the glucocorticoid receptor is required to reduce TGF-beta1-induced apoptosis in rat hepatocytes." *Hepatology*, 42(4), 925-34.

Spee, B., Arends, B., van den Ingh, T. S., Brinkhof, B., Nederbragt, H., Ijzer, J., Roskams, T., Penning, L. C., and Rothuizen, J. (2006a). "Transforming growth factor beta-1 signalling in canine hepatic diseases: new models for human fibrotic liver pathologies." *Liver Int*, 26(6), 716-25.

Spee, B., Arends, B., van den Ingh, T. S., Penning, L. C., and Rothuizen, J. (2006b). "Copper metabolism and oxidative stress in chronic inflammatory and cholestatic liver diseases in dogs." *J Vet Intern Med*, 20(5), 1085-92.

Sporea, I., Gilja, O. H., Bota, S., Sirli, R., and Popescu, A. (2013). "Liver elastography - an update." *Med Ultrason*, 15(4), 304-14.

Sridharan, S., Allen, A. L., Kidney, B., and Al-Dissi, A. N. (2015). "Metallothionein Expression in Dogs With Chronic Hepatitis and Its Correlation With Hepatic Fibrosis, Inflammation, and Ki-67 Expression." *Vet Pathol*, 52(6), 1127-33.

Sterczer, A., Gaal, T., Perge, E., and Rothuizen, J. (2001). "Chronic hepatitis in the dog--a review." *Vet Q*, 23(4), 148-52.

Strombeck, D. R., and Guilford, W. G. (1990). *Small Animal Gastroenterology*, Davis, Calif.: Stonegate Pub. Co.

Strombeck, D. R., Miller, L. M., and Harrold, D. (1988). "Effects of corticosteroid treatment on survival time in dogs with chronic hepatitis: 151 cases (1977-1985)." *J Am Vet Med Assoc*, 193(9), 1109-13.

Tamborini, A., Jahns, H., McAllister, H., Kent, A., Harris, B., Procoli, F., Allenspach, K., Hall, E. J., Day, M. J., Watson, P. J., and O'Neill, E. J. (2016). "Bacterial Cholangitis, Cholecystitis, or both in Dogs." *J Vet Intern Med*, 30(4), 1046-55.

Tao, H., Yang, J. J., Shi, K. H., Huang, C., Zhang, L., Lv, X. W., and Li, J. (2014). "The significance of YKL-40 protein in liver fibrosis." *Inflamm Res*, 63(4), 249-54.

Taura, K., Miura, K., Iwaisako, K., Osterreicher, C. H., Kodama, Y., Penz-Osterreicher, M., and Brenner, D. A. (2010). "Hepatocytes do not undergo epithelial-mesenchymal transition in liver fibrosis in mice." *Hepatology*, 51(3), 1027-36.

Trappoliere, M., Caligiuri, A., Schmid, M., Bertolani, C., Failli, P., Vizzutti, F., Novo, E., di Manzano, C., Marra, F., Loguercio, C., and Pinzani, M. (2009). "Silybin, a component of sylimarin, exerts

anti-inflammatory and anti-fibrogenic effects on human hepatic stellate cells." *J Hepatol*, 50(6), 1102-11.

Vaillant, B., Chiaramonte, M. G., Cheever, A. W., Soloway, P. D., and Wynn, T. A. (2001). "Regulation of hepatic fibrosis and extracellular matrix genes by the th response: new insight into the role of tissue inhibitors of matrix metalloproteinases." *J Immunol*, 167(12), 7017-26.

Van den Ingh, T. S., and Rothuizen, J. (1994). "Lobular dissecting hepatitis in juvenile and young adult dogs." *J Vet Intern Med*, 8(3), 217-20.

Van den Ingh, T. S. (2016). "Morphological classification of parenchymal disorders of the canine and feline liver", http:// www.vetvisuals.com/lms/moodle/mod/book/view.php?id=1001&chapterid=5285.

Vince, A. R., Hayes, M. A., Jefferson, B. J., and Stalker, M. J. (2016). "Sinusoidal endothelial cell and hepatic stellate cell phenotype correlates with stage of fibrosis in chronic liver disease in dogs." *J Vet Diagn Invest*, 28(5), 498-505.

Wang, B., Zhao, L., Fish, M., Logan, C. Y., and Nusse, R. (2015). "Self-renewing diploid Axin2(+) cells fuel homeostatic renewal of the liver." *Nature*, 524(7564), 180-5.

Wang, K. (2014). "Molecular mechanisms of hepatic apoptosis." *Cell Death Dis*, 5, e996.

Wang, K. (2015). "Molecular mechanisms of hepatic apoptosis regulated by nuclear factors." *Cell Signal*, 27(4), 729-38.

Washabau, R. J., and Day, M. J. (2013). *Canine & Feline Gastroenterology*, 1st ed., St. Louis, Mo.: Elsevier Saunders.

Wasmuth, H. E., Lammert, F., Zaldivar, M. M., Weiskirchen, R., Hellerbrand, C., Scholten, D., Berres, M. L., Zimmermann, H., Streetz, K. L., Tacke, F., Hillebrandt, S., Schmitz, P., Keppeler, H., Berg, T., Dahl, E., Gassler, N., Friedman, S. L., and Trautwein, C. (2009). "Antifibrotic effects of CXCL9 and its receptor CXCR3 in livers of mice and humans." *Gastroenterology*, 137(1), 309-19, 319 e1-3.

Watanabe, T., Niioka, M., Ishikawa, A., Hozawa, S., Arai, M., Maruyama, K., Okada, A., and Okazaki, I. (2001). "Dynamic change of cells expressing MMP-2 mRNA and MT1-MMP mRNA in the recovery from liver fibrosis in the rat." *J Hepatol*, 35(4), 465-73.

Watson, P. (2017). "Canine Breed-Specific Hepatopathies." *Vet Clin North Am Small Anim Pract*, 47(3), 665-682.

Watson, P. J. (2004). "Chronic hepatitis in dogs: a review of current understanding of the aetiology, progression, and treatment." *Vet J*, 167(3), 228-41.

Watson, P. J., Roulois, A. J., Scase, T. J., Irvine, R., and Herrtage, M. E. (2010). "Prevalence of hepatic lesions at post-mortem examination in dogs and association with pancreatitis." *J Small Anim Pract*, 51(11), 566-72.

Webster, C. R., and Cooper, J. (2009). "Therapeutic use of cytoprotective agents in canine and feline hepatobiliary disease." *Vet Clin North Am Small Anim Pract*, 39(3), 631-52.

Wells, R. G. (2014). "Portal Fibroblasts in Biliary Fibrosis." *Curr Pathobiol Rep*, 2(4), 185-190.

Wynn, T. A., and Vannella, K. M. (2016). "Macrophages in Tissue Repair, Regeneration, and Fibrosis." *Immunity*, 44(3), 450-62.

Xu, F., Liu, C., Zhou, D., and Zhang, L. (2016). "TGF-beta/SMAD Pathway and Its Regulation in Hepatic Fibrosis." *J Histochem Cytochem*, 64(3), 157-67.

Yoshizato, K., Thuy le, T. T., Shiota, G., and Kawada, N. (2016). "Discovery of cytoglobin and its roles in physiology and pathology of hepatic stellate cells." *Proc Jpn Acad Ser B Phys Biol Sci*, 92(3), 77-97.

Younis, N., Shaheen, M. A., and Abdallah, M. H. (2016). "Silymarin-loaded Eudragit((R)) RS100 nanoparticles improved the ability of silymarin to resolve hepatic fibrosis in bile duct ligated rats." *Biomed Pharmacother*, 81, 93-103.

11. Appendix

11.1 Legend of Figures

Figure 1 -14-
Figure 2 -30-
Figure 3 -37-
Figure 4 -54-
Figure 5 -65-
Figure 6 -67-
Figure 7 -68-
Figure 8 -70-
Figure 9 -71-
Figure 10 -72-
Figure 11 -73-
Figure 12 -74-

11.2 Legend of Tables

Table 1 -16-
Table 2 -25-26-
Table 3 -47-
Table 4 -49-
Table 5 -51-
Table 6 -56-64-

11.3 Supplementary Materials

Table S1 RNA Quality Control

Sample_ID	RNA Concentration (ng/µl)	OD_{260}/OD_{280}	OD_{260}/OD_{230}	RQN
Control				
1WV	727.5	1.97	1.34	7.4
2CW	535.5	1.89	1.19	7
3RY	3246.1	1.95	1.94	7.1
4MH	748.9	1.95	1.33	7.1
5SW	698.4	1.93	1.29	6.3
6.2PH	375	2.02	1.68	6
7.2GG	764.3	1.98	1.65	8
8CB	563.6	1.94	1.4	7.7
9CW	3354.7	1.95	1.81	6.6
10.2KD	2246.7	1.99	1.71	6.1
11DA/H	1006.4	2.04	1.77	8.2
12.2SSt	1346	2.04	2.2	7.9
Chronic Hepatitis				
1.2PP	618	2.11	2.16	7.2
3.2SF	93.1	2.07	1.61	7.9
4HB	20.5	2.45	1.06	7.4
5PA	264.6	2.09	2.12	7.3
6SB	33.3	2.04	0.53	8
7GH	49.8	2.05	1.51	7.3
8RP	11.5	1.99	0.25	6.1
9CG	43.1	2.08	0.42	7.6
10TB	10.4	2.61	0.05	7.3
11SLS	255.9	2.09	2.21	7.8
12HR	530.3	2.1	2.25	7.8
13MF	298.9	2.08	2	8.5
15BB	26.7	2.28	0.68	7.5
16.2BP	115.1	2.12	1.22	6.3
17LB	461.2	2.08	2.08	7.3
18DT	563.3	2.05	2.19	8.3

OD: optical density; OD ratio = indication of nucleid acid purity; RQN: RNA quality number; indication of total RNA integrity.

Table S2 Gene Table

Gene	Full Name	Chromosome	Fold Change	FDR-adjusted *P*-value
AADACL2	Arylacetamide Deacetylase-Like 2	23	8.45	2.36E-14
ABCC5	ATP Binding Cassette Subfamily C Member 5	34	-4.6	<0.001
ACKR3	Atypical Chemokine Receptor 3	25	-3.52	1.17E-08
ACOX2	Acyl-CoA Oxidase 2, Branched Chain	20	-2.56	1.82E-09
ACP5	Acid Phosphatase 5, Tartrate Resistant	20	2.96	2.48E-04
ACSM5	Acyl-CoA Synthetase Medium-Chain Family Member 5	6	-2.75	2.03E-04
ADAM28	ADAM Metallopeptidase Domain 28	25	3.67	5.26E-03
ADAMDEC1	ADAM-Like, Decysin 1	25	45.72	3.28E-07
ADAMTS12	ADAM Metallopeptidase With Thrombospondin Type 1 Motif 12	4	2.52	1.36E-03
ADGRD1	Adhesion G Protein-Coupled Receptor D1	26	2.97	0.02
ADIRF	Adipogenesis Regulatory Factor	4	2.78	0.01
ADRA1A	Adrenoceptor Alpha 1A	25	-2.5	2.11E-11
AGR2	Anterior Gradient 2, Protein Disulphide Isomerase Family Member	14	4.37	0.03
AKAP17A	A-Kinase Anchoring Protein 17A	X	-3.04	<0.001
AKAP8	A-Kinase Anchoring Protein 8	20	-3.77	<0.001
ALDH8A1	Aldehyde Dehydrogenase 8 Family Member A1	1	-2.74	<0.001
ALOX15	Arachidonate 15-Lipoxygenase	5	2.79	1.11E-04
AMICA1	Adhesion Molecule, Interacts With CXADR Antigen 1	5	4.54	3.84E-23
ANGPT4	Angiopoietin 4	24	2.52	8.98E-03
ANGPTL4	Angiopoietin Like 4	20	2.56	2.34E-04
ANLN	Anillin Actin Binding Protein	14	7.09	2.87E-05
ANTXR1	Anthrax Toxin Receptor 1	10	2.51	1.35E-03
ANXA1	Annexin A1	1	2.58	3.94E-15
ANXA2	Annexin A2	30	6.69	5.48E-31
ANXA4	Annexin A3	10	3.97	5.64E-08
ANXA5	Annexin A5	19	2.73	1.05E-06
APBB3	Amyloid Beta Precursor Protein Binding Family B Member 3	2	-3.58	2.14E-11
APOA4	Apolipoprotein A4	5	12.51	4.66E-09
ARHGAP11A	Rho GTPase Activating Protein 11A	30	5.53	2.08E-13
ARHGDIB	Rho GDP Dissociation Inhibitor Beta	27	2.63	6.40E-07
ARL4A	ADP Ribosylation Factor Like GTPase 4A	14	-2.67	5.00E-06
ARPC1B	Actin Related Protein 2/3 Complex Subunit 1B	6	2.63	2.33E-06
ASCL1	Achaete-Scute Family BHLH Transcription Factor 1	15	-5.38	4.75E-06
ASIC3	Acid Sensing Ion Channel Subunit 3	16	-5.84	7.18E-18
ASNS	Asparagine Synthetase (Glutamine-Hydrolyzing)	14	3.34	0.02
ATAT1	Alpha Tubulin Acetyltransferase 1	12	-3.19	1.81E-09
ATXN7L2	Ataxin 7 Like 2	6	-2.87	1.11E-07

AUTS2	Autism Susceptibility Candidate 2	6	-3.04	<0.001
B3GALNT1	Beta-1,3-N-Acetylgalactosaminyltransferase 1 (Globoside Blood Group)	34	3.28	2.19E-09
BCAS4	Breast Carcinoma Amplified Sequence 4	24	3.94	5.45E-08
BCAT1	Branched Chain Amino Acid Transaminase 1	27	6.85	2.34E-05
BCL2A1	BCL2 Related Protein A1	3	2.5	3.28E-03
BCL6	B-Cell CLL/Lymphoma 6	34	-2.78	<0.001
BGLAP	Bone Gamma-Carboxyglutamate Protein	7	-4.1	2.85E-36
BIRC3	Baculoviral IAP Repeat Containing 3	5	3.36	4.47E-14
BLNK	B-Cell Linker	28	3.03	9.90E-07
BPI	Bactericidal/Permeability-Increasing Protein	24	3.55	1.63E-05
BUB1B	BUB1 Mitotic Checkpoint Serine/Threonine Kinase B	30	6.65	6.80E-15
C20H19orf80	Chromosome 20 Open Reading Frame 80	20	-4.92	0.03
C31H21orf62	Chromosome 31 Open Reading Frame 62	31	2.75	8.89E-04
C6H16orf54	Chromosome 6 Open Reading Frame 54	6	3.59	3.16E-06
C7H1orf105	Chromosome 7 Open Reading Frame 105	7	-2.94	<0.001
C8H14orf180	Chromosome 14 Open Reading Frame 180	8	-3.18	1.36E-05
CA13	Carbonic Anhydrase 13	29	3.71	3.24E-04
CAPG	Capping Actin Protein, Gelsolin Like	17	4.2	1.18E-29
CAPS	Calcyphosine	20	3.05	0.02
CASC5	Cancer Susceptibility Candidate 5	30	5.59	6.12E-15
CAV1	Caveolin 1	14	2.75	2.57E-04
CCDC142	Coiled-Coil Domain Containing 142	17	-4.81	8.75E-33
CCDC18	Coiled-Coil Domain Containing 18	6	-2.73	1.20E-03
CCDC70	Coiled-Coil Domain Containing 70	22	-9.86	8.32E-06
CCDC78	Coiled-Coil Domain Containing 78	6	-8.68	6.13E-22
CCDC80	Coiled-Coil Domain Containing 80	33	3.67	2.89E-05
CCDC88A	Coiled-Coil Domain Containing 88A	10	2.94	1.89E-06
CCL2	C-C Motif Chemokine Ligand 2	9	8.39	1.94E-21
CCL21	C-C Motif Chemokine Ligand 21	11	3.1	2.25E-06
CCL5	C-C Motif Chemokine Ligand 5	9	13.75	1.39E-27
CCNA2	Cyclin A2	19	3.93	1.57E-03
CCNB2	Cyclin B2	30	2.59	6.58E-13
CCNL1	Cyclin L1	23	-3.56	<0.001
CCNL2	Cyclin L2	5	-2.87	<0.001
CCR1	C-C Motif Chemokine Receptor 1	20	3.89	1.42E-05
CCR5	C-C Motif Chemokine Receptor 1	20	3.76	5.69E-07
CD1A6	CD1A6 Molecule	38	7.33	2.88E-08
CD2	CD2 Molecule	17	3.88	5.00E-21
CD27	CD27 Molecule	27	4.25	6.64E-04
CD28	CD28 Molecule	37	-2.92	7.10E-04
CD34	CD34 Molecule	7	2.57	1.03E-10
CD3E	CD3E Molecule	5	7.17	8.66E-27
CD4	CD4 Molecule	27	2.96	0.01
CD48	CD48 Molecule	38	3.8	1.76E-05

CD6	CD6 Molecule	18	5.91	2.09E-04
CD84	CD84 Molecule	38	2.85	2.81E-04
CD8A	CD8A Molecule	17	6.01	1.66E-14
CD8B	CD8B Molecule	17	4.84	1.71E-15
CD9	CD9 Molecule	27	2.56	1.03E-03
CD96	CD96 Molecule	33	2.78	0.03
CDADC1	Cytidine And DCMP Deaminase Domain Containing 1	22	-3.75	5.65E-09
CDH13	Cadherin 13	5	4.27	2.93E-10
CDPF1	Cysteine Rich DPF Motif Domain Containing 1	10	-3.49	<0.001
CDR2L	Cerebellar Degeneration Related Protein 2 Like	9	2.59	1.43E-15
CENPE	Centromere Protein E	32	7.07	5.19E-07
CENPF	Centromere Protein F	7	11.41	2.84E-21
CFTR	Cystic Fibrosis Transmembrane Conductance Regulator	14	3.41	0.01
CGREF1	Cell Growth Regulator With EF-Hand Domain 1	17	3.01	1.96E-13
CHGA	Chromogranin A	8	9.72	2.11E-06
CHI3L1	Chitinase 3 Like 1	7	35.92	2.50E-25
CHRDL1	Chordin-Like 1	X	2.63	2.48E-06
CHST2	Carbohydrate Sulfotransferase 2	23	5.35	7.40E-08
CIART	Circadian Associated Repressor Of Transcription	17	-5.07	5.76E-50
CIITA	Class II, Major Histocompatibility Complex, Transactivator	6	2.76	2.19E-05
CKAP2	Cytoskeleton Associated Protein 2	25	3.11	8.60E-07
CLDN11	Claudin 11	34	4.46	1.78E-09
CLDN18	Claudin 18	23	6.03	3.59E-11
CLDN4	Claudin 4	6	2.97	1.85E-05
CLEC2D	C-Type Lectin Domain Family 2 Member D	27	2.83	4.63E-04
CLEC4A	C-Type Lectin Domain Family 4 Member A	27	-5.88	3.91E-17
CLIC5	Chloride Intracellular Channel 5	12	2.93	3.79E-05
CLK1	CDC Like Kinase 1	37	-3.81	1.17E-10
CLK4	CDC Like Kinase 4	11	-3.11	<0.001
COL12A1	Collagen Type XII Alpha 1	12	3.03	2.11E-03
COL15A1	Collagen Type XV Alpha 1	11	3.03	3.75E-10
COL16A1	Collagen Type XVI Alpha 1	2	3.68	1.25E-03
COL1A1	Collagen Type I Alpha 1	9	5.69	5.38E-22
COL1A2	Collagen Type I Alpha 2	14	2.59	1.94E-03
COL23A1	Collagen Type XXIII Alpha 1	11	2.98	1.73E-08
COL2A1	Collagen Type II Alpha 1	27	3.13	2.80E-04
COL3A1	Collagen Type III Alpha 1	36	2.98	3.95E-04
COL6A1	Collagen Type VI Alpha 1	31	3.58	1.52E-04
COL6A2	Collagen Type VI Alpha 2	31	3.42	5.28E-05
COL8A1	Collagen Type VIII Alpha 1	33	2.95	2.32E-03
CORO1A	Coronin 1A	6	2.64	5.89E-06
CPM	Carboxypeptidase M	10	4.84	2.89E-05
CPXM2	Carboxypeptidase X (M14 Family), Member 2	28	5.59	9.29E-04

CRIP1	Cysteine Rich Protein 1	8	2.67	7.54E-05
CRISPLD2	Cysteine Rich Secretory Protein LCCL Domain Containing 2	5	2.63	6.47E-09
CRYGS	Crystallin Gamma S	34	-6.34	1.24E-53
CRYM	Crystallin Mu	6	-2.96	1.32E-06
CSTB	Cystatin B	31	3.45	4.24E-05
CTGF	connective tissue growth factor	1	2.62	1.03E-06
CTSB	Cathepsin B	25	2.53	1.77E-04
CTSK	Cathepsin K	17	4.59	6.60E-18
CUX2	Cut Like Homeobox 2	26	6.09	1.06E-03
CX3CR1	C-X3-C Motif Chemokine Receptor 1	23	7.06	5.40E-29
CXCL10	C-X-C Motif Chemokine Ligand 10	32	19.05	1.69E-06
CYBASC3	Cytochrome B561 Family Member A3	18	2.69	0.01
CYGB	Cytoglobin, Stellate Cell Activation-Associated Protein	9	3.43	1.52E-18
CYP1B1	Cytochrome P450 Family 1 Subfamily B Member 1	17	5.82	5.14E-14
DAPP1	Dual Adaptor Of Phosphotyrosine And 3-Phosphoinositides	32	3.06	3.11E-04
DCDC2	Doublecortin Domain Containing 2	35	4.13	2.40E-03
DCLK1	Doublecortin Like Kinase 1	25	5.34	3.50E-06
DCN	Decorin	15	3.05	5.93E-04
DDR2	Discoidin Domain Receptor Tyrosine Kinase 2	38	4.59	1.30E-04
DFNA5	DFNA5, Deafness Associated Tumor Suppressor	14	3.65	0.01
DIAPH3	Diaphanous Related Formin 3	22	6.62	9.92E-07
DIO2	Deiodinase, Iodothyronine, Type II	8	-3.79	1.58E-03
DLA88	Major Histocompatibility Complex, Class I, B	12	2.96	0.01
DLA-DMA	Major Histocompatibility Complex, Class II, DM Alpha	12	3.03	9.60E-06
DLA-DMB	Major Histocompatibility Complex, Class II, DM Beta	12	3.23	1.27E-06
DLA-DQA1	Major Histocompatibility Complex, Class II, DQ Alpha 2	12	4.18	2.63E-07
DLA-DRA	Major Histocompatibility Complex, Class II, DR Alpha	12	3.13	2.95E-06
DOCK3	Dedicator Of Cytokinesis 3	20	-2.77	9.54E-11
DTX1	Deltex 1	26	4.13	1.06E-05
DTX4	Deltex 4, E3 Ubiquitin Ligase	18	3.62	7.85E-05
E2F1	E2F Transcription Factor 1	24	3.03	1.03E-03
E4F1	E4F Transcription Factor 1	6	-2.77	<0.001
EBI3	Epstein-Barr Virus Induced 3	20	2.5	6.52E-03
ECI1	Enoyl-CoA Delta Isomerase 2	6	3.84	3.57E-18
ECT2	Epithelial Cell Transforming 2	34	5.89	2.30E-21
EFEMP1	EGF Containing Fibulin-Like Extracellular Matrix Protein 1	10	4.73	5.14E-04
EGFL8	EGF Like Domain Multiple 8	12	-4.92	1.30E-12
ELOVL2	ELOVL Fatty Acid Elongase 2	35	26.12	1.89E-04
EMILIN2	Elastin Microfibril Interfacer 2	7	3.05	2.72E-15
EMP1	Epithelial Membrane Protein 1	27	6.62	1.57E-04

EMP3	Epithelial Membrane Protein 3	1	2.5	4.74E-19
ENPP6	Ectonucleotide Pyrophosphatase/Phosphodiesterase 6	16	2.56	0.04
ENTHD2	ENTH Domain Containing 2	9	-2.61	<0.001
EPHB6	EPH Receptor B6	16	3.55	4.44E-03
EPPK1	Epiplakin 1	13	-5.7	1.28E-08
ESRP2	Epithelial Splicing Regulatory Protein 2	5	-2.82	<0.001
ETNPPL	Ethanolamine-Phosphate Phospho-Lyase	32	-4.8	3.87E-03
EXOG	Endo/Exonuclease (5'-3'), Endonuclease G-Like	23	-3.18	<0.001
F13A1	Coagulation Factor XIII A Chain	35	5.3	5.38E-04
FAAP100	Fanconi Anemia Core Complex Associated Protein 100	9	-2.72	<0.001
FABP1	Fatty Acid Binding Protein 1	17	17.24	1.02E-28
FABP4	Fatty Acid Binding Protein 4	29	15.57	1.05E-03
FABP5	Fatty Acid Binding Protein 5	29	4.42	3.24E-04
FAM114A1	Family With Sequence Similarity 114 Member A1	3	2.77	5.59E-09
FAM129A	Family With Sequence Similarity 129 Member A	7	2.55	2.15E-24
FAM180A	Family With Sequence Similarity 180 Member A	16	2.66	2.28E-03
FAM76B	Family With Sequence Similarity 76 Member B	21	-2.89	<0.001
FAM81A	Family With Sequence Similarity 81 Member A	30	2.94	4.88E-14
FAP	Fibroblast Activation Protein Alpha	36	8.06	1.40E-04
FBLIM1	Filamin Binding LIM Protein 1	2	2.65	1.77E-03
FBXO44	F-Box Protein 44	2	-2.68	1.24E-06
FCGR1A	Fc Fragment Of IgG Receptor Ia	17	2.84	4.49E-08
FEZF1	FEZ Family Zinc Finger 1	14	4.91	2.13E-04
FKBP10	FK506 Binding Protein 10	9	4.21	3.03E-17
FLRT2	Fibronectin Leucine Rich Transmembrane Protein 2	8	3.58	4.59E-05
FNDC1	Fibronectin Type III Domain Containing 1	1	3.41	8.51E-10
FRMD6	FERM Domain Containing 6	8	2.69	1.62E-06
FSCN1	Fascin Actin-Bundling Protein 1	6	3.25	1.18E-08
FSD2	Fibronectin Type III And SPRY Domain Containing 2	3	-4.69	4.15E-14
FSIP1	Fibrous Sheath Interacting Protein 1	30	2.92	5.56E-28
FXYD5	FXYD Domain Containing Ion Transport Regulator 5	1	2.85	4.43E-20
FZD3	Frizzled Class Receptor 3	25	6.53	5.56E-04
G6PC	Glucose-6-Phosphatase Catalytic Subunit	9	-4.01	<0.001
GABRB1	Gamma-Aminobutyric Acid Type A Receptor Beta1 Subunit	13	6.35	0.03
GADD45A	Growth Arrest And DNA Damage Inducible Alpha	6	-3.59	7.03E-14
GADD45B	Growth Arrest And DNA Damage Inducible Beta	20	-4.31	5.45E-14
GADD45G	Growth Arrest And DNA Damage Inducible Gamma	1	-2.56	5.92E-15
GALNT3	Polypeptide N-Acetylgalactosaminyltransferase 3	36	2.59	1.43E-03
GALNT6	Polypeptide N-Acetylgalactosaminyltransferase 6	27	4.43	1.03E-03
GAS6	Growth Arrest Specific 6	22	3.03	4.17E-03
GAS7	Growth Arrest Specific 7	5	2.92	1.05E-20

GATA6	GATA Binding Protein 6	7	2.66	1.25E-13
GATM	Glycine Amidinotransferase	30	3.14	4.04E-04
GBP6	Guanylate Binding Protein Family Member 6	6	3.25	1.69E-03
GDF9	Growth Differentiation Factor 9	11	-3.47	2.68E-68
GGTA1	Glycoprotein, Alpha-Galactosyltransferase 1	9	2.74	1.61E-34
GIMAP2	GTPase, IMAP Family Member 2	16	3.46	1.97E-04
GIMAP4	GTPase, IMAP Family Member 4	16	3.01	1.05E-03
GIPC1	GIPC PDZ Domain Containing Family Member 1	20	2.94	3.01E-06
GLDN	Gliomedin	30	3.25	1.82E-11
GLI1	GLI Family Zinc Finger 1	10	2.84	1.49E-03
GNAT1	G Protein Subunit Alpha Transducin 1	20	-6.17	2.95E-12
GPM6A	Glycoprotein M6A	16	2.56	0.03
GPNMB	Glycoprotein Nmb	14	11.97	1.66E-06
GPR176	G Protein-Coupled Receptor 176	30	-3.18	<0.001
GRAMD1C	GRAM Domain Containing 1C	33	2.56	1.30E-03
GSN	Gelsolin	11	3.83	4.64E-18
GZMA	Granzyme A	2	5.13	1.37E-04
HAL	Histidine Ammonia-Lyase	15	-2.88	3.76E-04
HBEGF	Heparin Binding EGF Like Growth Factor	2	-3.06	3.74E-07
HELB	Helicase (DNA) B	10	-2.98	1.14E-12
HLA-DRB1	Major Histocompatibility Complex, Class II, DR Beta 1	12	3.67	2.35E-07
HMCN2	Hemicentin 2	9	-3.45	<0.001
HOXD8	Homeobox D8	36	4.67	0.01
HPSE	Heparanase	32	4.06	1.01E-04
HSPB8	Heat Shock Protein Family B (Small) Member 8	26	10.14	3.32E-06
HTRA3	HtrA Serine Peptidase 3	3	2.74	4.99E-04
HYKK	Hydroxylysine Kinase	13	-2.74	5.92E-08
ICOSLG	Inducible T-Cell Co-Stimulator Ligand	31	2.77	9.68E-04
IDO1	Indoleamine 2,3-Dioxygenase 1	16	9.01	5.30E-06
IFGGB1	Interferon-Gamma-Inducible GTPase B1	11	8.09	2.46E-14
IFGGB2	Interferon-Gamma-Inducible GTPase B2	11	2.6	4.69E-06
IFGGC1	Interferon-Gamma-Inducible GTPase C1	11	4.45	2.82E-11
IFIT1	Interferon Induced Protein With Tetratricopeptide Repeats 1	4	6.66	3.88E-04
IFNGR2	Interferon Gamma Receptor 2 (Interferon Gamma Transducer 1)	31	3.09	1.95E-08
IGFBP7	Insulin Like Growth Factor Binding Protein 7	13	2.57	8.56E-05
IKZF3	IKAROS Family Zinc Finger 3	9	3.97	3.31E-17
IL1RL2	Interleukin 1 Receptor Like 2	10	-5.61	<0.001
IL2RG	Interleukin 2 Receptor Subunit Gamma	X	5.9	7.16E-23
IL33	Interleukin 33	11	-2.9	<0.001
INA	Internexin Neuronal Intermediate Filament Protein Alpha	28	2.75	1.43E-04
INTS6	Integrator Complex Subunit 6	22	-2.55	7.79E-11
IRG1	Immune-Responsive Gene 1 Protein	22	8.39	8.30E-04
ISG20	Interferon Stimulated Exonuclease Gene 20kDa	3	4.19	9.35E-05

ITFG2	Integrin Alpha FG-GAP Repeat Containing 2	27	-2.65	1.49E-09
ITGA11	Integrin Subunit Alpha 11	30	3.01	9.24E-09
ITGAX	Integrin Subunit Alpha X	6	9.62	1.37E-11
ITGB4	Integrin Subunit Beta 8	9	2.55	8.64E-08
ITGB8	Integrin Subunit Beta 5	14	2.55	0.01
ITIH5	Inter-Alpha-Trypsin Inhibitor Heavy Chain Family Member 5	2	2.93	6.01E-04
JCHAIN	Joining Chain Of Multimeric IgA And IgM	13	4.77	2.23E-05
KCNA3	Potassium Voltage-Gated Channel Subfamily A Member 3	6	3.22	1.73E-05
KCNH2	Potassium Voltage-Gated Channel Subfamily H Member 2	16	-3.96	1.02E-05
KCNH7	Potassium Voltage-Gated Channel Subfamily H Member 7	36	-3.18	1.84E-05
KCNK17	Potassium Two Pore Domain Channel Subfamily K Member 17	12	3.43	4.94E-03
KIAA0101	-	30	4.98	4.21E-13
KIAA1549L	-	18	-3.89	3.48E-06
KIAA1644	-	10	5.23	8.52E-05
KIAA1755	-	24	2.66	1.68E-03
KIF11	Kinesin Family Member 11	28	8.67	2.50E-07
KIF20B	Kinesin Family Member 20B	28	2.52	1.61E-04
KIF23	Kinesin Family Member 23	30	3.95	1.82E-11
KISS1	KiSS-1 Metastasis-Suppressor	38	-5.22	6.84E-09
KLHL41	Kelch Like Family Member 41	36	-9.4	5.83E-13
KLRG1	Killer Cell Lectin Like Receptor G1	27	2.68	9.89E-05
KNTC1	Kinetochore Associated 1	26	4.94	3.95E-04
KRT19	Keratin 19	9	2.92	2.10E-11
KRT5	Keratin 5	27	5.26	9.72E-04
LAMA4	Laminin Subunit Alpha 4	12	4.56	1.27E-04
LAMC3	Laminin Subunit Gamma 3	9	3.15	8.33E-11
LBH	Limb Bud And Heart Development	17	3.13	4.21E-21
LCK	LCK Proto-Oncogene, Src Family Tyrosine Kinase	2	2.51	2.56E-03
LENG8	Leukocyte Receptor Cluster (LRC) Member 8	1	-3.14	<0.001
LGALS1	Lectin, Galactoside Binding Soluble 1	10	5.93	2.86E-08
LGALS3	Lectin, Galactoside Binding Soluble 3	8	9.88	4.12E-06
LGI4	Leucine-Rich Repeat LGI Family Member 4	1	-3.88	3.18E-61
LIPG	Lipase G, Endothelial Type	7	-3.51	<0.001
LMLN	Leishmanolysin Like Peptidase	33	3.2	2.34E-03
LOC100682772	-	14	-4.63	3.76E-05
LOC100683373	-	21	3.56	6.73E-13
LOC100684931	-	1	-12.53	<0.001
LOC100687054	-	26	3.26	2.11E-04
LOC100687459	-	16	3.37	6.93E-05
LOC100687463	-	17	40.38	4.51E-09
LOC100687983	-	1	6.95	1.35E-32
LOC100855630	-	26	7.74	7.23E-05

LOC100855940	-	17	-4.01	<0.001
LOC100856137	-	12	2.9	4.13E-04
LOC102151511	-	3	-53.77	3.27E-08
LOC102151654	-	16	-4.7	5.17E-07
LOC102152056	-	28	10.56	1.23E-06
LOC102152474	-	31	-3.58	2.45E-04
LOC102153199	-	9	-4.24	3.12E-14
LOC102153261	-	21	-3.36	2.16E-16
LOC102153586	-	17	-3.47	1.31E-14
LOC102154209	-	11	-4.12	1.52E-36
LOC102154781	-	5	-3.04	2.07E-21
LOC102155399	-	16	-5.51	1.03E-08
LOC102155424	-	X	4.88	1.09E-18
LOC102155487	-	1	-15.21	1.28E-76
LOC102155650	-	16	-5.03	3.93E-04
LOC102155751	-	25	-4.67	7.44E-10
LOC102155815	-	34	-3.74	1.42E-18
LOC102155886	-	21	39.19	2.79E-27
LOC102156060	-	2	-5.85	6.21E-14
LOC102156583	-	X	3.02	1.07E-19
LOC102156586	-	X	-7.99	1.41E-69
LOC102156852	-	10	-5.16	3.09E-23
LOC102156945	-	22	-5.96	5.67E-03
LOC102156955	-	13	-7.67	2.06E-20
LOC106557533	-	27	4.14	9.89E-05
LOC106559112	-	8	4.42	1.88E-04
LOC106559122	-	8	4.56	2.96E-03
LOC106559562	-	12	8.49	0.01
LOC106559915	-	17	-4.78	3.39E-39
LOC448801	-	6	4.62	1.91E-03
LOC475605	-	16	-3.52	5.30E-06
LOC476003	-	18	7.61	2.15E-05
LOC476006	-	18	3.5	1.40E-05
LOC476047	-	18	-2.7	4.31E-05
LOC476879	-	21	17.66	1.54E-19
LOC477562	-	26	-2.68	5.98E-05
LOC478384	-	31	2.66	1.28E-03
LOC478773	-	36	-2.91	1.59E-04
LOC479911	-	6	-3.45	4.56E-05
LOC482202	-	14	2.71	0.02
LOC482987	-	17	9.64	2.04E-14
LOC484897	-	20	2.65	0.01
LOC484960	-	20	-2.91	3.24E-10
LOC485464	-	22	-2.54	1.09E-05

LOC487375	-	2	17.82	1.30E-04
LOC487429	-	2	-2.86	<0.001
LOC490170	-	6	6.8	2.78E-04
LOC490172	-	6	6.09	1.59E-07
LOC490399	-	7	-2.66	1.57E-08
LOC490630	-	8	4.84	7.21E-04
LOC491379	-	16	-2.55	0.01
LOC491436	-	9	-2.73	1.57E-14
LOC607355	-	25	-8.04	7.08E-14
LOC607368	-	26	5.32	2.06E-05
LOC607692	-	6	-2.89	1.15E-10
LOC607890	-	17	3.19	5.07E-14
LOC607937	-	8	5.09	5.81E-06
LOC608848	-	38	4.17	3.61E-04
LOC609800	-	9	3.05	2.48E-07
LOC610528	-	7	-4.48	<0.001
LOC610677	-	6	-5.39	<0.001
LOC611363	-	6	10.69	2.27E-03
LOC611538	-	27	8.49	1.84E-06
LOC612054	-	26	4.16	8.82E-05
LOC612059	-	7	8.63	2.80E-18
LOC612122	-	26	4.89	1.85E-04
LOC612180	-	26	6.29	3.91E-05
LOC612200	-	X	3.46	7.57E-16
LPAR1	Lysophosphatidic Acid Receptor 1	11	3.28	1.27E-11
LPL	Lipoprotein Lipase	25	2.72	0.02
LRCH1	Leucine-Rich Repeats And Calponin Homology (CH) Domain Containing 1	22	-2.72	5.65E-09
LSP1	Lymphocyte-Specific Protein 1	18	4.28	1.68E-05
LUC7L	LUC7 Like	6	-3.2	<0.001
LUM	Lumican	15	7.02	1.22E-05
LY6G5B	Lymphocyte Antigen 6 Complex, Locus G5B	12	-7.36	1.51E-14
LYZ	Lysozyme	10	7.22	9.48E-13
MAFB	V-Maf Avian Musculoaponeurotic Fibrosarcoma Oncogene Homolog B	24	-3.22	1.66E-05
MAP1A	Microtubule Associated Protein 1A	30	2.61	6.03E-09
MAPK8IP3	Mitogen-Activated Protein Kinase 8 Interacting Protein 3	6	-3.49	5.23E-12
MARCKSL1	MARCKS-Like 1	2	3.06	8.47E-05
MATN3	Matrilin 3	17	10.68	5.32E-14
MBOAT1	Membrane Bound O-Acyltransferase Domain Containing 1	35	3.98	2.45E-07
MCAM	Melanoma Cell Adhesion Molecule	5	2.7	5.53E-09
MCM3	Minichromosome Maintenance Complex Component 3	12	2.54	8.79E-05
MCM5	Minichromosome Maintenance Complex Component 5	10	3.62	1.37E-05
MCM6	Minichromosome Maintenance Complex	19	3.3	1.05E-06

	Component 6			
MDM4	MDM4, P53 Regulator	38	-2.54	6.84E-09
MEGF6	Multiple EGF Like Domains 6	5	3.14	1.64E-14
MFAP4	Microfibrillar Associated Protein 4	5	7.28	4.84E-31
MFI2	Melanotransferrin	33	2.97	0.02
MGP	Matrix Gla Protein	27	4.73	7.39E-05
MKI67	Marker Of Proliferation Ki-67	28	10.04	2.45E-08
MLIP	Muscular LMNA-Interacting Protein	12	3.89	0.04
MLXIPL	MLX Interacting Protein Like	6	-4.3	<0.001
MME	Membrane Metallo-Endopeptidase	23	3.07	1.50E-18
MMP2	Matrix Metallopeptidase 2	2	7.22	3.31E-05
MMP9	Matrix Metallopeptidase 9	24	9.73	5.11E-06
MMRN1	Multimerin 1	32	3.95	0.03
MOB1A	MOB Kinase Activator 1A	17	2.75	4.71E-19
MOB1B	MOB Kinase Activator 1B	13	-2.93	7.52E-10
MRVI1	Murine Retrovirus Integration Site 1 Homolog	21	3.25	1.41E-10
MSC	Musculin	29	4.08	6.03E-04
MSH5	MutS Homolog 5	12	-3.34	9.96E-10
MTMR11	Myotubularin Related Protein 11	17	-2.55	<0.001
MTMR7	Myotubularin Related Protein 7	16	-2.51	5.52E-05
MXRA5	Matrix-Remodeling Associated 5	X	4.39	1.60E-12
MXRA8	Matrix-Remodeling Associated 8	5	2.78	7.18E-12
MYBL2	MYB Proto-Oncogene Like 2	24	3.79	5.55E-04
MYOF	Myoferlin	28	2.74	5.95E-04
N4BP2L1	NEDD4 Binding Protein 2-Like 1	25	-3.05	<0.001
NAA16	N(Alpha)-Acetyltransferase 16, NatA Auxiliary Subunit	22	-2.79	7.79E-11
NAMPT	Nicotinamide Phosphoribosyltransferase	18	-2.83	9.93E-04
NCAPG	Non-SMC Condensin I Complex Subunit G	3	3.13	1.18E-03
NECAB2	N-Terminal EF-Hand Calcium Binding Protein 2	5	-3.18	7.32E-10
NEFH	Neurofilament, Heavy Polypeptide	26	2.82	9.19E-05
NEIL1	Nei Like DNA Glycosylase 1	30	-2.79	5.25E-11
NELL2	Neural EGFL Like 2	27	-2.52	3.52E-04
NEPN	Nephrocan	1	3.7	2.58E-22
NET1	Neuroepithelial Cell Transforming 1	2	2.67	4.23E-04
NEURL3	Neuralized E3 Ubiquitin Protein Ligase 3	17	8.14	3.48E-17
NFKBIZ	NFKB Inhibitor Zeta	33	-2.9	2.89E-05
NICN1	Nicolin 1	20	-4.45	7.87E-12
NID2	Nidogen 2	8	3.81	8.59E-04
NKD2	Naked Cuticle Homolog 2	34	-5.06	6.23E-21
NKTR	Natural Killer Cell Triggering Receptor	23	-2.99	<0.001
NOCT	Nocturnin	19	-7.69	<0.001
NOD1	Nucleotide Binding Oligomerization Domain Containing 1	14	-3.45	1.16E-09
NOL6	Nucleolar Protein 6	11	-2.91	<0.001
NOV	Nephroblastoma Overexpressed	13	3.24	0.01

NPY1R	Neuropeptide Y Receptor Y1	15	15.54	0.01
NR4A1	Nuclear Receptor Subfamily 4 Group A Member 1	27	-4.34	7.39E-05
NR5A2	Nuclear Receptor Subfamily 5 Group A Member 2	7	-2.6	<0.001
NRP2	Neuropilin 2	37	2.8	3.54E-05
OAT	Ornithine Aminotransferase	28	-3.96	7.90E-06
OGT	O-Linked N-Acetylglucosamine (GlcNAc) Transferase	X	-2.61	<0.001
OLFM4	Olfactomedin 4	22	3.36	0.03
OLFML2A	Olfactomedin Like 2A	9	2.84	2.45E-22
OLFML2B	Olfactomedin Like 2B	38	2.72	3.08E-03
OLR1	Oxidized Low Density Lipoprotein Receptor 1	27	9.7	1.77E-04
OPRK1	Opioid Receptor Kappa 1	29	-2.75	1.76E-03
OXER1	Oxoeicosanoid (OXE) Receptor 1	10	-11.8	9.26E-23
P4HA1	Prolyl 4-Hydroxylase Subunit Alpha 1	4	-2.77	2.95E-04
PADI2	Peptidyl Arginine Deiminase 2	2	3.44	1.77E-03
PAMR1	Peptidase Domain Containing Associated With Muscle Regeneration 1	18	5.55	1.20E-03
PAN2	PAN2 Poly(A) Specific Ribonuclease Subunit	10	-2.61	<0.001
PAQR7	Progestin And AdipoQ Receptor Family Member 7	2	4.27	3.98E-05
PARP6	Poly(ADP-Ribose) Polymerase Family Member 6	30	-2.95	<0.001
PAXBP1	PAX3 And PAX7 Binding Protein 1	31	-2.54	1.92E-08
PBK	PDZ Binding Kinase	25	10.48	1.50E-05
PCK1	Phosphoenolpyruvate Carboxykinase 1	24	-2.6	0.02
PDE1C	Phosphodiesterase 1C	14	2.56	0.02
PDGFD	Platelet Derived Growth Factor D	5	4.24	8.19E-16
PDLIM3	PDZ And LIM Domain 3	16	2.54	4.98E-04
PDZK1IP1	PDZK1 Interacting Protein 1	15	4.2	1.25E-03
PER1	Period Circadian Clock 1	5	-4.2	<0.001
PER2	Period Circadian Clock 2	25	-2.83	1.27E-08
PGPEP1L	Pyroglutamyl-Peptidase I-Like	3	-4.11	7.79E-10
PHYHD1	Phytanoyl-CoA Dioxygenase Domain Containing 1	9	-2.58	<0.001
PI3	Peptidase Inhibitor 3	24	44.49	8.67E-08
PIGA	Phosphatidylinositol Glycan Anchor Biosynthesis Class A	X	-5.02	4.08E-118
PIGC	Phosphatidylinositol Glycan Anchor Biosynthesis Class C	7	-2.58	5.26E-11
PIGV	Phosphatidylinositol Glycan Anchor Biosynthesis Class V	2	-2.9	<0.001
PKD1L1	Polycystin 1 Like 1, Transient Receptor Potential Channel Interacting	16	-5.5	4.38E-10
PKIB	Protein Kinase (CAMP-Dependent, Catalytic) Inhibitor Beta	1	4.41	8.79E-28
PLAC8	Placenta Specific 8	32	2.5	1.99E-04
PLEKHS1	Pleckstrin Homology Domain Containing S1	28	4.75	0.02
PLK4	Polo Like Kinase 4	19	5.02	6.15E-04
PLP2	Proteolipid Protein 2 (Colonic Epithelium-Enriched)	X	3.04	6.31E-23
PLXDC1	Plexin Domain Containing 1	9	7.42	1.50E-19

PODN	Podocan	5	3.31	9.54E-15
PPARGC1A	PPARG Coactivator 1 Alpha	3	-4.32	<0.001
PPFIA2	PTPRF Interacting Protein Alpha 2	15	-3.84	1.64E-11
PRC1	Protein Regulator Of Cytokinesis 1	3	4.26	9.42E-04
PRKCA	Protein Kinase C Alpha	9	-3.42	<0.001
PROM1	Prominin 1	3	3.91	5.93E-03
PRPF40B	Pre-MRNA Processing Factor 40 Homolog B	27	-2.84	7.49E-13
PRRX1	Paired Related Homeobox 1	7	4.11	2.38E-08
PRSS12	Protease, Serine 12	32	-5.23	1.44E-16
PRSS8	Protease, Serine 8	6	2.53	8.75E-03
PSAT1	Phosphoserine Aminotransferase 1	1	5.56	3.59E-18
PSD	Pleckstrin And Sec7 Domain Containing	28	-3.79	3.41E-10
PTCHD2	Patched Domain-Containing Protein 2	2	-2.82	5.11E-08
PTGDS	Prostaglandin D2 Synthase	9	5.52	2.44E-15
PTGFRN	Prostaglandin F2 Receptor Inhibitor	17	2.55	2.69E-26
PTGR1	Prostaglandin Reductase 1	11	3.26	5.02E-16
PTPN18	Protein Tyrosine Phosphatase, Non-Receptor Type 18	25	2.7	1.66E-04
PTPRC	Protein Tyrosine Phosphatase, Receptor Type C	7	2.76	9.37E-19
PTPRCAP	Protein Tyrosine Phosphatase, Receptor Type C Associated Protein	18	3.43	8.42E-05
PYROXD2	Pyridine Nucleotide-Disulphide Oxidoreductase Domain 2	28	-3.47	<0.001
RARRES1	Retinoic Acid Receptor Responder 1	23	3.03	3.26E-08
RARRES3	Retinoic Acid Receptor Responder 3	18	3.69	2.58E-04
RASD1	Ras Related Dexamethasone Induced 1	5	4.65	2.40E-12
RBM3	RNA Binding Motif (RNP1, RRM) Protein 3	X	-2.84	1.12E-13
RBSN	Rabenosyn, RAB Effector	20	-2.57	8.68E-11
REN	Renin	38	-4.93	1.54E-05
RFTN1	Raftlin, Lipid Raft Linker 1	23	2.82	3.86E-19
RGS5	Regulator Of G-Protein Signaling 5	38	2.51	5.85E-04
RGS7	Regulator Of G-Protein Signaling 7	7	-3.87	1.14E-06
RHNO1	RAD9-HUS1-RAD1 Interacting Nuclear Orphan 1	27	-3.08	4.44E-13
RIC3	RIC3 Acetylcholine Receptor Chaperone	21	-4.34	3.32E-16
RNF152	Ring Finger Protein 152	1	-2.51	<0.001
RNF183	Ring Finger Protein 183	11	5.36	3.97E-15
ROPN1L	Rhophilin Associated Tail Protein 1 Like	34	-3.44	<0.001
RRAGD	Ras Related GTP Binding D	12	2.71	2.54E-04
RRM2	Ribonucleotide Reductase Regulatory Subunit M2	17	11.97	5.32E-30
RSPH1	Radial Spoke Head 1 Homolog	31	-2.52	1.96E-07
RSRP1	Arginine And Serine Rich Protein 1	2	-3.12	4.43E-04
RUNX3	Runt Related Transcription Factor 3	2	3.2	1.48E-05
S100A10	S100 Calcium Binding Protein A10	17	3.53	1.96E-24
S100A4	S100 Calcium Binding Protein A4	7	7.77	2.09E-27
S100A6	S100 Calcium Binding Protein A6	7	5.21	1.33E-28
S100P	S100 Calcium Binding Protein P	3	4.47	1.66E-03

SAA1_1	Serum Amyloid A1	21	5.87	5.72E-05
SAA1_2	Serum Amyloid A1	21	-5.46	5.43E-07
SAFB2	Scaffold Attachment Factor B2	20	-2.93	<0.001
SALL1	Spalt-Like Transcription Factor 1	2	-2.69	<0.001
SAMHD1	SAM Domain And HD Domain 1	24	3.05	4.52E-06
SBSN	Suprabasin	1	20.53	1.47E-20
SCML1	Sex Comb On Midleg-Like 1 (Drosophila)	X	-4.19	<0.001
SCN1A	Sodium Voltage-Gated Channel Alpha Subunit 1	36	-4.23	8.21E-13
SCN3A	Sodium Voltage-Gated Channel Alpha Subunit 3	36	-3.54	3.02E-10
SCN4A	Sodium Voltage-Gated Channel Alpha Subunit 4	9	-9.12	<0.001
SCN8A	Sodium Voltage-Gated Channel Alpha Subunit 8	27	-2.65	7.67E-09
SCRN1	Secernin 1	14	3.27	1.17E-04
SDPR	Serum Deprivation Response	37	2.64	2.66E-04
SDS	Serine Dehydratase	26	-3.34	9.64E-03
SEBOX	SEBOX Homeobox	9	-5.22	<0.001
SELM	Selenoprotein M	26	3.26	2.60E-05
SEMA3C	Semaphorin 3C	18	3.56	1.20E-03
SEMA3G	Semaphorin 3G	20	4	7.23E-04
SERPINB5	Serpin Family B Member 5	1	4.68	3.00E-19
SERPINE1	Serpin Family E Member 1	6	2.97	0.02
SERPINE2	Serpin Family E Member 2	37	13.71	1.01E-06
SFPQ	Splicing Factor Proline/Glutamine-Rich	15	-2.51	5.77E-14
SFRP5	Secreted Frizzled-Related Protein 5	28	2.58	7.45E-03
SGOL2	Shugoshin 2	37	2.92	8.93E-06
SH2D1A	SH2 Domain Containing 1A	X	2.84	3.22E-08
SHROOM1	Shroom Family Member 1	11	-4.9	<0.001
SIK1	Salt Inducible Kinase 1	31	-3.41	2.66E-08
SLAMF7	SLAM Family Member 7	38	4.69	7.36E-06
SLC17A4	Solute Carrier Family 17 Member 4	35	-4.26	1.89E-04
SLC17A9	Solute Carrier Family 17 Member 9	24	2.92	4.00E-05
SLC19A3	Solute Carrier Family 19 Member 3	25	3.52	8.60E-07
SLC1A1	Solute Carrier Family 1 Member 1	1	-2.64	1.51E-07
SLC22A2	Solute Carrier Family 22 Member 2	1	4.54	1.70E-19
SLC22A3	Solute Carrier Family 22 Member 3	1	-2.62	1.65E-14
SLC25A25	Solute Carrier Family 25 Member 25	9	-3.44	3.81E-11
SLC25A27	Solute Carrier Family 25 Member 27	12	-2.81	7.26E-06
SLC25A34	Solute Carrier Family 25 Member 34	2	-2.84	5.82E-05
SLC25A37	Solute Carrier Family 25 Member 37	25	-2.71	6.98E-08
SLC37A2	Solute Carrier Family 37 Member 2	5	4.79	5.98E-17
SLC51B	Solute Carrier Family 51 B	30	7.56	5.41E-17
SLC5A6	Solute Carrier Family 5 Member 6	17	-2.92	<0.001
SLC6A1	Solute Carrier Family 6 Member 1	20	2.63	2.26E-04
SLC6A14	Solute Carrier Family 6 Member 14	X	-6.4	<0.001
SLC6A8	Solute Carrier Family 6 Member 8	X	3.63	3.75E-20

SLC9A7	Solute Carrier Family 9 Member 7	X	-6.6	2.91E-37
SLCO3A1	Solute Carrier Organic Anion Transporter Family Member 3A1	3	3.96	1.49E-04
SLIT3	Slit Guidance Ligand 3	4	3.62	1.33E-04
SLITRK2	SLIT And NTRK Like Family Member 2	X	9.5	5.02E-09
SLITRK4	SLIT And NTRK Like Family Member 4	X	2.51	1.76E-06
SLITRK6	SLIT And NTRK Like Family Member 6	22	3.92	0.01
SLPI	Secretory Leukocyte Peptidase Inhibitor	24	69.78	9.87E-07
SMPDL3A	Sphingomyelin Phosphodiesterase Acid Like 3A	1	5.57	1.24E-18
SNCG	Synuclein Gamma	4	3.1	0.01
SNRNP70	Small Nuclear Ribonucleoprotein U1 Subunit 70	1	-3.13	<0.001
SOAT1	Sterol O-Acyltransferase 1	7	2.5	6.90E-10
SOCS2	Suppressor Of Cytokine Signaling 2	15	-3.18	4.60E-04
SPARCL1	SPARC Like 1	32	4.82	2.43E-04
SPC25	SPC25, NDC80 Kinetochore Complex Component	36	9.34	1.57E-04
SPINT1	Serine Peptidase Inhibitor, Kunitz Type 1	30	2.55	4.96E-12
SPN	Sialophorin	6	3.12	1.61E-05
SPNS3	Spinster Homolog 3 (Drosophila)	5	4.5	5.20E-10
SPON1	Spondin 1	21	3.44	3.05E-11
SPON2	Spondin 2	3	5.26	3.48E-03
SPP1	Secreted Phosphoprotein 1	32	5.88	5.19E-07
SPRY3	Sprouty RTK Signaling Antagonist 3	X	-5.94	2.79E-79
SRC	SRC Proto-Oncogene, Non-Receptor Tyrosine Kinase	24	2.59	2.66E-08
SREK1	Splicing Regulatory Glutamic Acid/Lysine-Rich Protein 1	2	-2.65	1.64E-11
SRRM2	Serine/Arginine Repetitive Matrix 2)	6	-4.08	<0.001
SRSF11	Serine/Arginine-Rich Splicing Factor 11	6	-2.54	<0.001
SRSF2	Serine/Arginine-Rich Splicing Factor 2	9	-3.15	<0.001
SRSF6	Serine/Arginine-Rich Splicing Factor 6	24	-2.51	4.34E-11
ST6GALNAC2	ST6 N-Acetylgalactosaminide Alpha-2,6-Sialyltransferase 2	9	4.94	1.67E-12
STEAP4	STEAP4 Metalloreductase	14	9.44	2.43E-05
STK17A	Serine/Threonine Kinase 17a	18	2.65	1.79E-07
STMN1	Stathmin 1	2	4.36	3.13E-07
STMN2	Stathmin 2	29	3.35	6.69E-03
STX11	Syntaxin 11	1	2.87	6.26E-24
STX3	Syntaxin 3	21	-4.14	<0.001
SULF1	Sulfatase 1	29	2.72	0.01
SULF2	Sulfatase 2	24	3.22	7.97E-07
SVOP	SV2 Related Protein	26	-5.63	8.03E-08
SYBU	Syntabulin	13	-2.56	1.83E-11
SYT17	Synaptotagmin 17	6	-4.11	3.77E-12
SYTL1	Synaptotagmin Like 1	2	4.65	6.25E-05
TACC3	Transforming Acidic Coiled-Coil Containing Protein 3	3	2.53	0.01
TAGLN	Transgelin	5	3.69	4.90E-18

TAT	Tyrosine Aminotransferase	5	-2.52	8.54E-08
TBX20	T-Box 20	14	3.74	2.11E-05
TBXAS1	Thromboxane A Synthase 1	16	3.82	4.55E-05
TCTE1	T-Complex-Associated-Testis-Expressed 1	12	-2.65	1.85E-09
TDRD15	Tudor Domain Containing 15	17	-2.58	<0.001
TERT	Telomerase Reverse Transcriptase	34	-3.88	9.76E-79
TEX14	Testis Expressed 14	9	-2.89	2.87E-10
TFEC	Transcription Factor EC	14	3.99	1.32E-04
THBS1	Thrombospondin 1	30	2.97	4.36E-31
THBS2	Thrombospondin 2	1	3.76	4.62E-22
THBS4	Thrombospondin 4	3	9.28	5.93E-03
THY1	Thy-1 Cell Surface Antigen	5	4.89	1.27E-28
TIA1	TIA1 Cytotoxic Granule-Associated RNA Binding Protein	10	-2.76	8.56E-11
TIMP1	TIMP Metallopeptidase Inhibitor 1	X	11.81	1.62E-30
TIRAP	Toll-Interleukin 1 Receptor (TIR) Domain Containing Adaptor Protein	5	-4.8	1.55E-62
TK1	Thymidine Kinase 1	9	2.59	3.25E-11
TLR2	Toll Like Receptor 2	15	3.29	9.21E-06
TLR8	Toll Like Receptor 8	X	2.89	4.79E-13
TM4SF19	Transmembrane 4 L Six Family Member 19	33	5.38	0.02
TMEM117	Transmembrane Protein 117	27	2.8	1.32E-04
TMEM119	Transmembrane Protein 119	26	6.67	1.13E-04
TMEM25	Transmembrane Protein 25	5	-7.5	<0.001
TMEM37	Transmembrane Protein 37	19	2.61	6.51E-05
TMEM55A	Transmembrane Protein 55A	29	-2.71	4.63E-08
TMSB10	Thymosin Beta 10	17	3.01	4.48E-33
TNFAIP2	TNF Alpha Induced Protein 2	8	2.88	1.16E-04
TNFRSF12A	Tumor Necrosis Factor Receptor Superfamily Member 12A	6	3.1	2.10E-03
TNFRSF21	Tumor Necrosis Factor Receptor Superfamily Member 21	12	2.51	7.26E-06
TNFSF13B	Tumor Necrosis Factor Superfamily Member 13b	22	4.44	4.00E-04
TOB1	Transducer Of ERBB2, 1	9	-3.23	<0.001
TOMM40L	Translocase Of Outer Mitochondrial Membrane 40 Like	38	-2.75	4.27E-06
TOP2A	Topoisomerase (DNA) II Alpha	9	4.85	2.72E-27
TP53I13	Tumor Protein P53 Inducible Protein 13	9	-4.38	<0.001
TP53INP1	Tumor Protein P53 Inducible Nuclear Protein 1	29	-3.67	5.19E-12
TPM4	Tropomyosin 4	20	2.53	2.09E-06
TPX2	TPX2, Microtubule Nucleation Factor	24	6.25	1.10E-06
TRIB3	Tribbles Pseudokinase 3	24	-5.91	6.17E-10
TRPV6	Transient Receptor Potential Cation Channel Subfamily V Member 6	16	-3.62	1.50E-07
TTC31	Tetratricopeptide Repeat Domain 31	17	-2.91	<0.001
TTN	Titin	36	-3.88	<0.001
TUSC3	Tumor Suppressor Candidate 3	16	2.67	5.30E-06
UBD	Ubiquitin D	35	13.93	4.44E-03

UBE2C	Ubiquitin Conjugating Enzyme E2 C	24	6.87	9.22E-06
UCHL1	Ubiquitin C-Terminal Hydrolase L1	3	4.25	5.32E-04
ULK1	Unc-51 Like Autophagy Activating Kinase 1	26	-3.37	<0.001
USP2	Ubiquitin Specific Peptidase 2	5	-2.84	1.48E-14
VAMP2	Vesicle Associated Membrane Protein 2	5	-2.69	4.33E-30
VCAN	Versican	3	3.97	4.53E-03
VEGFA	Vascular Endothelial Growth Factor A	12	-3.2	<0.001
VIM	Vimentin	2	2.73	4.91E-05
VWA2	Von Willebrand Factor A Domain Containing 2	28	2.51	0.02
WDR90	WD Repeat Domain 90	6	-3.25	<0.001
WFDC2	WAP Four-Disulfide Core Domain 2	24	15.5	8.51E-05
WHAMM	WAS Protein Homolog Associated With Actin, Golgi Membranes And Microtubules	3	-3.99	6.20E-14
WISP2	WNT1 Inducible Signaling Pathway Protein 2	24	11.31	3.28E-07
WSB1	WD Repeat And SOCS Box Containing 1	9	-3.83	<0.001
WT1	Wilms Tumor 1	18	3.86	5.21E-04
XPNPEP2	X-Prolyl Aminopeptidase (Aminopeptidase P) 2, Membrane-Bound	X	2.69	5.41E-07
XRCC3	X-Ray Repair Complementing Defective Repair In Chinese Hamster Cells 3	8	-8	1.05E-26
ZBTB16	Zinc Finger And BTB Domain Containing 16	5	-3.13	<0.001
ZFAND5	Zinc Finger AN1-Type Containing 5	1	-2.85	<0.001
ZP2	Zona Pellucida Glycoprotein 2	6	-3.86	1.57E-04
ZPR1	ZPR1 Zinc Finger	5	-2.5	6.72E-14

FDR: false discovery rate.

Table S3 Transcript Table

Transcript	**Chromosome**	**Fold Change**	**FDR-adjusted *P*-value**
AADACL2_1	23	11.17	1.91E-14
ABCA8_6	9	-3.4	<0.001
ABCC5_1	34	-5.44	<0.001
ABCC5_2	34	-3.97	<0.001
ABCC5_3	34	-4.44	<0.001
ABCC5_4	34	-3.84	<0.001
ABCC5_5	34	-5.43	<0.001
ABCD4_2	8	3.1	1.49E-03
ABHD2_1	3	2.8	3.64E-07
ABLIM1_16	28	2.5	5.73E-03
ABR_6	9	2.5	8.56E-10
ACADL_1	37	-2.77	2.78E-04
ACADSB_1	28	-4.3	7.65E-09
ACKR3_1	25	-3.22	1.25E-04
ACKR3_3	25	-5.1	3.27E-06

ACKR3_4	25	-3.41	9.25E-04
ACOX2_6	20	-4.99	9.92E-08
ACOX2_7	20	-4.22	7.59E-09
ACP5_1	20	4.06	8.81E-05
ACP5_2	20	2.52	0.02
ACSM5_2	6	-5.72	4.32E-10
ACTB_1	6	-3.3	2.29E-05
ADAM28_1	25	3.96	5.93E-03
ADAM9_1	16	2.57	2.28E-05
ADAMDEC1_1	25	47.9	9.91E-06
ADAMTS12_1	4	2.62	9.76E-04
ADCY1_1	16	3.21	0.04
ADGRD1_2	26	3.71	0.02
ADGRL1_3	20	-2.62	4.36E-04
ADIPOR2_2	27	-3.67	4.06E-09
ADIRF_1	4	2.85	7.16E-03
ADNP_1	24	3.08	1.47E-06
AGMAT_2	2	-2.67	0.02
AGR2_3	14	5.46	8.27E-03
AGR2_4	14	6.14	0.02
AJUBA_4	8	-3.43	1.96E-11
AKAP17A_1	X	-3.1	<0.001
AKAP17A_2	X	-2.7	<0.001
AKAP8_1	20	-3.71	<0.001
ALAS1_2	20	-10.21	3.12E-12
ALDH1B1_4	11	-3.14	5.75E-13
ALDH8A1_4	1	-3.85	<0.001
ALG1_5	6	-3.24	9.48E-09
ALOX15_1	5	2.99	1.26E-04
ALPI_1	25	9.05	0.04
ALPL_1	2	-2.61	5.06E-03
AMDHD2_2	6	-4.22	2.01E-10
AMICA1_1	5	4.94	5.01E-24
ANGPT4_2	24	3.85	3.61E-04
ANGPTL4_1	20	2.6	3.45E-04
ANK2_9	32	3.78	0.03
ANK3_5	4	2.56	0.01
ANK3_6	4	3.82	4.61E-04
ANKRD33B_2	34	2.59	1.12E-06
ANLN_1	14	5.53	1.34E-03
ANLN_3	14	7.46	1.38E-03
ANTXR1_1	10	2.61	6.73E-04
ANXA1_1	1	2.69	3.54E-15
ANXA2_1	30	6.72	1.37E-29

ANXA4_1	10	4.18	4.28E-08
ANXA5_1	19	2.92	1.12E-06
ANXA8L1_1	4	5.19	2.09E-06
AOAH_2	14	2.86	6.28E-03
AP1S2_1	X	2.57	2.05E-13
AP5S1_4	24	-3.57	5.19E-10
APBB1IP_1	2	3.02	7.55E-06
APBB3_7	2	-5.71	6.41E-13
APOA4_1	5	13.29	9.44E-09
APOF_2	10	-2.5	0.02
ARFGAP2_1	18	-2.64	4.37E-04
ARHGAP11A_1	30	6.57	7.65E-11
ARHGDIB_1	27	2.78	2.09E-06
ARHGEF3_4	20	3.49	1.99E-05
ARID5B_2	4	-2.71	4.67E-04
ARL4A_1	14	-2.75	2.15E-04
ARL4A_2	14	-3.21	3.90E-05
ARPC1B_1	6	2.72	6.11E-06
ASCL1_1	15	-5.47	1.32E-05
ASNS_1	14	5.03	9.89E-03
ATF3_2	7	2.68	9.30E-09
ATG13_11	18	-2.53	1.25E-04
ATG2B_2	8	-3	7.18E-06
ATG2B_5	8	-2.61	6.39E-05
ATP2A3_3	9	3.23	8.92E-20
AUTS2_2	6	-2.89	4.61E-07
AUTS2_4	6	-3.74	8.32E-08
B3GNT9_1	5	2.68	8.47E-12
B4GALT3_3	38	-3.19	1.19E-07
BAAT_5	11	-3.59	<0.001
BASP1_1	4	3.22	3.03E-05
BAZ2A_2	10	-2.7	1.46E-06
BBOX1_2	21	-2.64	<0.001
BBS12_1	19	2.95	5.51E-03
BCAS4_1	24	4.19	4.70E-08
BCAT1_1	27	7.23	4.83E-05
BCAT1_2	27	7.19	2.83E-05
BCL2A1_1	3	2.52	3.94E-03
BCL6_3	34	-3.54	<0.001
BCL6_4	34	-3.74	<0.001
BCL9_6	17	-3.48	<0.001
BGLAP_1	7	-4.03	1.15E-34
BMP1_3	25	-3.85	1.08E-08
BPI_1	24	3.7	2.32E-05

BPI_2	24	3.64	1.76E-05
BPI_3	24	3.98	5.08E-05
BRD1_1	10	-2.54	1.57E-05
BTBD3_3	24	-2.73	8.34E-04
C20H19orf80_1	20	-4.87	0.04
C29H8orf22_1	29	-2.59	1.32E-04
C31H21orf62_2	31	2.71	0.04
C6_1	4	2.96	4.87E-03
C6_2	4	3.11	4.56E-03
C6H16orf54_1	6	3.72	4.44E-06
C7H1orf105_4	7	-3.65	<0.001
CA13_1	29	3.83	2.79E-04
CAD_1	17	-2.89	<0.001
CAP1_3	15	2.53	8.66E-04
CAPG_3	17	7.5	2.13E-27
CAPS_1	20	3.09	0.02
CASP4_1	5	6.8	9.83E-25
CAST_13	3	3.21	7.51E-04
CAV1_1	14	3.2	5.70E-05
CAV1_2	14	2.83	5.33E-03
CAV2_1	14	2.66	1.02E-03
CCDC125_2	2	-2.99	4.83E-07
CCDC148_1	36	-3.64	2.26E-03
CCDC18_1	6	-4.38	7.59E-04
CCDC80_1	33	3.53	4.53E-05
CCDC88A_1	10	3.45	3.08E-05
CCDC88A_2	10	3.44	5.76E-04
CCL2_1	9	8.65	2.40E-21
CCL21_1	11	3.22	9.56E-07
CCL5_1	9	14.07	1.06E-27
CCNA2_1	19	4.18	8.74E-04
CCNB2_1	30	3.26	9.79E-14
CCND3_4	12	2.8	3.73E-05
CCNL1_1	23	-3.59	<0.001
CCNL2_1	5	-2.87	<0.001
CCNL2_2	5	-3	1.49E-51
CCNT2_5	19	-3.14	1.87E-05
CCR1_2	20	4.09	3.13E-05
CCS_1	18	-2.9	5.26E-07
CD163_2	27	-2.61	5.84E-04
CD1A6_1	38	7.74	1.10E-08
CD2_1	17	4.04	5.69E-21
CD27_1	27	4.49	5.13E-04
CD28_1	37	-2.99	5.59E-04

CD34_1	7	2.62	1.01E-10
CD3E_1	5	7.7	7.44E-27
CD4_1	27	3.17	0.01
CD44_4	18	2.9	8.12E-03
CD48_1	38	3.68	9.13E-06
CD6_1	18	10.18	2.98E-04
CD74_1	4	5.26	3.84E-09
CD74_2	4	4.26	1.65E-07
CD83_1	35	2.59	1.82E-03
CD84_3	38	5.38	2.03E-06
CD86_4	33	2.42	8.90E-03
CD8A_1	17	6.27	7.93E-15
CD8B_1	17	5.06	9.28E-16
CD9_1	27	2.72	1.17E-03
CD96_1	33	4.19	0.02
CDADC1_1	22	-3.48	1.95E-07
CDADC1_2	22	-11.12	6.13E-12
CDC25B_1	24	2.53	3.11E-05
CDH13_1	5	4.75	1.75E-10
CDHR2_1	4	32.29	1.69E-14
CDKN1A_1	12	3.17	0.04
CDKN2B_1	11	2.52	1.89E-08
CDPF1_4	10	-3.94	<0.001
CENPE_1	32	7.5	3.54E-06
CENPE_2	32	6.16	1.01E-05
CENPF_1	7	11.59	1.93E-21
CFTR_1	14	3.38	0.01
CGREF1_2	17	5.71	5.94E-14
CHGA_1	8	9.74	3.70E-06
CHI3L1_2	7	42.68	4.84E-21
CHKA_3	18	3.06	3.26E-03
CHST2_1	23	5.31	1.42E-07
CIART_1	17	-5.63	1.17E-38
CIRBP_3	20	-2.79	1.03E-06
CIRBP_4	20	-3.07	3.53E-08
CLDN11_1	34	4.33	1.70E-09
CLDN18_2	23	8.6	4.17E-12
CLDN4_1	6	3.08	3.21E-05
CLEC12A_1	27	2.62	2.54E-03
CLEC2D_1	27	2.99	3.87E-04
CLEC4A_1	27	-5.55	2.58E-17
CLIC5_2	12	3.93	7.74E-05
CLK1_1	37	-4.36	6.38E-07
CLK1_2	37	-2.76	3.75E-04

CLK1_3	37	-3.51	6.38E-07
CLK4_1	11	-2.62	<0.001
CLK4_2	11	-2.8	<0.001
CLK4_3	11	-3.48	<0.001
COL12A1_3	12	3.37	1.43E-03
COL15A1_1	11	2.99	9.47E-09
COL15A1_2	11	3.36	2.85E-09
COL15A1_3	11	3.26	7.45E-10
COL16A1_1	2	3.77	4.04E-04
COL1A1_1	9	5.87	1.56E-21
COL1A2_1	14	2.56	3.22E-03
COL23A1_1	11	3.44	1.34E-08
COL2A1_1	27	3.35	6.99E-04
COL2A1_2	27	3.5	3.31E-04
COL2A1_3	27	3.14	4.95E-04
COL3A1_1	36	3.21	2.37E-04
COL6A1_1	31	3.36	5.00E-04
COL6A2_1	31	3.22	2.11E-04
COL6A3_4	25	2.59	0.03
COL6A3_7	25	2.85	0.01
COL6A5_4	23	3.56	6.32E-07
COL6A5_6	23	3.16	6.44E-07
COL8A1_1	33	2.87	2.55E-03
COMT_2	26	2.65	2.24E-03
CORO1A_1	6	2.97	3.77E-06
CPM_1	10	5.08	2.84E-05
CPXM2_4	28	8.47	1.94E-03
CRAMP1_2	6	-4.47	2.56E-09
CREBZF_1	21	-2.6	<0.001
CREM_26	2	-5.91	3.03E-12
CRHR2_1	14	-2.75	0.02
CRHR2_4	14	-2.67	0.02
CRHR2_5	14	-2.56	0.03
CRHR2_6	14	-2.54	0.03
CRIP1_1	8	2.7	2.64E-04
CRISPLD2_1	5	2.91	3.26E-09
CRY2_2	18	-2.83	3.43E-04
CRYAB_1	5	3.16	4.28E-17
CRYGS_2	34	-7.53	1.89E-37
CRYL1_3	25	-2.62	4.46E-05
CRYM_1	6	-2.85	1.43E-05
CSTB_1	31	3.25	1.79E-04
CTGF_1	1	2.69	9.96E-07
CTSB_1	25	2.62	2.02E-04

CTSK_1	17	4.8	6.48E-18
CUX2_1	26	4.1	3.13E-04
CUX2_2	26	10.76	3.82E-03
CXCL10_1	32	19.35	2.61E-06
CYBASC3_1	18	5.03	0.01
CYBASC3_3	18	2.88	0.01
CYBASC3_5	18	2.52	0.04
CYGB_1	9	3.78	6.85E-19
CYP1A2_3	30	-2.97	1.57E-13
CYP1B1_1	17	6.04	1.86E-14
CYSLTR2_2	22	2.65	2.73E-04
CYTIP_2	36	3.87	6.37E-06
DAPP1_1	32	3.46	8.69E-04
DAZAP1_3	20	-3.08	8.71E-07
DBNDD2_1	24	2.98	1.76E-06
DCDC2_1	35	4.02	1.86E-03
DCLK1_8	25	9.35	2.48E-06
DCN_1	15	3.05	0.02
DCN_3	15	6.38	1.58E-04
DCN_4	15	2.74	1.21E-03
DDR2_3	38	3.14	0.01
DDR2_4	38	3.59	1.05E-03
DDR2_6	38	9.51	3.38E-04
DFNA5_1	14	3.61	0.01
DGKA_1	10	3.65	1.96E-03
DGKQ_3	3	-4.06	6.48E-07
DIO2_1	8	-3.73	1.81E-03
DLA-79_2	18	3.02	2.76E-05
DLA88_1	12	4.45	4.00E-03
DLA-DMA_1	12	4.42	1.77E-05
DLA-DMA_2	12	2.94	8.30E-04
DLA-DMA_3	12	2.92	3.76E-03
DLA-DMA_4	12	3.14	1.67E-03
DLA-DMA_5	12	3.14	1.92E-03
DLA-DMB_1	12	3.51	1.45E-06
DLA-DRA_2	12	4.65	1.97E-05
DNASE1_2	6	2.65	2.75E-03
DTX1_1	26	4.31	4.21E-05
DTX4_1	18	3.67	1.02E-04
E4F1_1	6	-2.68	4.05E-13
ECI1_1	6	3.98	1.22E-15
ECSCR_3	2	3.67	6.08E-03
EFEMP1_2	10	7.15	2.08E-04
EFEMP1_3	10	4.52	2.62E-03

EFNA1_3	7	-2.61	6.52E-13
EGR2_2	4	2.7	0.01
ELF3_2	7	3.1	1.33E-07
ELOVL2_1	35	19.8	3.07E-04
ELOVL2_2	35	45.65	3.07E-04
ELOVL2_3	35	25.6	1.45E-04
ELOVL2_4	35	15.01	1.82E-03
EMB_1	4	3.14	3.86E-06
EMILIN2_1	7	3.11	2.47E-15
EMP1_1	27	7.05	2.04E-04
ENPP5_2	12	2.93	8.04E-05
ENPP6_1	16	2.74	0.03
ENTHD2_1	9	-2.54	<0.001
EPHB6_1	16	3.86	2.57E-03
EPPK1_1	13	-5.69	3.00E-08
ETNPPL_1	32	-4.8	3.32E-03
EVA1A_6	17	-2.82	<0.001
EXD1_10	30	-2.92	6.93E-15
EXOG_1	23	-3.17	6.99E-25
EXOG_2	23	-3.17	2.57E-34
F10_2	22	-2.78	3.17E-05
F12_1	4	-2.67	4.69E-06
F13A1_1	35	5.14	5.53E-04
F2R_3	3	2.51	4.24E-05
FAAP100_1	9	-2.68	<0.001
FABP1_1	17	17.98	2.94E-28
FABP4_1	29	16.3	7.08E-04
FABP5_1	29	4.58	2.64E-04
FAM114A1_1	3	3.54	3.46E-07
FAM129A_2	7	2.87	2.65E-15
FAM13A_3	32	-2.51	1.32E-03
FAM180A_1	16	2.88	2.17E-03
FAM193B_5	4	-5.56	1.49E-11
FAM193B_6	4	-6.71	1.41E-13
FAM193B_7	4	-5.53	1.46E-11
FAM214A_2	30	-2.69	2.13E-11
FAM214A_3	30	-2.73	<0.001
FAM76B_3	21	-2.7	2.00E-18
FAM92A1_5	29	-4.23	2.79E-04
FAN1_8	3	-2.93	2.16E-05
FAP_1	36	7.75	5.93E-05
FAP_2	36	6.95	3.03E-04
FAP_3	36	4.45	5.69E-04
FAP_4	36	14.54	3.06E-04

FAR1_1	21	3.04	5.65E-19
FBLIM1_1	2	2.7	6.67E-04
FBXO21_3	26	-2.54	1.64E-03
FBXO44_1	2	-2.71	4.83E-07
FBXO9_2	12	-2.71	1.55E-03
FEZF1_1	14	4.88	2.67E-04
FICD_4	26	-2.62	1.18E-03
FKBP10_1	9	4.36	2.55E-17
FKBP5_3	12	-2.99	4.91E-04
FKBP5_6	12	-2.66	1.55E-03
FLRT2_1	8	4.98	4.13E-05
FMR1_1	X	-3.58	5.28E-23
FNBP4_3	18	-2.57	1.13E-04
FOLH1_1	21	3.38	5.92E-13
FOSL2_5	17	-2.87	1.90E-14
FRA10AC1_4	28	-2.57	9.58E-05
FSCN1_1	6	3.37	8.84E-08
FSIP1_1	30	2.72	1.70E-19
FSIP1_2	30	2.98	1.22E-23
FSIP1_3	30	3.15	4.71E-15
FXYD5_1	1	2.95	8.51E-20
FYB_1	4	2.52	5.95E-04
G6PC_1	9	-3.89	<0.001
GABRB1_1	13	6.5	0.02
GADD45A_1	6	-3.48	3.54E-12
GADD45B_1	20	-4.23	1.09E-12
GALNT3_1	36	2.82	4.60E-03
GALNT3_2	36	2.67	1.79E-03
GALNT3_3	36	2.8	0.01
GALNT6_1	27	5.88	4.95E-04
GAS6_1	22	3.23	2.96E-03
GATA6_1	7	2.7	7.71E-14
GATM_1	30	3.19	2.62E-04
GBP6_1	6	3.37	1.49E-03
GCA_3	36	-3.91	4.07E-10
GDF9_1	11	-2.98	1.04E-36
GIGYF1_5	6	-2.64	3.37E-04
GIMAP2_1	16	3.71	1.01E-04
GIMAP4_1	16	2.86	3.62E-03
GIMAP4_3	16	3.9	1.79E-03
GIMAP4_4	16	3.71	2.79E-03
GIMAP6_1	16	2.56	8.29E-05
GLDN_1	30	3.25	7.93E-12
GLIPR2_1	11	2.64	2.95E-22

GLS2_4	10	-2.79	1.33E-03
GLS2_5	10	-6.04	5.25E-08
GMEB2_1	24	-3.56	1.25E-18
GMEB2_3	24	2.65	5.56E-05
GMPPA_3	37	-2.67	3.90E-05
GNAT1_1	20	-6.56	1.69E-11
GON4L_1	7	-2.5	3.56E-30
GON4L_2	7	-2.55	5.50E-32
GPM6A_1	16	2.74	0.03
GPNMB_1	14	11.81	3.19E-06
GPR176_1	30	-2.76	<0.001
GPR176_2	30	-3.69	<0.001
GPSM2_3	6	4.04	4.44E-06
GRAMD1C_5	33	4.64	1.03E-05
GRB14_3	36	-2.57	4.86E-11
GSN_1	11	4.03	1.15E-18
GULP1_4	36	5.61	0.02
GULP1_7	36	3.68	0.02
GULP1_8	36	3.56	0.01
GZMA_1	2	5.76	8.65E-06
GZMK_1	4	6.4	5.61E-05
HAL_1	15	-2.89	5.05E-04
HAVCR1_5	4	4.87	9.20E-04
HBEGF_2	2	-2.73	1.23E-05
HDAC11_2	20	-4.52	2.32E-11
HKDC1_1	4	-4.96	9.76E-07
HLA-DRB1_1	12	3.97	1.95E-07
HMCN2_1	9	-2.58	1.68E-06
HMCN2_2	9	-3.97	4.05E-25
HMCN2_3	9	-3.94	2.08E-23
HNRNPDL_3	32	-5.08	4.87E-10
HOPX_1	13	2.57	0.01
HOXD8_1	36	5.04	7.29E-03
HPN_2	1	-6.26	<0.001
HPN_3	1	-8.01	<0.001
HPSE_1	32	4.07	1.33E-04
HSPB8_1	26	10.73	2.05E-06
HTRA3_1	3	2.74	3.53E-04
HYKK_3	13	-2.79	1.13E-06
ICOSLG_1	31	2.6	2.34E-03
IDO1_1	16	9.65	2.56E-06
IDO2_2	16	-4.14	3.25E-07
IDUA_3	3	-3.2	2.81E-09
IFGGB1_2	11	12.22	2.98E-15

IFGGB2_1	11	2.68	3.08E-06
IFGGB2_2	11	3.02	1.14E-05
IFGGC1_1	11	4.73	1.06E-11
IFIT1_1	4	7.04	3.30E-04
IFIT3_1	4	3.19	1.09E-04
IFNGR2_1	31	3.47	2.15E-09
IGF2_3	18	-3.69	2.11E-06
IGFBP7_1	13	2.53	2.15E-04
IKZF5_2	28	-2.93	4.13E-06
IL16_3	3	3.85	2.01E-05
IL1RL2_1	10	-4.01	3.52E-06
IL1RL2_2	10	-5.03	4.18E-15
IL1RL2_3	10	-7.25	1.55E-15
IL1RL2_4	10	-4.94	1.54E-15
IL1RL2_5	10	-4.93	1.30E-15
IL1RL2_6	10	-6.02	7.44E-12
IL2RG_1	X	7.55	2.76E-20
IL2RG_2	X	4.37	1.50E-13
IL33_2	11	-3.32	<0.001
ILKAP_1	25	-3.67	4.97E-10
INA_1	28	2.66	4.71E-04
INTS6_2	22	-3.88	1.47E-07
IRG1_1	22	8.77	8.19E-03
IRG1_2	22	8.63	2.50E-03
ISG20_1	3	4.23	5.83E-05
ITFG2_1	27	-3.64	3.31E-09
ITGA11_1	30	2.99	1.14E-08
ITGA3_1	9	2.56	2.46E-13
ITGA6_1	36	3.03	1.85E-04
ITGAX_1	6	9.97	7.45E-11
ITGB2_1	31	2.7	2.94E-03
ITGB4_1	9	2.64	5.43E-08
ITGB7_1	27	2.55	1.08E-03
ITGB8_4	14	3.41	0.04
ITIH1_2	20	-5.5	1.85E-12
ITIH5_1	2	2.87	3.42E-04
ITK_1	4	2.58	2.41E-03
JCHAIN_1	13	5.28	2.58E-04
JCHAIN_2	13	3.04	1.75E-05
KALRN_8	33	-3.08	4.93E-13
KCNA3_1	6	3.35	1.68E-05
KCNH2_1	16	-3.77	2.88E-05
KCNK17_1	12	3.69	2.38E-03
KDM4A_5	15	-4.25	3.02E-09

KIAA0101_2	30	5.35	4.59E-11
KIAA1524_2	33	2.99	8.70E-04
KIAA1644_1	10	5.48	8.77E-05
KIAA1755_1	24	2.82	8.90E-04
KIAA1804_1	4	-3.27	4.69E-05
KIF11_1	28	8.31	2.14E-07
KIF23_1	30	4.02	1.41E-11
KISS1_2	38	-8.87	7.02E-11
KISS1_3	38	-4.84	1.70E-08
KLC1_5	8	-2.81	5.54E-12
KLC1_6	8	-2.81	4.16E-13
KLC1_7	8	-2.84	6.40E-11
KLHL41_1	36	-8.75	4.86E-11
KLRG1_3	27	2.91	9.86E-05
KPNA2_1	9	2.52	3.34E-12
KRT19_1	9	3.01	1.91E-11
KRT5_1	27	5.56	1.09E-03
KTN1_1	8	4.43	4.00E-07
KTN1_8	8	2.58	1.86E-03
LAMA4_1	12	4.85	9.64E-05
LAMB2_1	20	3.39	2.19E-03
LAMC3_1	9	4.07	1.27E-10
LARP1B_1	19	-2.51	2.90E-06
LARP6_1	30	3.87	1.25E-11
LBH_1	17	3.25	3.86E-21
LCK_1	2	2.69	5.57E-04
LENG8_1	1	-3	<0.001
LENG8_2	1	-2.88	<0.001
LENG8_3	1	-3.33	<0.001
LENG8_4	1	-2.88	<0.001
LGALS1_1	10	6.21	4.92E-08
LGALS3_1	8	15.99	3.70E-06
LGALS3_2	8	8.3	2.95E-04
LGALS3_3	8	5.58	3.96E-06
LGI4_1	1	-3.73	2.44E-54
LIPG_1	7	-3.45	<0.001
LMLN_1	33	3.17	4.01E-03
LOC100682772_1	14	-4.68	4.93E-05
LOC100683373_1	21	3.84	2.33E-14
LOC100683419_11	17	-2.89	4.62E-19
LOC100683419_7	17	-2.76	7.44E-16
LOC100684931_1	1	-18.17	6.09E-46
LOC100687054_1	26	3.31	6.87E-04
LOC100687459_1	16	4	3.37E-04

LOC100687459_3	16	4.67	9.98E-05
LOC100687983_1	1	7.21	6.05E-32
LOC100855630_1	26	7.71	2.48E-04
LOC100855940_1	17	-3.84	<0.001
LOC100856137_1	12	3.16	3.73E-04
LOC100856302_1	24	2.61	0.02
LOC100856622_1	31	-5.74	3.08E-13
LOC102151511_1	3	-54.28	3.19E-08
LOC102151654_1	16	-4.52	9.36E-07
LOC102151654_2	16	-4.15	4.02E-05
LOC102152056_1	28	10.15	1.77E-06
LOC102152474_1	31	-3.8	1.79E-04
LOC102153199_1	9	-4.13	1.19E-13
LOC102153586_1	17	-3.34	4.76E-14
LOC102154209_1	11	-3.92	9.24E-34
LOC102154748_3	12	-2.53	3.73E-05
LOC102154781_1	5	-2.83	2.68E-18
LOC102155229_4	31	-2.83	5.04E-05
LOC102155399_1	16	-5.21	7.35E-08
LOC102155424_1	X	5.15	2.23E-18
LOC102155487_1	1	-14.73	5.06E-76
LOC102155751_1	25	-4.5	1.63E-09
LOC102155815_1	34	-3.81	5.85E-20
LOC102155886_1	21	42.3	8.67E-28
LOC102156583_1	X	3.17	3.06E-19
LOC102156586_1	X	-7.54	1.26E-65
LOC102156852_1	10	-7.07	1.75E-16
LOC102156955_1	13	-7.71	3.28E-21
LOC106557533_1	27	4.38	9.21E-05
LOC106559112_1	8	4.42	3.83E-04
LOC106559122_1	8	4.54	3.27E-03
LOC106559562_1	12	8.97	7.74E-03
LOC106559915_1	17	-4.6	2.51E-35
LOC448801_1	6	4.8	1.30E-03
LOC475605_1	16	-3.43	2.50E-04
LOC475935_1	18	4.64	8.87E-05
LOC476006_1	18	3.58	4.24E-05
LOC476047_1	18	-2.68	1.55E-04
LOC476047_2	18	-2.91	4.42E-04
LOC476879_1	21	15.34	6.20E-14
LOC476879_2	21	19.09	5.07E-19
LOC476879_3	21	15.9	1.62E-17
LOC477562_2	26	-4.06	2.71E-06
LOC477562_3	26	-2.67	2.44E-04

LOC478384_2	31	2.53	0.01
LOC478773_3	36	-2.83	4.06E-03
LOC479911_1	6	-3.36	9.07E-05
LOC481227_4	10	2.59	2.75E-05
LOC482202_1	14	2.64	0.01
LOC482987_1	17	9.98	6.46E-15
LOC483345_3	9	2.72	7.08E-25
LOC484897_1	20	3.39	0.03
LOC484960_1	20	-2.87	2.55E-09
LOC487375_1	2	18.44	1.29E-05
LOC487429_2	2	-3.12	<0.001
LOC487429_4	2	-4.92	1.14E-25
LOC488622_1	38	3.69	8.86E-03
LOC488622_5	38	2.92	7.77E-03
LOC489851_3	6	-2.68	0.01
LOC490170_1	6	7.07	2.16E-04
LOC490172_1	6	6.32	3.71E-07
LOC490399_3	7	-4.96	<0.001
LOC490630_1	8	4.88	8.75E-04
LOC491379_1	16	-3.48	7.05E-04
LOC491379_2	16	-4.1	5.71E-06
LOC607355_1	25	-7.85	2.27E-13
LOC607368_1	26	6.24	1.12E-04
LOC607368_11	26	3.05	6.14E-03
LOC607368_12	26	5.57	3.78E-04
LOC607368_16	26	6.72	1.18E-03
LOC607368_17	26	6.24	5.64E-04
LOC607368_2	26	7.89	1.71E-03
LOC607368_21	26	8.65	7.50E-04
LOC607368_23	26	5.76	1.85E-04
LOC607368_25	26	6.56	5.02E-04
LOC607368_26	26	8.65	4.21E-05
LOC607368_27	26	7.07	3.90E-04
LOC607368_28	26	3.34	9.42E-03
LOC607368_3	26	7.06	1.07E-04
LOC607368_30	26	9.12	2.35E-04
LOC607368_34	26	4.24	6.14E-03
LOC607368_36	26	3.64	3.30E-03
LOC607368_37	26	5.86	7.72E-04
LOC607368_38	26	7.95	6.27E-04
LOC607368_39	26	4.93	1.43E-03
LOC607368_4	26	5.09	0.01
LOC607368_40	26	4.6	4.02E-04
LOC607368_41	26	4.04	4.25E-03

LOC607368_43	26	7.69	1.40E-03
LOC607368_49	26	3.84	4.25E-03
LOC607368_50	26	4.02	2.49E-03
LOC607368_6	26	4.17	1.36E-03
LOC607692_1	6	-3.42	1.42E-07
LOC607692_3	6	-2.64	2.93E-05
LOC607890_1	17	3.32	3.34E-14
LOC607937_1	8	5.14	1.61E-05
LOC608848_2	38	4.45	2.33E-04
LOC608975_2	12	3.88	1.11E-04
LOC609452_2	24	2.51	6.25E-05
LOC609800_1	9	3.14	1.44E-07
LOC610528_1	7	-4.4	<0.001
LOC610677_1	6	-5.22	<0.001
LOC611363_1	6	11.27	1.53E-03
LOC611538_1	27	9.02	1.16E-06
LOC611922_1	6	2.56	2.43E-05
LOC612054_1	26	4.1	2.71E-04
LOC612059_2	7	12.02	7.66E-15
LOC612122_1	26	4.64	4.43E-04
LOC612180_1	26	6.44	1.42E-04
LOC612200_1	X	3.65	9.93E-16
LPCAT2_4	2	2.73	3.42E-04
LPL_1	25	2.85	0.01
LRCH1_1	22	-2.57	2.96E-07
LSP1_1	18	4.86	1.93E-04
LSP1_2	18	4.54	3.78E-04
LSP1_4	18	5.02	1.28E-07
LTBP1_4	17	2.71	1.29E-07
LTBP4_1	1	3.17	3.42E-10
LUC7L_3	6	-4.36	4.64E-11
LUC7L2_6	16	-4.15	1.10E-08
LUM_1	15	7.05	2.95E-05
LY6G5B_1	12	-6.9	7.57E-14
LY9_1	38	2.77	3.53E-03
LYN_2	29	2.6	7.08E-04
LYZ_1	10	7.68	7.05E-12
MADD_25	18	-2.57	1.56E-03
MAFB_1	24	-3.05	8.52E-05
MAFG_4	9	-2.82	<0.001
MAOA_1	X	2.62	1.20E-17
MAP1A_1	30	2.61	3.50E-09
MAP4_8	20	4.69	1.79E-05
MAP4_9	20	3.4	6.90E-06

MAPK8IP3_1	6	-3.37	2.01E-10
MARC1_1	38	-6.46	1.70E-08
MARCKSL1_1	2	3.17	2.17E-05
MASP2_1	2	-3.02	<0.001
MATN3_1	17	11.12	1.44E-14
MAU2_1	20	-2.52	8.71E-07
MAVS_4	24	-2.79	8.23E-14
MBOAT1_1	35	3.83	1.15E-03
MBOAT1_2	35	6.29	1.08E-06
MBOAT1_4	35	6.15	1.34E-07
MCM3_1	12	2.76	4.31E-05
MCM5_1	10	3.81	1.58E-05
MCM6_1	19	3.51	1.58E-06
MDC1_9	12	-3.21	9.34E-07
MDFIC_2	14	2.98	2.31E-03
MDM4_1	38	-2.72	7.83E-07
MDM4_4	38	-2.63	3.44E-06
MEGF6_1	5	3.46	7.14E-15
METTL22_5	6	-3.32	4.38E-06
MFAP4_1	5	8.07	5.64E-30
MFI2_1	33	2.85	0.02
MFSD2A_4	15	-3.2	2.29E-03
MGP_1	27	5.01	9.96E-05
MINA_2	33	-2.57	2.34E-07
MKI67_1	28	9.67	2.39E-08
MLLT4_12	1	-3.35	<0.001
MLXIPL_1	6	-3.76	1.74E-05
MLXIPL_4	6	-5.52	<0.001
MLXIPL_5	6	-6.09	<0.001
MMP2_1	2	7.54	5.60E-06
MMP9_1	24	15.6	2.35E-06
MMRN1_1	32	3.98	0.03
MOB1A_1	17	2.85	2.05E-14
MOB1A_2	17	2.85	1.89E-11
MOB1B_1	13	-2.94	3.00E-09
MRVI1_1	21	5.66	2.75E-11
MRVI1_2	21	3.15	8.08E-07
MRVI1_3	21	2.59	6.53E-06
MRVI1_4	21	3.24	7.50E-08
MSC_1	29	4.27	3.64E-04
MSH5_1	12	-3.12	8.61E-09
MSN_2	X	3.16	1.74E-26
MTIF3_7	25	-2.91	3.26E-07
MTMR11_2	17	-2.63	<0.001

MTSS1_3	13	-3.44	5.23E-08
MXRA5_1	X	4.65	1.15E-12
MXRA8_1	5	3.06	3.17E-12
MYBL2_1	24	4.02	3.75E-04
MYL9_2	24	2.89	3.11E-05
MYOF_2	28	3.21	2.35E-03
N4BP2L1_1	25	-2.97	8.70E-12
NAA16_1	22	-2.64	9.25E-09
NAMPT_1	18	-2.79	1.69E-03
NANOS1_1	28	-3.14	1.31E-04
NCAPG_1	3	3.14	9.69E-04
NCAPH2_5	10	-3	3.92E-05
NDOR1_2	9	-3.51	<0.001
NECAB2_1	5	-2.96	5.27E-08
NEIL1_3	30	-3.57	7.79E-12
NELL2_2	27	-2.56	5.18E-04
NEPN_1	1	3.85	1.07E-22
NET1_1	2	2.78	5.69E-05
NEURL3_1	17	8.53	1.68E-17
NFAM1_1	10	2.51	3.32E-04
NFKBIZ_1	33	-2.93	4.53E-05
NICN1_1	20	-4.39	1.07E-11
NID2_1	8	3.87	9.92E-04
NKD2_1	34	-5.21	1.57E-21
NKTR_1	23	-2.87	<0.001
NKTR_2	23	-3.21	<0.001
NKTR_3	23	-2.85	<0.001
NKTR_4	23	-2.8	<0.001
NKTR_6	23	-3.29	<0.001
NKTR_7	23	-2.84	<0.001
NOCT_1	19	-9.06	6.89E-12
NOCT_2	19	-6.47	5.24E-12
NOCT_3	19	-7.43	6.10E-12
NOCT_4	19	-3.67	9.84E-09
NOD1_2	14	-3.67	1.55E-05
NOD1_3	14	-4.05	5.50E-09
NOD1_4	14	-4.02	5.50E-09
NOL6_1	11	-2.76	<0.001
NOSTRIN_4	36	-5.03	3.77E-04
NOV_1	13	3.16	0.01
NR4A1_2	27	-5.44	2.31E-05
NR4A1_4	27	-5.32	4.95E-04
NR5A2_1	7	-3.26	<0.001
NRP2_2	37	3.96	2.90E-05

NRP2_3	37	2.55	6.40E-04
NRP2_4	37	2.63	3.34E-04
NRP2_5	37	2.95	8.90E-05
NRXN1_10	10	2.61	5.42E-04
NRXN1_3	10	2.75	0.02
NUDT12_7	3	3.25	3.53E-04
OAT_2	28	-3.07	0.04
OAT_3	28	-5.92	3.22E-05
OGT_1	X	-2.72	<0.001
OLFM4_1	22	3.6	0.02
OLFML2A_2	9	3.46	3.54E-18
OLFML2B_1	38	2.62	3.30E-03
OLR1_2	27	11.04	2.87E-04
OPRK1_1	29	-2.73	1.10E-03
ORAI2_2	6	2.75	7.58E-04
OSMR_1	4	2.61	0.01
OTUD3_3	2	-2.57	2.24E-05
OTUD6B_2	29	-3.16	4.23E-06
OXER1_1	10	-11.23	1.97E-21
P4HA1_2	4	-4.1	1.85E-04
PACSIN3_3	18	-3.63	4.25E-08
PADI2_1	2	3.65	4.53E-04
PAQR7_1	2	4.62	3.93E-06
PARP6_3	30	-3.03	2.40E-15
PARP6_5	30	-3.12	2.37E-29
PAXBP1_1	31	-2.68	5.98E-09
PCK1_1	24	-2.57	0.03
PCM1_3	16	2.53	0.01
PDGFD_1	5	4.7	8.64E-16
PDLIM3_1	16	2.88	4.70E-04
PDZK1IP1_3	15	4.87	1.36E-03
PER2_5	25	-5.37	<0.001
PFKFB1_4	X	-2.64	<0.001
PFKFB2_6	7	-2.58	<0.001
PFKFB3_1	2	-3.05	9.28E-06
PFKP_2	2	3	1.36E-03
PGPEP1L_2	3	-5.84	5.80E-13
PHF5A_2	10	-2.68	5.47E-05
PHYHD1_1	9	-2.65	<0.001
PHYHD1_3	9	-2.75	<0.001
PI16_2	12	2.86	0.02
PI3_1	24	47.76	1.10E-07
PIGA_1	X	-4.69	9.02E-91
PIGA_2	X	-4.71	2.23E-78

PIGC_3	7	-3.26	6.13E-11
PIGV_1	2	-4.52	1.37E-15
PIGV_5	2	-3.76	<0.001
PIK3R1_5	2	-3.55	2.40E-08
PKD1L1_1	16	-5.1	7.64E-09
PKIB_4	1	7.74	3.32E-26
PKIB_7	1	7.23	2.02E-18
PLA2G6_1	10	-2.95	1.55E-07
PLAC8_1	32	3.39	1.01E-05
PLK4_1	19	5.36	3.69E-04
PLLP_1	2	2.55	4.61E-04
PLP2_1	X	3.21	4.55E-22
PLXDC1_1	9	7.63	1.13E-19
PMF1_1	7	-3.45	4.01E-21
PML_8	30	-3.62	<0.001
PNISR_4	12	-5.58	1.28E-06
POMK_5	16	-2.75	8.37E-06
PPARGC1A_1	3	-3.16	8.57E-08
PPARGC1A_4	3	-5.28	2.70E-08
PPARGC1A_5	3	-5.33	<0.001
PPFIA2_1	15	-3.84	1.54E-11
PPRC1_3	28	-2.97	1.18E-07
PQBP1_5	X	-3.08	1.80E-50
PRAP1_3	28	6.32	7.05E-03
PRC1_1	3	4.27	6.91E-04
PRF1_1	4	6.89	2.38E-04
PRKACB_2	6	2.66	1.51E-04
PRKCA_1	9	-2.9	<0.001
PRKCA_2	9	-3.56	<0.001
PRKCD_1	20	2.5	2.08E-03
PROSER2_3	2	-3.02	1.23E-07
PRPF39_4	8	-3.53	2.48E-05
PRPF4B_2	35	-3.14	1.86E-03
PRPF4B_3	35	-2.59	0.02
PRPH_1	27	2.55	3.87E-04
PRRX1_1	7	4.9	3.39E-09
PRSS12_1	32	-5.21	1.74E-15
PRSS8_1	6	2.61	6.82E-03
PSAT1_1	1	5.83	2.39E-18
PTCHD2_2	2	-3.25	1.07E-07
PTGDS_1	9	5.72	1.10E-15
PTGFRN_1	17	2.65	1.81E-26
PTGR1_1	11	3.64	2.01E-13
PTGR1_3	11	3.71	1.61E-15

PTPN12_3	18	2.6	5.31E-04
PTPN13_1	32	2.69	8.40E-04
PTPN18_1	25	2.8	1.26E-04
PTPRC_1	7	2.93	1.08E-12
PTPRC_2	7	3.5	2.59E-10
PTPRC_6	7	3.36	3.65E-10
PTPRCAP_1	18	3.49	1.09E-04
PXDC1_2	35	-7.45	5.91E-13
PXN_5	26	2.86	0.01
PYROXD2_1	28	-3.6	<0.001
RAB3IP_7	10	-2.87	2.37E-05
RAB43_2	20	-5.02	3.12E-12
RAB43_3	20	-5.55	9.62E-11
RAB7B_1	38	2.57	2.69E-03
RAB7B_2	38	3.11	1.05E-03
RARRES1_1	23	2.99	3.34E-08
RARRES3_1	18	3.74	3.96E-04
RASD1_2	5	4.88	1.96E-11
RBM3_3	X	-4.77	<0.001
RBPMS_13	16	-2.86	1.58E-04
RBSN_1	20	-3.91	7.10E-07
RBSN_2	20	-3.69	4.44E-05
RDH16_7	10	-3.6	<0.001
REN_1	38	-6.3	1.03E-09
REN_3	38	-6.46	6.73E-07
REXO1_2	20	-4.23	3.35E-09
RFTN1_1	23	2.81	7.79E-19
RGS10_1	28	2.98	4.42E-04
RHNO1_5	27	-5.63	3.96E-10
RNF183_1	11	5.71	1.16E-15
RNF31_4	8	-2.5	4.71E-04
ROPN1L_2	34	-6.66	6.47E-36
RRAGD_1	12	2.93	1.31E-04
RRM2_1	17	12.49	1.35E-29
RSPH1_3	31	-2.69	7.21E-04
RSRP1_1	2	-3.04	2.16E-04
RTEL1_3	24	-2.5	4.91E-04
RUNX3_1	2	3.32	9.80E-07
S100A10_1	17	3.66	4.49E-24
S100A4_1	7	7.69	6.77E-23
S100A4_2	7	8.15	1.61E-20
S100A6_1	7	5.33	1.60E-27
S100P_1	3	4.47	9.86E-04
SAA1_1_1	21	8.44	5.21E-06

SAA1_1_2	21	4.06	1.27E-03
SAA1_2_1	21	-4.57	8.10E-05
SAA1_2_2	21	-5.51	3.50E-06
SAA1_2_3	21	-5.38	2.80E-06
SAFB2_1	20	-2.94	<0.001
SAFB2_2	20	-2.74	1.96E-13
SAFB2_3	20	-2.98	<0.001
SAFB2_4	20	-2.86	<0.001
SALL1_2	2	-2.59	2.94E-11
SAMHD1_1	24	4.31	1.76E-06
SASH3_1	X	2.81	7.98E-12
SAT1_1	X	4.41	1.04E-13
SCN1A_1	36	-4.45	4.60E-05
SCN1A_2	36	-4.3	3.82E-07
SCN1A_6	36	-4.32	1.46E-04
SCN1A_7	36	-4.31	1.96E-06
SCN3A_1	36	-3.28	1.81E-08
SCN4A_1	9	-10.2	<0.001
SCN7A_1	36	3.73	0.04
SCN7A_4	36	4.52	0.04
SCN8A_1	27	-3.21	1.93E-08
SDPR_1	37	2.65	3.52E-04
SDS_1	26	-3.31	0.01
SDSL_4	26	-4.51	9.58E-05
SEBOX_1	9	-2.63	5.96E-15
SEBOX_2	9	-7.77	<0.001
SELM_1	26	3.39	6.12E-05
SELPLG_1	26	2.53	2.15E-04
SEMA3C_1	18	3.62	1.27E-03
SEMA3G_1	20	4.04	1.08E-03
SERPINB5_3	1	7.29	4.94E-17
SERPINE2_1	37	13.58	5.56E-05
SF3B1_1	37	4.17	1.72E-04
SFPQ_1	15	-2.51	1.54E-11
SFSWAP_2	26	-4.48	3.27E-12
SFXN2_2	28	-3.03	7.78E-06
SGCE_4	14	2.82	0.03
SGMS2_6	32	2.63	1.10E-03
SGOL2_1	37	3.4	3.55E-05
SH2D1A_1	X	3.01	6.00E-09
SH3PXD2B_1	4	-4.36	1.22E-12
SHROOM1_1	11	-4.65	<0.001
SIK1_1	31	-3.61	1.14E-08
SIRT3_4	18	-3.31	6.63E-11

SIRT3_8	18	-3.02	4.25E-08
SIRT3_9	18	-2.62	1.19E-03
SKAP2_1	14	2.99	3.37E-04
SLAMF7_1	38	5.22	5.18E-06
SLAMF7_2	38	5.07	5.58E-05
SLAMF7_3	38	3.43	3.78E-04
SLC12A2_1	11	2.57	9.27E-11
SLC17A1_1	35	-2.54	1.15E-03
SLC17A3_1	35	-2.91	3.24E-03
SLC17A4_1	35	-4.44	8.22E-05
SLC17A9_1	24	3.34	8.52E-05
SLC1A1_1	1	-2.59	2.43E-07
SLC22A2_1	1	4.72	4.63E-20
SLC25A25_1	9	-2.81	3.18E-08
SLC25A25_2	9	-2.79	5.33E-08
SLC25A25_3	9	-2.77	3.55E-08
SLC25A25_4	9	-2.79	5.06E-08
SLC25A25_5	9	-2.97	1.12E-08
SLC25A25_6	9	-2.81	2.65E-08
SLC25A25_7	9	-6.12	<0.001
SLC25A34_1	2	-2.83	2.91E-05
SLC25A37_1	25	-2.6	3.31E-06
SLC38A1_3	27	2.64	0.01
SLC39A14_3	25	-3.01	4.51E-06
SLC43A2_1	9	3.81	1.04E-20
SLC51B_3	30	12.4	1.37E-13
SLC5A6_1	17	-2.94	<0.001
SLC5A6_2	17	-2.81	<0.001
SLC5A6_3	17	-2.75	<0.001
SLC5A6_4	17	-2.76	<0.001
SLC5A6_5	17	-2.75	<0.001
SLC5A6_6	17	-2.9	<0.001
SLC6A1_1	20	2.68	2.76E-04
SLC6A14_1	X	-5.96	<0.001
SLC6A8_1	X	3.86	2.50E-20
SLC8B1_3	26	-2.82	1.81E-06
SLC9A7_1	X	-6.67	5.65E-31
SLC9A7_2	X	-5.67	9.30E-27
SLCO3A1_2	3	4.15	4.69E-05
SLIT3_1	4	3.71	1.42E-04
SLPI_1	24	74.54	1.67E-06
SMARCD2_4	9	-2.97	<0.001
SMC3_1	28	2.56	8.15E-06
SMC4_1	34	3.1	3.28E-16

SMPDL3A_1	1	7.94	2.43E-18
SMPDL3A_2	1	3.31	4.50E-12
SNCG_1	4	3.2	7.16E-03
SNRNP70_1	1	-3.56	<0.001
SNRPB2_2	24	2.76	8.19E-05
SNX20_1	2	2.55	3.93E-04
SOCS2_2	15	-4.88	9.87E-05
SOCS2_3	15	-2.74	0.03
SOCS2_5	15	-5.49	4.82E-06
SORBS2_4	16	2.72	4.18E-03
SPARCL1_1	32	5.82	1.00E-03
SPARCL1_2	32	3.38	9.49E-04
SPARCL1_3	32	5.01	5.80E-05
SPARCL1_4	32	5.07	2.17E-03
SPC25_1	36	9.97	6.31E-05
SPI1_1	18	2.67	3.50E-03
SPINT1_1	30	2.56	3.72E-12
SPN_1	6	3.24	2.85E-05
SPON1_1	21	5.08	4.65E-13
SPON2_1	3	5.27	2.80E-03
SPP1_1	32	6.06	9.32E-07
SPP1_2	32	5.81	2.61E-06
SPRY3_1	X	-4.8	5.10E-43
SPRY3_2	X	-4.68	1.77E-32
SPRY3_3	X	-8.44	1.93E-66
SPRY3_4	X	-4.97	1.37E-44
SRC_4	24	5.59	7.23E-10
SREK1_7	2	-4.17	1.43E-10
SRGAP2_4	38	-3.53	3.44E-06
SRRM1_10	2	-3.1	9.96E-05
SRRM2_12	6	-4.21	3.19E-12
SRRM2_3	6	-4.09	2.12E-07
SRRM2_4	6	-5.23	<0.001
SRRM2_6	6	-4.63	1.74E-12
SRRM2_9	6	-5.38	<0.001
SRSF2_1	9	-4.16	<0.001
SRSF5_2	8	-4.19	5.41E-07
SRSF6_2	24	-7.71	<0.001
ST6GALNAC2_1	9	5.11	7.77E-13
STAU2_1	29	2.89	6.29E-03
STEAP2_1	14	-2.94	6.94E-03
STEAP4_1	14	4.44	1.27E-03
STEAP4_2	14	13.21	1.94E-04
STK17A_1	18	2.7	2.79E-06

STK36_11	37	-3.51	1.44E-05
STMN1_1	2	4.4	7.06E-07
STMN1_2	2	4.61	3.32E-07
STMN1_3	2	4.22	7.21E-08
STMN2_1	29	3.45	6.21E-03
STOX1_1	4	3.04	6.86E-06
STX16_12	24	-2.52	3.07E-09
STX16_9	24	-2.68	1.47E-06
STX3_1	21	-4.96	1.17E-27
STX3_3	21	-4.65	1.83E-23
STX3_5	21	-3.19	1.68E-25
STX3_6	21	-3.52	4.75E-22
STX3_7	21	-5.07	3.55E-25
STX3_9	21	-2.93	1.13E-21
SULF2_1	24	3.2	3.58E-05
SULF2_2	24	3.8	1.30E-06
SULF2_3	24	3.22	3.71E-06
SVOP_1	26	-5.85	3.74E-08
SYBU_1	13	-2.55	2.20E-10
SYT17_1	6	-4.01	3.72E-09
SYTL1_1	2	6.07	5.32E-06
SZT2_4	15	-3.82	6.97E-10
TACC3_1	3	2.55	7.60E-03
TAF1D_1	21	-2.85	4.23E-23
TAF1D_15	21	-3	3.15E-24
TAF1D_16	21	-3.29	5.16E-26
TAF1D_9	21	-2.61	5.36E-18
TAGLN_1	5	4.07	3.15E-18
TBC1D1_1	3	3.25	1.05E-04
TBX20_1	14	3.67	4.93E-05
TBXAS1_1	16	2.82	5.01E-04
TBXAS1_2	16	4.16	9.98E-05
TBXAS1_3	16	5.2	1.73E-04
TCTN1_5	26	2.63	1.48E-03
TCTN2_1	26	2.63	1.13E-03
TDRD15_6	17	-5.53	1.09E-24
TERT_1	34	-3.92	8.36E-78
TEX14_6	9	-2.97	3.66E-09
TEX14_7	9	-2.83	1.30E-07
TFEC_4	14	4.81	0.01
TFEC_7	14	6.42	1.45E-04
TFR2_1	6	2.63	1.04E-03
THBS1_1	30	2.99	1.73E-31
THBS2_1	1	3.9	3.91E-22

THBS4_1	3	9.1	6.23E-03
THOC5_1	26	-3.55	2.05E-06
THY1_1	5	5.36	3.79E-28
TIA1_1	10	-4.24	7.44E-12
TIA1_6	10	-2.56	8.32E-06
TIMP1_1	X	12.43	9.16E-30
TK1_1	9	2.66	2.25E-11
TKFC_6	18	-3.18	3.28E-05
TKFC_7	18	-4.09	6.14E-05
TLR2_1	15	3.59	1.01E-05
TLR8_2	X	3.15	2.22E-09
TLR9_2	20	2.51	4.17E-06
TLR9_3	20	-9.78	1.66E-07
TM4SF19_1	33	5.28	0.02
TMEM132A_1	18	4.02	1.70E-04
TMEM154_2	15	2.52	1.50E-06
TMEM170B_2	35	-2.63	2.41E-03
TMEM37_1	19	2.8	4.26E-05
TMEM55A_1	29	-2.64	5.58E-07
TMSB10_1	17	3.12	4.60E-32
TNFAIP2_1	8	2.92	2.57E-04
TNFRSF12A_1	6	3.22	1.84E-03
TNFRSF21_1	12	2.71	9.26E-06
TNFSF13B_1	22	4.73	2.00E-04
TNRC6A_6	6	-2.58	2.67E-04
TNRC6A_8	6	-3.74	3.48E-08
TOB1_1	9	-3.14	<0.001
TOMM40L_1	38	-3.84	3.56E-08
TP53I13_1	9	-6.88	<0.001
TP53I13_2	9	-3.14	<0.001
TP53INP1_1	29	-4.1	1.53E-09
TP53INP1_4	29	-5.12	1.53E-09
TPC3_4	17	2.5	3.40E-08
TPM4_1	20	2.52	6.76E-06
TPM4_2	20	2.64	6.42E-06
TPM4_3	20	2.67	3.00E-05
TPMT_3	35	3.36	2.47E-03
TPX2_4	24	17.51	8.36E-06
TRA2A_3	14	-3.23	3.19E-06
TRIB3_2	24	-6.73	3.81E-09
TRIM34_1	21	2.63	1.46E-11
TRPV6_1	16	-4.79	7.35E-08
TRPV6_3	16	-4.02	2.07E-07
TRPV6_4	16	-2.88	4.62E-03

TRPV6_5	16	-3.86	1.72E-06
TSC22D3_5	X	-2.5	2.11E-10
TSHZ2_1	24	2.53	4.91E-04
TSKU_1	21	2.84	3.93E-16
TSKU_2	21	3.11	5.07E-19
TSKU_3	21	3.06	2.04E-14
TSKU_4	21	2.9	1.68E-11
TSKU_5	21	-2.93	9.58E-09
TTC31_1	17	-2.5	6.62E-13
TTC31_2	17	-3.63	3.89E-30
TTC31_3	17	-2.67	3.22E-30
TTN_1	36	-3.61	1.94E-11
TTPAL_1	24	-2.83	6.09E-03
TTPAL_4	24	-3.06	2.87E-05
TTPAL_5	24	-2.74	5.55E-05
TUSC3_1	16	2.86	1.33E-05
UBD_1	35	13.53	1.86E-03
UBE2C_1	24	11.45	1.98E-05
UBFD1_7	6	-3.01	3.34E-06
UCHL1_1	3	4.27	4.15E-04
UCP2_1	21	2.7	2.36E-16
UEVLD_8	21	-2.61	2.21E-14
UHMK1_2	38	-2.93	6.75E-06
ULK1_3	26	-5.95	<0.001
UNC5B_1	4	5.73	9.86E-07
UNKL_3	6	-2.59	9.19E-04
UNKL_6	6	-3.02	1.37E-04
UVSSA_4	3	-2.64	4.18E-05
UVSSA_5	3	-2.97	4.15E-04
VAMP2_1	5	-2.5	<0.001
VARS2_1	12	-2.66	3.73E-05
VCAM1_1	6	2.64	4.43E-03
VCAN_1	3	2.76	5.49E-03
VCAN_2	3	2.78	4.15E-03
VCAN_3	3	5.21	6.59E-03
VEGFA_1	12	-3.73	9.47E-10
VIM_1	2	2.81	5.64E-06
VWA1_1	5	2.58	4.80E-11
VWA2_1	28	3.71	7.46E-03
WDR37_5	2	-2.81	8.65E-06
WDR90_4	6	-4.4	7.45E-11
WFDC2_1	24	16.5	4.53E-04
WFS1_1	13	2.9	1.46E-05
WFS1_6	13	-5.39	5.92E-09

WHAMM_1	3	-4.02	5.49E-13
WIPF1_3	36	2.61	1.41E-05
WISP2_1	24	9.81	1.79E-06
WISP2_2	24	15.12	1.47E-06
WNT2_2	14	3.05	4.86E-04
WSB1_2	9	-3.95	<0.001
WT1_1	18	3.92	4.42E-04
XG_2	X	2.86	5.49E-09
XPNPEP2_1	X	2.78	1.97E-07
XPO4_5	25	-3.09	1.26E-04
YPEL5_1	17	2.97	6.31E-11
YPEL5_3	17	-2.53	<0.001
ZFAND5_2	1	-3.03	<0.001
ZNF133_1	24	-3.02	2.48E-04
ZNF35_3	20	-2.6	7.47E-05
ZNF7_4	13	-2.89	1.15E-05
ZNRF3_4	26	-2.7	1.11E-05
ZP2_1	6	-3.74	2.07E-04
ZPR1_1	5	-2.52	2.05E-10
ZSWIM8_5	4	-2.54	1.08E-06

FDR: false discovery rate.

12. Publications

A part of the results of the RNA sequencing study was published as an abstract: 'High-throughput RNA Sequencing and Differential Gene Expression Analysis in Dogs with Chronic Hepatitis' **(**VM Eulenberg, YA Lawrence, JS Suchodolski, JM Steiner, and JA Lidbury) in the *2017 ACVIM Forum Research Abstract Program.* DOI: 10.1111/jvim.14778.

Parts of the literature review were published in the review 'Hepatic fibrosis in dogs' (VM Eulenberg, JA Lidbury), *Journal of Veterinary Internal Medicine, Jan/Feb 2018*. DOI:10.111/jvim.14891.

13. Danksagung

I would like to thank Dr. Jörg Steiner, Dr. Barbara Kohn, and Dr. Jonathan Lidbury for providing the possibilities for this doctoral work. I'd like to thank Dr. Jonathan Lidbury for being the most accurate supervisor I've ever met and Dr. Jan Suchodolski for giving us advice when needed.

In addition, I want to thank Jonathan, Jörg, Yuri, Julia, Mookky, and Ago for reading and editing my manuscripts.

I thank Mookky for finally finding her way to the GiLab.

I also need to thank the GiLab staff for their always helpful support and Nancy for keeping things organized and reminding us of important rules. I also thank Texas A&M and the PDA for all the great learning opportunities.

Last not least danke ich meinen Hunden, Sonya und Rudi, for their goofy support und meinem Kater Hans, für sein beruhigendes Schnurren.

14. Selbstständigkeitserklärung

Hiermit bestätige ich, dass ich die vorliegende Arbeit selbständig angefertigt habe und versichere, ausschlieβlich die angegebenen Quellen und Hilfen in Anspruch genommen zu haben.

Berlin, den 08.03.2018 Vera M. Eulenberg

mbvberlin mensch und buch verlag

49,90,00 Euro | ISBN: 978-3-86387-886-3